“Enhanced innate immune response in the olfactory sensory system of the zebrafish”

Tesis entregada a la

UNIVERSIDAD DE VALPARAÍSO

En Cumplimiento Parcial de los requisitos para optar al grado de

Doctor en Ciencias con Mención en Neurociencia

Facultad de Ciencias

Por

María Fernanda Palominos Chacón

Marzo, 2021

Tesis dirigida por:

Dr. Kathleen E. Whitlock

FACULTAD DE CIENCIAS

UNIVERSIDAD DE VALPARAÍSO

INFORME DE APROBACIÓN DE TESIS DE DOCTORADO

Se informa a la Facultad de Ciencias que la Tesis de Doctorado presentada por:

María Fernanda Palominos Chacón

Ha sido aprobada por la comisión de Evaluación de la tesis como requisito para optar al grado de Doctor en Ciencias con mención en Neurociencia, en el exam de Defensa de Tesis rendido el día 27 de Abril de 2021.

Directora de Tesis:

Dr. Kathleen E. Whitlock .....

Comisión de Evaluación de Tesis

Dr. John Ewer Lothian .....

Dr. Pablo R. Moya .....

Dr. Carmen G. Feijoo .....

Para Elena, la niña del futuro

AGRADECIMIENTOS

Esta tesis es obra de quienes han confiado en mí, de aquellos que vieron “algo” que a veces ni yo misma puedo ver, y eligieron apoyarme. Agradezco el apoyo incondicional y libre de mi tutora, la Dra. Kate Whitlock, con quien a través de la comunicación sincera, a veces de risas y/o llantos, me brindó su amistad y confianza. Debe haber sido difícil acarrear a los que nos perdemos rápido en el bosque para mirar en detalle los árboles y las ramas (a veces hasta las hojas…).

Agradezco también el apoyo y las críticas constructivas de mi comisión de tesis, Dra. Carmen G. Feijoo, Dr. Pablo R. Moya, y en especial, a Dr. John Ewer, quien era el Director del Doctorado en Neurociencia cuando ingresé al Programa y quien rigurosamente revisó este tesis. También quisiera agradecer especialmente el apoyo constante de la Dra. Ana María Cárdenas. Gracias a Andrea Moscoso, Trini Órdenes, y Stephany Alaniz por tener a los peces felices y alimentados, por su amistad y cariño. A mis compañeras y compañeros de lab: Eugenius, Angie, Vale, Lili, Cata, Caro, Danissa, Justin, Javier A., Javier C., Cristian, Pablo, Ricardo; gracias por la amistad, las risas, los buenos momentos, y las noches de Valpo. Por último, quisiera agradecer al Prof. Dr. Juan Fernández Hidalgo y al Prof. Dr. Eduardo Couve, quienes ahora pertenecen al plano de la memoria pero que influenciaron fuertemente mi carrera científica.

Finalmente, pero siendo la base fundamental para el desarrollo de esta tesis, agradezco a mi familia; a Diego, a mis amigas y amigos. Ellos son mi fortaleza.

TABLE OF CONTENTS

INDEX OF FIGURES

Summary

The olfactory system detects odorants in the environment and relays this information to the central nervous system via the olfactory nerve. Over fifty years ago researchers showed that fluids pass from the arachnoid space of the brain across the cribriform plate separating the brain from the peripheral olfactory organs. We now know that fluids drain across the cribriform plate along perineural spaces associated with the olfactory nerves passing through the nasal mucosa to cervical lymph nodes. This olfactory/nasal lymphatic route remains poorly characterized with respect to the potential immune contribution in the protection of the brain from inflammation caused by damage, and viral or bacterial infections.

Here we showed that the zebrafish olfactory sensory system has an extensive network of blood-lymphatic vasculature and associated immune cells (neutrophils and macrophages) that forms during early development. This network of lymphatic and blood vasculature is associated with the migration of immune cells towards the olfactory organs in response to copper induced damage and migration of neutrophils is dependent on calcium signaling mediated by L-type Ca^{2+} channels.

In adult animals we showed that the blood-lymphatic vasculature extends across the cribriform plate connecting the peripheral olfactory organs and central nervous system. Two distinct lymphatic cell types were identified in the olfactory organs, one of which accompanies the blood vasculature as it connects the olfactory organs and the central nervous system. Finally, the adult olfactory organs have a large population of resident neutrophils that rapidly increased on number in response to copper-induced damage.

The extensive population of resident neutrophils within the olfactory organs suggests that the olfactory organs may act as an immune defense niche for the adult brain. Furthermore, I anticipate that these results will lay the foundations for future research that will shed light on the

role of this interface in the life-long neurogenic capacities of the olfactory epithelium, the systemic responses of nasal-delivered drugs, as well as its potential to be used as a point of entry to pathogens (such as the SARS-CoV2 virus, which can access the brain through the olfactory pathway).

CHAPTER 1: INTRODUCTION

The olfactory route as a port of entry to the brain

The olfactory sensory system is composed of the peripheral olfactory epithelium (OE), where the continually renewing olfactory sensory neurons (OSNs) are located. The axons of the OSNs reach the central nervous system (CNS) via the olfactory nerve (ON), where they make their first synapses in the olfactory bulb (OB) (Sakano 2010; Whitlock 2015). Thus, unlike other sensory systems, the first synapses of the sensory receptor neurons lie within the CNS. This unique organization creates a potential gateway for chemical or biological agents to enter the CNS because the OSNs can be easily damaged, triggering an inflammatory response, and the nasally transmitted substances can cross the cribriform plate, the bony plate that separates the CNS and the olfactory neuroepithelium.

Mucosal barriers are the interfaces between the external world (Air, food etcetera) and the internal world of the animal, and, as a consequence, mucosal barriers are armed with components from the innate and adaptive immune systems. The immune cells and molecules they secrete form the mucosal-associated immune tissues (MALTs) and are essential in mounting a rapid immune response as the first line of defense. In humans, the nasopharyngeal-associated lymphoid tissue (NALT) is the Waldeyer's tonsillar ring, an arrangement of lymphoid tissues (tonsils) in the naso- oropharyngeal cavity that protects us against invasion by neurotropic microorganisms, including viruses. The pharyngeal tonsil, or adenoids, is the lymphatic structure closest to the nasal mucosa, and its equivalent has been found in rat, mouse, and chick (Kiyono and Fukuyama, 2004; Sosa and Roux, 2004; Kang et al., 2013). In contrast, in fish, limited studies suggest the presence of a diffuse and scattered network of lymphoid and myeloid cells in the olfactory organ, resembling mammalian NALT (Tacchi et al., 2014); but also sparse CX3CR1-monocytes (co-expressing MHC-II and CD68) have been observed localized in the olfactory epithelium of adult mouse (Ruitenberg et al., 2008). Despite being

anatomically next to the OE-ON interface, there a few studies (Platt et al., 2020) linking NALT (whether diffuse in the olfactory epithelia or organized in tonsil-like structures) tissues to immune responses in the CNS (Platt et al., 2020; Sepahi et al., 2016).

CNS immune surveillance and recent re-discovery of the meningeal lymphatics

The brain was considered an immune-privileged organ until the recent "re-discovery" of lymphatic vasculature associated with the meninges (which drain metabolic waste & CNS-derived antigens, Aspelund et al., 2015; Louveau et al., 2015), a series of overlapping membranes containing a diverse array of immune cells (Rua & McGavern2018) that contribute actively to not only CNS homeostasis but also to brain immunity. In mammals, resident and circulating myeloid cells can enter the adult CNS via the choroid plexus, the subarachnoid space, and/or the perivascular space (Ransohoff, Kivisäkk, and Kidd, 2003). However, little is known about the immune response in peripheral sensory tissues, such as the olfactory epithelium (OE), and the potential link to CNS surveillance. The olfactory system is unusual because, unlike most other cranial nerves, the meningeal covering of the CNS extends to the peripheral OE, thus the newly described meningeal immunity may play an important role in this part of the peripheral nervous system. To date the identity and motile characteristics of the immune cells that populate and interact with peripheral sensory systems, like the olfactory system, are mostly unknown.

Neutrophils and macrophages in immune defense

The central nervous system and its meningeal coverings are populated by myeloid immune cells, including microglia, perivascular and meningeal macrophages, dendritic cells, and granulocytes (such as neutrophils and mast cells; Herz et al., 2017). Little is known about the role of immune cell function in brain homeostasis, but several studies suggest that there may be non-bone marrow sources of immune cells in the adult brain. Damage to the CNS resulted in an increase in immune cells including microglia, and these cells appeared to arise from a bone marrow-

independent pool of CNS-resident progenitors (Ajami et al., 2007; Herz et al., 2017). Most recently, infection of the brain by Rift Valley Fever virus through aerial inhalation was first observed in the olfactory bulbs followed by the brain stem and spinal cord (Walter et al., 2019), and infection resulted in the recruitment of neutrophils and macrophages, not lymphocytes, in an anterior to posterior movement in the brain (Albe et al., 2019). In these studies it is still unclear whether the numbers of neutrophils and macrophages increased by infiltration from the peripheral circulation, or from a pool of local myeloid cells that change their gene expression and morphology after damage.

Neutrophils are the main type of circulating leukocyte and are widely known as the first line of defense against pathogens (Wittamet et al., 2011). Traditionally, they were thought to be exclusively active in innate immunity, but recently they have been implicated in different adaptive responses *in vivo* and *in vitro* (Puga et al., 2011; Dragana Odobasic, et al. 2016; C.-W.Yang et al. 2010; Rua et al., 2019, Mohanty et al., 2019; Parker Harp et al., 2019). Macrophages are primarily responsible for the phagocytosis of pathogens and cellular debris. Along with neutrophils (Yipp et al., 2017; Herz et al., 2017; Li et al., 2019), macrophages are able to coexist in specialized tissue-specific functions (Epelman et al., 2014; Theret et al., 2019), as well to coordinate adaptive immune responses through T lymphocyte antigen presentation (Li et al., 2019; Hilhorst et al., 2014). In their ontogeny, neutrophils and macrophages constitute a heterogeneous type of phagocytic innate immune cell derived from the myeloid lineage. In both mice and humans, the hematopoietic stem cells of the bone marrow give rise to myeloid progenitors that will generate monocytes including macrophages, neutrophils, dendritic cells, erythrocytes, and megakaryocytes (Wolf et al., 2019). In mammals, circulating neutrophils and macrophages are produced in the bone marrow, whereas microglia (the resident macrophage population in the CNS), originate from mesodermally-derived tissues during embryonic

development and populate the brain (Epelman et al., 2014; Blériot et al., 2020). In contrast, in teleost fish, the hematopoietic stem cells are derived from the intermediate cell mass (ICM), the aorta- gonad mesonephros (AGM) region and caudal hematopoietic tissue (CHT) in successive waves of differentiation with circulating adult neutrophils and macrophages arising from the head kidney and spleen (Orkin and Zon 2008). Originally the CNS was thought to lack immune cells and an inflammatory response in part because the tissue damage would affect the brain; with the re-analysis of the lymphatic vasculature of the brain and meninges it is now important to understand how neutrophils and macrophages infiltrate the CNS in response to damage.

In response to tissue injury and infection, neutrophils and macrophages migrate in coordinated behaviors to the damage site using cues such as damage-associated molecular patterns (DAMPs) and reactive oxygen species (ROS) (Moreira et al., 2010), but also chemokines and leukotrienes (Chen and Nuñez, 2010; Lämmerman and Germain, 2014). Using the circulation, leukocytes, such as neutrophils, can reach distant tissues traveling inside the endothelial lumen of vessels, and then passing to the interstitial tissue through a coordinated multi-step choreography that includes tethering, rolling, adhesion, crawling, and transendothelial migration (McDonald and Kubes, 2011). During chemotactic migration, neutrophils primarily employ fast-speed amoeboid motility, becoming polarized by asymmetrically distributing actin and microtubule networks, while macrophages display characteristics of both amoeboid and lower speed mesenchymal mode of migration (Barros- Becker et al., 2017). The orchestration of adaptive immune responses in vertebrates relies on innate immunity for its initiation. Recently, neutrophils have been shown to transport antigens from the injured tissues in reverse migration (de Oliveira et al., 2016; Christoffersson and Phillipson, 2018) to lymph nodes via High-Endothelial Venules (HEVs), where they can coordinate early adaptive immune responses (Hampton et al. 2015, Hampton and Chtanova 2016). Furthermore, macrophages are highly heterogeneous scavengers

that can also recognize and transport antigens to control the proliferation and differentiation of type 1 and 2 helper T cells (Mills and Ley, 2014).

We have previously performed microarray and RNAseq (Harden et al., 2006; Calfun et al., 2016) analyses using the olfactory epithelia of adult zebrafish looking for differentially expressed genes related to the formation of olfactory memory or imprinting (Harden et al., 2006; Whitlock, 2006). In addition to known genes, such as olfactory receptors (Calfun et al., 2016), we found specific changes in genes from both the innate and adaptive immune systems (Calfun et al., in preparation). Moreover, other labs have previously reported that the OE of both mouse (Chum et al., 1991) and zebrafish (Jessen et al. 2001) express genes from the adaptive immune system such as the recombination activating-gene Rag1/2, which is specifically expressed in lymphocytes for correct immunoglobulin recombination (Mombaerts et al., 1992)

Peripheral sensory systems such as the olfactory epithelium are traditionally thought to lack immune cells (Rasohoff and Brown, 2012; Herz et al., 2017), however the presence of meningeal covering along the olfactory nerve and extending to the olfactory epithelia (Faber, 1937), coupled with the localization of myeloid cells in organized or diffuse NALT in the olfactory epithelium of mice, rat, and rainbow trout (Kiyono and Fukuyama, 2004; Sosa and Roux, 2004; Kang et al., 2013; Ruitenberg et al., 2008; Tacchi et al., 2014) suggests that there are immune cells associated with the olfactory sensory system. Furthermore, the infiltration of immune cells in an anterior-posterior appearance (from the olfactory bulb to the spinal cord) in response to viral infection of the brain suggests that the olfactory sensory system may be a source of immune cells in the CNS. Because the olfactory sensory system is exposed to the external environment with direct connections to the CNS, it may have a robust immune response associated with an extensive immune architecture in both the developing and the adult animal.

For my thesis work, I used the zebrafish, *Danio rerio,* as a model organism to describe the localization of neutrophils and macrophages in the developing and adult olfactory sensory system. I then analyzed the dynamics of immune cell movement in response to copper-induced death of olfactory sensory neurons in the developing and adult olfactory system. Concurrently, I described the structure of the blood and lymphatic vasculature in the olfactory sensory system of developing and adult zebrafish. Finally, using a genetically encoded calcium indicator expressed in neurons, I showed that large calcium transients generated by copper-induced damage trigger immune cell recruitment to the developing olfactory sensory system, and that attenuation of these calcium transients blocks immune cell recruitment.

References

Ajami, Bahareh, et al. “Local Self-Renewal Can Sustain CNS Microglia Maintenance and Function throughout Adult Life.” *Nature Neuroscience*, vol. 10, no. 12, 2007, pp. 1538–43, doi:10.1038/nn2014.

Albe, Joseph R., et al. “Neutrophil and Macrophage Influx into the Central Nervous System Are Inflammatory Components of Lethal Rift Valley Fever Encephalitis in Rats.” *PLoS Pathogens*, vol. 15, no. 6, 2019, pp. 1–26, doi:10.1371/journal.ppat.1007833.

Aspelund, Aleksanteri, et al. “A Dural Lymphatic Vascular System That Drains Brain Interstitial Fluid and Macromolecules.” *Journal of Experimental Medicine*, vol. 212, no. 7, 2015, pp. 991–99, doi:10.1084/jem.20142290.

Barros-Becker, Francisco, et al. “Live Imaging Reveals Distinct Modes of Neutrophil and Macrophage Migration within Interstitial Tissues.” *Journal of Cell Science*, vol. 130, no. 22, 2017, pp. 3801–08, doi:10.1242/jcs.206128.

Blériot, Camille, et al. “Determinants of Resident Tissue Macrophage Identity and Function.” *Immunity*, vol. 52, no. 6, June 2020, pp. 957–70, doi:10.1016/j.immuni.2020.05.014.

Calfún, Cristian, et al. “Changes in Olfactory Receptor Expression Are Correlated With Odor Exposure During Early Development in the Zebrafish (Danio Rerio).” *Chemical Senses*, vol. 00, 2016, p. bjw002, doi:10.1093/chemse/bjw002.

Chen, Grace Y., and Gabriel Nuñez. “Sterile Inflammation: Sensing and Reacting to Damage.” *Nature Reviews Immunology*, vol. 10, no. 12, Nature Publishing Group, 2010, pp. 826–37, doi:10.1038/nri2873.

Christoffersson, Gustaf, and Mia Phillipson. “The Neutrophil: One Cell on Many Missions or Many Cells with Different Agendas?” *Cell and Tissue Research*, vol. 371, no. 3, Cell and

Tissue Research, 2018, pp. 415–23, doi:10.1007/s00441-017-2780-z.

Chun, Jerold J. M., et al. “The Recombination Activating Gene-1 (RAG-1) Transcript Is Present in the Murine Central Nervous System.” *Cell*, vol. 64, no. 1, 1991, pp. 189–200, doi:10.1016/0092-8674(91)90220-S.

Epelman, Slava, et al. “Origin and Functions of Tissue Macrophages.” *Immunity*, vol. 41, no. 1, Elsevier Inc., 2014, pp. 21–35, doi:10.1016/j.immuni.2014.06.013.

Faber, William M. “The Nasal Mucosa and the Subarachnoid Space.” *American Journal of Anatomy*, vol. 62, no. 1, 1937, pp. 121–48, doi:10.1002/aja.1000620106.

Hampton, Henry R., et al. “Microbe-Dependent Lymphatic Migration of Neutrophils Modulates Lymphocyte Proliferation in Lymph Nodes.” *Nature Communications*, vol. 6, no. May, Nature Publishing Group, 2015, pp. 1–11, doi:10.1038/ncomms8139.

Hampton, Henry R., and Tatyana Chtanova. “The Lymph Node Neutrophil.” *Seminars in Immunology*, vol. 28, no. 2, Elsevier Ltd, 2016, pp. 129–36, doi:10.1016/j.smim.2016.03.008.

Harden, Maegan V., et al. “Olfactory Imprinting Is Correlated with Changes in Gene Expression in the Olfactory Epithelia of the Zebrafish.” *Journal of Neurobiology*, vol. 66, no. 13, Nov. 2006, pp. 1452–66, doi:10.1002/neu.20328.

Herz, Jasmin, et al. “Myeloid Cells in the Central Nervous System.” *Immunity*, vol. 46, no. 6, Elsevier Inc., 2017, pp. 943–56, doi:10.1016/j.immuni.2017.06.007.

Hilhorst, Marc, et al. “T Cellâ€“Macrophage Interactions and Granuloma Formation in Vasculitis.” *Frontiers in Immunology*, vol. 5, Sept. 2014, doi:10.3389/fimmu.2014.00432.

Kang, Haihong, et al. “Characteristics of Nasal-Associated Lymphoid Tissue (NALT) and Nasal Absorption Capacity in Chicken.” *PLoS ONE*, vol. 8, no. 12, 2013, doi:10.1371/journal.pone.0084097.

Kiyono, Hiroshi, and Satoshi Fukuyama. “Nalt-versus Peyer’s-Patch-Mediated Mucosal

Immunity." *Nature Reviews Immunology*, vol. 4, no. 9, 2004, pp. 699–710, doi:10.1038/nri1439.

Lämmermann, Tim, and Ronald N. Germain. "The Multiple Faces of Leukocyte Interstitial Migration." *Seminars in Immunopathology*, vol. 36, no. 2, 2014, pp. 227–51, doi:10.1007/s00281-014-0418-8.

Li, Yang, et al. "The Regulatory Roles of Neutrophils in Adaptive Immunity." *Cell Communication and Signaling*, vol. 17, no. 1, Cell Communication and Signaling, 2019, pp. 1–11, doi:10.1186/s12964-019-0471-y.

Louveau, Antoine, et al. "Structural and Functional Features of Central Nervous System Lymphatic Vessels." *Nature*, vol. 523, no. 7560, July 2015, pp. 337–41, doi:10.1038/nature14432.

McDonald, Braedon, and Paul Kubes. "Cellular and Molecular Choreography of Neutrophil Recruitment to Sites of Sterile Inflammation." *Journal of Molecular Medicine*, vol. 89, no. 11, 2011, pp. 1079–88, doi:10.1007/s00109-011-0784-9.

Mills, Charles D., and Klaus Ley. "M1 and M2 Macrophages: The Chicken and the Egg of Immunity." *Journal of Innate Immunity*, vol. 6, no. 6, 2014, pp. 716–26, doi:10.1159/000364945.

Mohanty, Tirthankar, et al. "Neutrophil Extracellular Traps in the Central Nervous System Hinder Bacterial Clearance during Pneumococcal Meningitis." *Nature Communications*, vol. 10, no. 1, Springer US, 2019, doi:10.1038/s41467-019-09040-0.

Mombaerts, Peter, et al. "RAG-1-Deficient Mice Have No Mature B and T Lymphocytes." *Cell*, vol. 68, no. 5, Mar. 1992, pp. 869–77, doi:10.1016/0092-8674(92)90030-G.

Moreira, Severina, et al. "Prioritization of Competing Damage and Developmental Signals by Migrating Macrophages in the Drosophila Embryo." *Current Biology*, vol. 20, no. 5, Elsevier Ltd, Mar. 2010, pp. 464–70, doi:10.1016/j.cub.2010.01.047.

Odobasic, Dragana, et al. “Neutrophil-Mediated Regulation of Innate and Adaptive Immunity: The Role of Myeloperoxidase.” *Journal of Immunology Research*, vol. 2016, 2016, doi:10.1155/2016/2349817.

Oliver, Guillermo, and Mark L. Kahn Editors. *Lymphangiogenesis*. Edited by Guillermo Oliver and Mark L. Kahn, vol. 1846, Springer New York, 2018, doi:10.1007/978-1-4939-8712-2.

Orkin, Stuart H., and Leonard I. Zon. “Hematopoiesis: An Evolving Paradigm for Stem Cell Biology.” *Cell*, vol. 132, no. 4, 2008, pp. 631–44, doi:10.1016/j.cell.2008.01.025.

Parker Harp, Chelsea R., et al. “Neutrophils Promote VLA-4–Dependent B Cell Antigen Presentation and Accumulation within the Meninges during Neuroinflammation.” *Proceedings of the National Academy of Sciences of the United States of America*, vol. 116, no. 48, 2019, pp. 24221–30, doi:10.1073/pnas.1909098116.

Platt, Maryann P., et al. “Th17 Lymphocytes Drive Vascular and Neuronal Deficits in a Mouse Model of Postinfectious Autoimmune Encephalitis.” *Proceedings of the National Academy of Sciences of the United States of America*, vol. 117, no. 12, 2020, pp. 6708–16, doi:10.1073/pnas.1911097117.

Puga, Irene, et al. “B Cell-Helper Neutrophils Stimulate the Diversification and Production of Immunoglobulin in the Marginal Zone of the Spleen.” *Nature Immunology*, vol. 13, no. 2, 2012, pp. 170–80, doi:10.1038/ni.2194.

Ransohoff, Richard M., et al. “Three or More Routes for Leukocyte Migration into the Central Nervous System.” *Nature Reviews Immunology*, vol. 3, no. 7, July 2003, pp. 569–81, doi:10.1038/nri1130.

Ransohoff, Richard M., and Melissa A. Brown. “Review Series Innate Immunity in the Central Nervous System.” *The Journal of Clinical Investigation*, vol. 122, no. 4, 2012, pp. 1164–71, doi:10.1172/JCI58644.1164.

Rua, Rejane, et al. “Infection Drives Meningeal Engraftment by Inflammatory Monocytes That

Impairs CNS Immunity." *Nature Immunology*, vol. 20, no. 4, Springer US, 2019, pp. 407–19, doi:10.1038/s41590-019-0344-y.

Rua, Rejane, and Dorian B. McGavern. "Advances in Meningeal Immunity." *Trends in Molecular Medicine*, vol. 24, no. 6, Elsevier Ltd, 2018, pp. 542–59, doi:10.1016/j.molmed.2018.04.003.

Ruitenberg, Marc J., et al. "CX3CL1/Fractalkine Regulates Branching and Migration of Monocyte-Derived Cells in the Mouse Olfactory Epithelium." *Journal of Neuroimmunology*, vol. 205, no. 1–2, Elsevier B.V., 2008, pp. 80–85, doi:10.1016/j.jneuroim.2008.09.010.

Sakano, Hitoshi. "Neural Map Formation in the Mouse Olfactory System." *Neuron*, vol. 67, no. 4, Elsevier Inc., 2010, pp. 530–42, doi:10.1016/j.neuron.2010.07.003.

Sosa, Gustavo A., and María E. Roux. "Development of T Lymphocytes in the Nasal-Associated Lymphoid Tissue (NALT) from Growing Wistar Rats." *Clinical and Developmental Immunology*, vol. 11, no. 1, 2004, pp. 29–34, doi:10.1080/10446670410001670463.

Tacchi, Luca, et al. "Nasal Immunity Is an Ancient Arm of the Mucosal Immune System of Vertebrates." *Nature Communications*, vol. 5, no. May, Nature Publishing Group, Oct. 2014, p. 5205, doi:10.1038/ncomms6205.

Theret, Marine, et al. "The Origins and Non-Canonical Functions of Macrophages in Development and Regeneration." *Development (Cambridge)*, vol. 146, no. 9, 2019, pp. 1–14, doi:10.1242/dev.156000.

Walters, Aaron W., et al. "Vascular Permeability in the Brain Is a Late Pathogenic Event during Rift Valley Fever Virus Encephalitis in Rats." *Virology*, vol. 526, no. August 2018, Elsevier Inc., Jan. 2019, pp. 173–79, doi:10.1016/j.virol.2018.10.021.

Whitlock, Kathleen E. "The Loss of Scents: Do Defects in Olfactory Sensory Neuron Development Underlie Human Disease?" *Birth Defects Research Part C - Embryo Today:*

Reviews, vol. 105, no. 2, 2015, pp. 114–25, doi:10.1002/bdrc.21094.

Whitlock, Kathleen E. *The Sense of Scents : Olfactory Behaviors in the Zebrafish*. Vol. 3, no. 2, 2006.

Wittamer, Valerie, et al. "Characterization of the Mononuclear Phagocyte System in Zebrafish." *Blood*, vol. 117, no. 26, June 2011, pp. 7126–35, doi:10.1182/blood-2010-11-321448.

Wolf, Anja A., et al. "The Ontogeny of Monocyte Subsets." *Frontiers in Immunology*, vol. 10, no. JULY, 2019, doi:10.3389/fimmu.2019.01642.

Yang, Chiao-Wen, et al. "Neutrophils Influence the Level of Antigen Presentation during the Immune Response to Protein Antigens in Adjuvants." *The Journal of Immunology*, vol. 185, no. 5, 2010, pp. 2927–34, doi:10.4049/jimmunol.1001289.

Yipp, Bryan G., et al. "The Lung Is a Host Defense Niche for Immediate Neutrophil-Mediated Vascular Protection." *Science Immunology*, vol. 2, no. 10, 2017, pp. 1–14, doi:10.1126/sciimmunol.aam8929.

CHAPTER 2: THE OLFACTORY ORGAN IS POPULATED BY NEUTROPHILS AND MACROPHAGES DURING EARLY DEVELOPMENT

The olfactory organ is populated by neutrophils and macrophages during early development

M. Fernanda Palominos and Kathleen E. Whitlock

Centro Interdisciplinario de Neurociencia de Valparaíso (CINV)

Facultad de Ciencia

Universidad de Valparaíso

Pasaje Harrington 287

Valparaíso, Chile

Teléfono: 56-32-299-5510, 56-32-250-8040

FAX: 56-32-250-8027

Correspondence to be sent to: Kathleen Whitlock

Instituto de Neurociencia, Universidad de Valparaíso, Valparaíso, Chile

e-mail: kathleen.whitlock@uv.cl

Key words: immune, macrophage, olfactory, neuron, vasculature, zebrafish, microglia, nervous system

Worked published on 18 January of 2021 in:

Frontiers in Cell and Developmental Biology

DOI:10.3389/fcell.2020.604030

Abstract

The immune system of vertebrates is characterized by innate and adaptive immunity that function together to form the natural defense system of the organism. During development innate immunity is the first to become functional and is mediated primarily by phagocytic cells, including macrophages, neutrophils, and dendritic cells. In the olfactory sensory system, the same sensory neurons in contact with the external environment have their first synapse within the central nervous system. This unique architecture presents a potential gateway for the entry of damaging or infectious agents to the nervous system. Here we used zebrafish as a model system to examine the development of the olfactory organ and to determine whether it shares immune characteristics of a host defense niche described in other tissues. During early development both neutrophils and macrophages appear coincident with the generation of the primitive immune cells. The appearance of neutrophils and macrophages in the olfactory organs occurs as the blood and lymphatic vascular system is forming in the same region. Making use of the neurogenic properties of the olfactory organ we show that damage to the olfactory sensory neurons in larval zebrafish triggers a rapid immune response by local and non-local neutrophils. In contrast macrophages, though present in greater numbers, mount a slower response to damage. We anticipate our findings will open new avenues of research into the role of the olfactory-immune response during normal neurogenesis and damage-induced regeneration, and contribute to our understanding of the formation of a potential host defense immune niche in the peripheral nervous system.

Introduction

The olfactory sensory system is composed of the peripheral olfactory epithelium (OE), where the continually renewing olfactory sensory neurons (OSNs) are located. The axons of the OSNs reach the central nervous system (CNS) via the olfactory nerve (ON), where they make their first synapses in the olfactory bulb (OB) [1];[2]. Thus, unlike other sensory systems the first synapses of the OSNs lie within the CNS. This unique organization creates a potential pathway for chemical or biological agents to enter the CNS. Yet, although pathogens can enter the CNS via the olfactory epithelium [3], it is striking that our brains are not besieged by infections that enter through this direct olfactory portal.

Recently it has been shown that in mammals "host defense niches" exist where myeloid cell types, such as neutrophils, remain associated with the tissue instead of patrolling the body [4]. These resident cells have been described in the lungs, a tissue that like the olfactory epithelia come in contact with potential damaging airborne substances. In mammals the airways of the nose and mouth have a network of lymphoid tissue in the pharynx and palate (tonsils), called nasopharynx-associated lymphoid tissue (NALT) that protect against invasion by neurotropic microorganisms, including viruses. Like mammals, zebrafish have the basic myeloid cell types including monocytes, neutrophils, eosinophils, mast cells and dendritic cells, yet they do not have organized lymphoid structures such as tonsils/lymph nodes. Limited studies suggest that fish have a diffuse network of lymphoid and myeloid cells associated with the olfactory organ that may resemble mucosal immune tissues [5].

Similar to mammals zebrafish generate blood/immune cells in successive waves during development. In zebrafish, during the first phase of hematopoiesis precursors arise from the mesoderm generating the rostral blood island (RBI) and intermediate cell mass (ICM) before entering the circulation [6]. Myeloid cell precursors including monocytes/macrophages and

granulocytes develop by 12 hours post fertilization (hpf) [7] and functional macrophages and neutrophils are present by 30 hpf [8; 9]. The RBI will also give rise to larval microglia via primitive macrophages [8; 10; 11]. The larval zebrafish has been used to study immune system development and function due to the optical clarity, availability of reporter lines expressed in immune cell types, and sequenced genome [12; 13; 14]. Because of the regenerative properties of fish, in tissues such as the tail and fins, zebrafish are readily amenable to wounding studies (induced by cutting the tail for example) where the response of the innate immune system can be visualized and manipulated in intact living animals [15]. Here we make use of the peripheral olfactory sensory system to explore the early development of immune cells types and their potential association with the olfactory organ.

Previously, through microarray and RNAseq analyses of adult OE zebrafish [16] [17], we found that in addition to OE specific genes, genes normally expressed in both the innate and the adaptive immune systems were also expressed. These findings prompted us to investigate the potential "immune architecture" of the OE. Because of the early development of innate immune system [18], we investigated the presence and dynamics of neutrophils and macrophages in the olfactory sensory system of developing zebrafish to better characterize the immune cells as well as understand their potential response to damage in the developing olfactory organ.

Materials and Methods

Animals: Zebrafish were maintained in a re-circulating system (Aquatic Habitats Inc, Apopka, FL) at 28°C on a light-dark cycle of 14 and 10 hours respectively. All fish were maintained in the Whitlock Fish Facility at the Universidad de Valparaiso. Wild-type (WT) fish of the Cornell strain (derived from Oregon AB) were used. All protocols and procedures employed were reviewed and approved by the Institutional Committee of Bioethics for Research with Experimental Animals, University of Valparaiso (#BA084-2016). Embryos were obtained from natural spawnings in laboratory conditions and raised at 28.5°C in Embryo medium as previously described [19]. Staging was done according to Kimmel [20]. At 5 dpf larvae were transferred to finger bowls, and fed daily with Larval AP100 dry diet (Zeigler ®) until processed. Larvae were defined as ranging from 3 to 14 dpf; and 21 dpf animals were considered as juveniles. Transgenic lines were used to visualize specific cell types. *Tg(BACmpx:gfp)i114*, *Tg(mpx:GFP) Tg(mpx:EGFP),* [12]; (Tg(fli1a:EGFP)y1, Tg(fli1a:EGFP), [21]; *Tg(−5.2lyve1b:DsRed)*^{nz101}, *Tg(2lyve1b:DsRed) Tg(−5.2lyve1b:EGFP)*^{nz151} *Tg(lyve1b:EGFP)*, [22]; *Tg(gata1a:DsRed)*^{sd2}, *Tg(gata1a:DsRed)* [23]; *Tg(pOMP2k:gap-YFP)*^{rw032a}, *(OMP:YFP)*, *Tg(pOMP2k:lyn-mRFP)*^{rw035a}, *Tg(OMP:RFP*), *Tg(pTRPC4.5k:gap-Venus)*^{rw037a} [24]; *Tg(mpeg1:mCherry)* [25]; and *Tg(lysC:DsRED2),* [14].

Copper Exposure: Initial dose response analysis was performed based on previous work in zebrafish and salmon [26]; [27]. A stock solution of 10 mM $CuSO_4$ was diluted in filtered embryo medium [19] for a final concentration of 10 μM $CuSO_4$. Staged larvae were exposed to 10 μM $CuSO_4$ for 4 hours and then washed out. The long-term effects of copper on neutrophil movement to the OO were quantified in individual larvae using adapted ChIn assay [28].

Immunocytochemistry and Cell Labeling: Staged larvae were fixed in 4% PFA in 0.1M phosphate buffer, pH 7.3, or 1X phosphate-buffered saline PBS pH 7.3. Larvae were rinsed three times in phosphate buffer or PBS, permeabilized in acetone at -20 ºC for 10 minutes then incubated for two hours in blocking solution (10 mg/ml BSA, 1% DMSO, 0.5% Triton X-100 (Sigma) and 4% normal goat serum in 0.1M phosphate buffer or 1X PBS). Primary antibodies used were anti-RFP (rabbit 1:250, Life Technologies), anti-GFP (mouse 1:500, Life Technologies), anti-GFP (rabbit 1:500, Invitrogen), anti-SOX2 (mouse 1:250, Abcam), anti-DsRed (mouse 1:500, Santa Cruz Biotechnology) and anti-HuC/D (rabbit 1:500, Invitrogen). Larvae up to 14 days were incubated in primary antibodies for 3-4 days. After washes, tissues were incubated overnight in any of the following secondary antibodies as appropriate: Dylight 488 conjugated anti-mouse antibody (goat 1:500, Jackson Immuno Research), Alexa Fluor 488 conjugated anti-rabbit antibody (goat 1:1000, Molecular Probes), Alexa Fluor 568 conjugated anti-rabbit antibody (goat 1:1000, Molecular Probes), Alexa Fluor 568 conjugated anti-mouse antibody (goat 1:1000, Molecular Probes), Dylight 650 conjugated anti-rabbit antibody (goat 1:500, Jackson Immuno Research). Tissues were then rinsed in 0.1M phosphate buffer or 1X PBS with 1% DMSO, stained for DAPI (1 µg/ml, Sigma), washed in 0.1M phosphate buffer or 1X PBS and mounted in 1.5 % low melting temperature agarose (Sigma) in an Attofluor Chamber for subsequent imaging (see below).

Cryosectioning. 7 dpf larvae were sacrificed, then fixed and embedded in 5% sucrose/ 1.5 % agarose in mqH_2O. Blocks were then submerged in 30% sucrose for 2-3 days and then stored covered by O.C.T. Compound (Tissue-Tek®) in cryomolds at -20ºC. Twenty-five µm cryosections were processed for immunofluorescense as described above; primary and secondary antibodies were incubated overnight.

TUNEL Labeling: Larvae were processed using *In Situ* Cell Death Detection Kit, Fluorescein (Roche) according manufacturer recommendations. Briefly, larvae were permeabilized for 1

hour at 37 ºC, washed twice and labeled at the same temperature for 1 hour. DAPI staining was used for nuclear labeling. Larvae were mounted in 2% low melting temperature agarose (Sigma) in an Attofluor Chamber for imaging (see below). Fluorescent signals in TUNEL labeled preparations were quantified by mean pixel intensities from green (fluorescein from TUNEL staining), green (GFP from *trpc2:GFP*) and red (RFP from *OMP:RFP*) in OE and OB (selected as different ROIs in FIJI). Values were normalized by mean pixel intensity of the DAPI stained whole head (as another ROI).

Microscopy: Fluorescent images were acquired using a Spinning Disc microscope Olympus BX-DSU (Olympus Corporation, Shinjuku-ku, Tokyo, Japan) with ORCA IR2 Hamamatsu camera (Hamamatsu Photonics, Higashi-ku, Hamamatsu City, Japan) and Olympus CellR software (Olympus Soft Imaging Solutions, Munich, Germany) or confocal laser scanning microscope (Nikon C1 Plus; Nikon, Tokyo, Japan). Images were deconvoluted in AutoQuantX 2.2.2 (Media Cybernetics, Bethesda, MD, USA) and processed using FIJI (National Institute of Health, Bethesda, Maryland, USA; [29] and CellProfiler [30].

Live imaging: For live imaging of the olfactory sensory system, larvae were anesthetized (2% Tricaine Sigma) mounted in a cut tip of plastic Pasteur pipette in 2% low temperature agarose (Sigma) in embryo medium [19]. The larvae were imaged in frontal view in an Attofluor Chamber (Thermo Fisher Scientific) filled with Embryo medium. The agarose covering the olfactory system was removed. Temperature was maintained at 26-28ºC and images were captured using a Spinning disc confocal microscope (Olympus) with a 20X 0.95 NA water immersion LUMPlanFL/IR objective.

Time-lapse videos of copper exposure: To generate the time-lapse movies (Fig. 5, 6, 8, 9), stacks of images were collected with 3um/optical sections in a total depth of 150 um depth. All tracking data from time-lapse microscopy in control and copper-exposed larvae were processed using MTrackJ tracker in FIJI. Chemotactic index (CI) was calculated as described by [31], taking left

or right OO as reference. Briefly, CI was defined as cos(α) with α as the angle between the distance vector to the damage site (OO) and the actual movement vector.

Image Analyses For analysis of neutrophils and macrophages: Only cells within the boundaries of the sensory tissue in were counted and the values were given as the average of total number of mpx:GFP positive or mpeg1:mCh positive in both OOs with standard deviation. Values given for paired sensory structure are a sum of the individual sensory tissues. For time-lapse videos all counts of neutrophils and macrophages in the two olfactory organs were combined for each animal and the mean/SEM calculated for each time point.

Statistics. Data are presented as means ± standard deviations. Experiments number and statistical analysis were done using Prism 6 (Graphpad), and are indicated in each figure legend. Unpaired Student's t-tests were performed unless otherwise indicated. P values are indicated as follows: *: $P < 0.05$, **: $P < 0.01$, ***: $P < 0.001$, ****: $P < 0.0001$.

Acknowledgements

We thank A. Moscoso, T. Ordenes and S. Alanis for care of the zebrafish, especially with the difficulties brought on by the pandemic. Funding: Fondo Nacional de Desarrollo Científico y Tecnológico (FONDECYT) 1160076 (KEW); Centro Interdisciplinario de Neurociencia de Valparaíso (CINV) ICM ANID Millennium Institute project code ICN09-022, CINV (KEW) and Graduate Fellowship (CONICYT) 21161437 (MFP).

Results

Phagocytic cell populations in the developing olfactory organ

We first quantified phagocytic cells (neutrophils and macrophages) of the immune system to determine whether they were present in peripheral sensory systems during early development. We used the *Tg(mpx:GFP)* line to visualize neutrophils, a leukocyte sub-type with strong myeloperoxidase (mpx) activity, and the *Tg(mpeg1:mCh)* line (macrophage-expressed gene, *mpeg1.1*, encodes perforin-2, a pore-forming protein associated with host defense against pathogens) to visualize macrophages in fixed wholemount larvae (Fig. 1). Olfactory sensory structures do not appear as a stratified epithelium until later in development thus we refer to the tissue as an olfactory organ (OO, Fig. 1A, E). At 7 days post fertilization (dpf) mpx:GFP+ neutrophils were found associated with the OOs (Fig. 1, B, green, arrows) and anti-Sox2 positive taste buds (Fig. 1, B, arrowheads). In contrast few neutrophils were directly associated with the ear (Fig. 1, C, green). When quantifying neutrophils in the developing sensory systems (Fig. 1, D) the olfactory sensory system has more neutrophils than other sensory systems (n=30 animals per sensory system, 1-way ANOVA, Tukey test, $p < 0.05$). No neutrophils were observed in the retina. In contrast to neutrophils, at 7 dpf there were many more macrophages in the OOs (Fig. 1, F), but not in the ear (Fig. 1, G). Unlike the situation with neutrophils, the OO and eye had equal numbers of macrophages (Fig. 1, H) yet the gustatory (mouth) and auditory (ear) number remained lower (n=30 animals per sensory system, 1-way ANOVA, Tukey test, $p < 0.05$).

We next quantified the number of mpx:GFP+ neutrophils (Fig. 2, A-C) and mpeg1:mCh+ macrophages (Fig. 2, D-F) associated with the OOs during early development. At 3 dpf neutrophils started to appear associated with the OOs (Fig. 2, C; 1.4 ± 0.1) and by 7 dpf (Fig. 2, A, B, green) there was an average of 3.6 ± 0.2 (Fig. 2, C), and neutrophil numbers increased steadily through the first two weeks (Fig. 2, C; 6.0 ± 0.3). Like neutrophils, at 3 dpf macrophages started to appear associated with the OOs (Fig. 2, F; 1,1 ± 0.1) and by 7 dpf (Fig.

2, D, D', E, red) there was an average of 8.2 ± 0.2 macrophages (Fig. 2, F). Macrophage numbers increased steadily through the first two weeks (Fig. 2, F, 11 ± 0.4).

Blood-Lymphatic system in the developing olfactory organ

Recently the lymphatic vasculature (LV) of the zebrafish brain has been described [32]; [33] [34], but little is known about the developing blood vasculature (BV) and LV associated with the olfactory sensory system. Using the *Tg(lyve1b:DsRed);Tg(OMP:YFP)* double transgenic line at 5 dpf we found LV on the dorsal-lateral surface of the telencephalon (Fig. 3, A, red, arrows) extending around the region of the forming OB. By 7 dpf the LV encircled the olfactory bulb region (Fig. 3, B, OB) where the axons of the olfactory sensory neurons (OSNs) terminate (Fig. 3, B, asterisks, yellow). At two weeks post fertilization the dorsal projections were maintained (Fig. 3, C, red, arrows) and lyve1b:DsRed+ branches were apparent on the ventral side of the OOs (Fig. 3, C, red, arrowheads, G, G', NL). We visualized the development of BV using the *Tg(fli1a:EGFP)* line *(*Fig 3, D-F, G, G', green). At 5 dpf the BV was already apparent on the dorsal surface of the brain and was found associated with the OOs before the LV. The nasal artery/nasal veins (NA/NV) [35] are the most rostrally-projecting of vessels until at least 7 dpf, with two branches enclosing the OO at 15 dpf (Fig. 3, F, G, G', yellow), a time when the ventral-lateral branch of the LV can be seen entering the OO (Fig. 3, C, red, arrowhead, G', NL, red). The nuclei of the NV wrapping along the medial OO (Fig. 3, D-F, G', green) are positive for both the LV (lyve1b:DsRed) and the BV marker *(*fli1a:EGFP), suggesting it is venous–lymphoid in nature. The later developing LV entering the ventral lateral region of the OO (NL in Fig. 3, F, G', red) expressed only lyve1b:DsRed suggesting it is differentiated LV.

Responses of neutrophils and macrophages to tissue damage in the OO

Previously it has been shown that copper exposure at concentrations ranging from 10^{-9} to 10^{-5} M [36] damages the olfactory sensory epithelia of zebrafish and that the unique neurogenic

characteristics of the OE allow for the replacement of the olfactory sensory neurons [37]. In order to confirm that copper caused cell death in the developing OO, 5 dpf larvae were exposed to 10 μM $CuSO_4$ (Fig. 4) and processed for TUNEL labeling (Fig. 4, A-C). At 5 dpf whole-mount control fish showed no cell death (Fig. 4, A). After exposure to 10 μM $CuSO_4$ only the OOs were positive for TUNEL (Fig. 4, B, green, arrows). Quantification of TUNEL fluorescence in control and treated animals showed a statistically significant increase in fluorescence in the OOs of copper treated animals (Fig. 4, C).

The olfactory sensory system has several sensory cell types and the *Tg(OMP:RFP)* reporter line is expressed only in ciliated OSNs, the most abundant sensory neuron type in the OO. Because differential sensitivity has been reported for ciliated and microvillous OSNs we visualized the microvillous OSNs using the *Tg(trpc2:GFP)* line combined with *Tg(lysc:DsRed)* to visualize neutrophils in red (Fig. 4, D, E). Quantification of pixel intensity changes for Trpc2:GFP+ fluorescence confirmed that, unlike ciliated OSNs (see Fig. 5), microvillous OSNs were largely unaffected by copper exposure (Fig. 4, D, E, green; F, grey bar). For all experiments (Fig. 4, D, E) 25 larvae were processed and examined (control and copper-exposed). Of these, 3 different animals were analyzed from each treatment group. These results confirm that the damage caused by copper exposure is consistent and comparable with previous studies in zebrafish [37].

In vivo neutrophil response to cell damage

To confirm whether copper induced damage affected the ciliated olfactory sensory neurons (OSNs) and triggered a neutrophil response, we exposed 5 dpf *Tg(mpx:GFP);Tg(OMP:RFP*) to copper (Fig. 5, A-A'', OSNs: red, neutrophils: green) and assayed the changes in fluorescence in the OSNs (Fig. 5, B). After 4 hrs of copper exposure neutrophils were found in the OO (Fig. 5, A', green) and the OSNs degenerated as evidenced by loss of OMP:RFP fluorescence (Fig. 5, A', red). Quantification of pixel intensity changes in OMP:RFP+ fluorescence confirmed that OSNs degenerated when scored immediately after copper exposure (Fig. 5, B, red bar). When

scored at twenty-four hours after exposure (Fig. 5, B, green bar) and forty-eight hours after exposure a steady increase in OMP:RFP fluorescence was observed where OSN fluorescence in the OB returned to pre-copper exposure levels (control, Fig. 5, A), indicating the OSNs had recovered (Fig. 5, C, blue bar). Analyses were performed both in the OO where the cell bodies of the OSNs are located and in the OB where the axons form their terminations (Fig. 5, A, arrows; B, asterisks, respectively).

To better understand the dynamics of neutrophil response to OSN damage in the OO we performed time lapse imaging in whole-mount preparations using a *Tg(OMP:RFP):Tg(mpx:GFP)* double transgenic line to visualize OSNs (Fig. 5, C-C‘’’; red) and neutrophils *in vivo* (Fig. 5, C-C’’’; green; Supplementary Video 1). Before copper exposure, local neutrophils (defined as those associated with the OO prior to initiating the time lapse; Fig. 5, C, green) were associated with the OSNs at the margins of the OO (Fig. 5, C, red, asterisk indicates boxed area). During copper exposure local neutrophils were associated with the OO (Fig. 5, C’, arrow) and olfactory nerve (Fig. 5, C’, arrowhead, asterisk indicates boxed area). Subsequently, neutrophils in the OO (Fig. 5, C, asterisk indicates boxed area) were joined by neutrophils associated with the axons of OSNs in the OB (Fig. 5, C’’’, asterisk indicates boxed area), and by patrolling non-local neutrophils (Fig. 5, C’’’, arrows) in an apparent “swarming behavior” (Supplementary Video 1).

Analysis of the 2D path of individual neutrophils showed that copper exposure triggered the migration of non-local neutrophils from the dorsal and ventral sides of the head (Fig. 5, C’’’, D’-D’’’, arrows), and these entered the OO and OB regions via pathways separate from the olfactory nerve (Fig. 5, C’’’, arrows). During the time of copper exposure (4 hours) the number of neutrophils increased from a pre-exposure average of 5.2 ± 1.7 to 15.0 ± 2.4 (Fig. 5, E, data from analysis of 6 different time lapse videos). The mean speed of neutrophils after copper exposure increased from a pre-exposure velocity of 7.1 ± 0.2 μm/min, to a post exposure

velocity of 7.8 ± 0.1μm/min (Fig. 5, F, n=30 neutrophils; 1 representative video). Both velocities were in the range of the reported 11 μm/min for randomly migrating neutrophils in the ventral region of the head of 3 dpf zebrafish larvae [38]. Analysis of the chemotactic index (Fig. 5, G) showed a significant increase in orientation towards the OO [CI of - 0.05 (range: -0.21 to 0.15) to 0.24 (from -0.33 to 0.78)] but with a separation of groups, reflecting different patterns of movement of local neutrophils, which moved within the OO, vs. those of non-local populations, which appeared to circulate in and out of the OO region (Fig. 5, D'-D''', arrows, G, red). The number of neutrophils in the OOs remained elevated in the continued presence of copper (9.8 ± 1.9) and decreased after wash-out (Fig. 5, H). A second increase is seen twenty-four hours after copper treatment (8.1 ± 1.9; *n*=48), which may be associated with the replacement of ciliated OSNs (Fig. 5, A-A'', B), which have a life-long program of cell renewal that is distinct from damage-induced regeneration. The number of neutrophils then returned to baseline at the end of the second day post exposure (Fig. 5, H) a time when the OSNs have recovered (Fig. 5, B). Thus, consistent with previous reports, in juvenile zebrafish damage triggers a rapid mobilization of neutrophils, and chemotaxis contributes to the migration of neutrophils to the site of damage [13], which also correlates with the time course of neuronal regeneration.

Macrophage response to cell damage

To better understand the dynamics of the macrophage response to OSN damage in the OO we performed time lapse imaging in whole-mount preparations using a *Tg(mpeg1:mCh);Tg*(*OMP:RFP)* double transgenic line to visualize macrophages (Fig. 6, A-A''; red) and OSNs (Fig. 6, A-A'''; green; Supplementary Video 2). Before copper exposure, an extensive population of macrophages was found both associated with the OO (Fig. 6, A, green) as well as extending dorsal and ventral to the OOs (Fig. 6, A, red). In contrast to neutrophil migration induced during copper exposure, macrophages were closely associated with the OO (Fig. 6, A, arrows) and olfactory nerve (Fig. 6, A). During copper exposure macrophages in the

OOs (Fig. 6, A, red) were joined by macrophages located outside the OOs (Fig. 6, A'-'A'', arrows; Supplementary Video 2). Analysis of the 2D path of only the macrophages associated with the OOs showed that copper exposure resulted in a statistically significant increase in the number of macrophages in the OOs (Fig. 6, B-B''', C), with specific non-local macrophages moving toward the OOs (Fig. 6, B'-B''', arrows). These macrophages entered the OO and OB via pathways separate from the olfactory nerve (Fig. 6, A''', arrows). Similar to neutrophils, exposure to copper resulted in an increased number of macrophages (Fig. 6, C; 11.5 ± 0.4) associated with the OO when compared to the controls (Fig. 6, C; 6.2 ± 0.3; data from analysis of six independent time lapse videos). In contrast to neutrophil dynamics, no significant difference in instantaneous velocity of the macrophages was observed (Fig. 6, D, pre-exposure velocity of 1.7 ± 0.7 μm/min to a post exposure velocity of 2.2 ± 0.6 μm/min; n=26 macrophages; 1 video), and both velocities were significantly slower than that observed for neutrophils after exposure to copper (pre 7.1 ± 0.2 μm/min / post 7.8 ± 0.1μm/min). When quantifying the total displacement of the tracked macrophages there was a significant difference between two groups of macrophages (Fig. 6, E): local macrophages that remained in close association with the OOs, moving less than 100 μm, and non-local (or wandering) macrophages that exceeded this total displacement (n=51 macrophages, 16 local, 25 non local, 1 representative time lapse). During copper exposure there is a steady increase in macrophages associated with the OO (Fig. 6, F) that starts to decrease when copper is removed. Like neutrophils, twenty-four hours post-exposure there is a statistically significant increase of macrophages in the OOs that returns to baseline values at forty-eight hours post treatment (see Fig. 5, F).

To better understand the dynamics of macrophage movements in the OOs we analyzed the movements of macrophages and neutrophils relative to copper induced damage of the OSNs in *Tg(mpeg1:mCh):Tg(mpx:EGFP)*:*Tg*(*OMP:YFP)* triple transgenic larvae (Fig. 7, A-C;

Supplementary Video 3). As the OSNs degenerated, evidenced by the fading of green signal (Fig. 7, A-A'''), the macrophages associated with the OSNs (Fig. 7, A-A''', arrow) and those at the perimeter of the OMP:YFP+ population (Fig. 7 A-A''', arrowheads) swell over time, (see Fig. 6, A'-A''', red; Fig. 7 D-D', red), potentially reflecting their role in phagocytosis of damaged OSNs. In further analysis of the macrophage movements using cell tracking, two distinct populations were observed: fixed macrophages (Fig. 7, B), (previously called local macrophages) that were always in the OOs, and "wandering" or non-local macrophages (Fig. 7, C), that were able to enter the OOs when damage occurs, but were patrolling the head before olfactory damage. Therefore the local or fixed macrophages, observed using the *Tg(mpeg1:mCh)* line, were found in the OO and their behavior contrasts sharply with the wandering phenotype perhaps reflecting different roles and subtypes of the phagocytic cells within the zebrafish head.

In response to copper induced damage of the OSNs, both local and non-local macrophages changed their shape from a ramified-star-like shape (Fig. 7, D, red, arrowheads) to a rounded swollen-morphology (Fig. 7, D', red, arrowheads). In contrast to neutrophils, in response to copper macrophages formed multiple vesicles and phagosome-like structures (Fig. 7, D, D') [39], that were observed engulfing the OMP:YFP+ degenerating OSNs (Fig. 7, D', arrowheads). Thus the macrophages associated with the OOs during early development are greater in number, respond more slowly to copper induced damage, and show distinct phagocytic behaviors.

Blood-Lymphatic vasculature and neutrophil migration

Because this was the first reported analysis of neutrophil responses in the OO and our data on individual *in vivo* cell tracking suggested that neutrophils used pre-existing pathways to reach the OOs in response to copper exposure, we further examined the neutrophil migration routes. To determine whether neutrophils migrated using BV and/or LV, we used *Tg(mpx:GFP); Tg(lyve1b:DsRed)* double transgenic larvae to follow neutrophil movements associated with LV. Initially there was no association of neutrophils with the developing rostral LV (data not shown),

but in 7 dpf larvae neutrophils were localized in the ventral-lateral OO (Fig. 8, A, A', asterisks). After copper exposure the number of neutrophils increased (Fig. 8, A', B', green, asterisks), and were found associated with the lyve1b:DsRed+ branch of the ventral-lateral OO (Fig. 8, A', B', red, arrowheads; Fig. 3, G', NL, red). To analyze the potential role of BV in neutrophil migration, we generated a quadruple reporter line *Tg(fli1a:EGFP);Tg(gata1a:DsRed);Tg(mpx:GFP);Tg(OMP:RFP)* allowing us to image in 5 dpf larvae *in vivo*: neutrophils (Fig. 8, C, C', D, D'', green), the blood vasculature surrounding the OO (Fig. 8, C, C', D, D'', green), the OSN (Fig. 8, C, C', D, D'', red), and the erythrocytes within blood vessels (Fig. 8, C, C', D, D'', green). Consistent with previous reports, we found that neutrophils showed a close association with the BV system in the developing embryo. In larvae exposed to copper, neutrophils moved along the NV on the medial side of the OO (Fig. 8, D, D', asterisks, Supplementary Video 4). As the neutrophils migrate they maintained intimate contact with the BV, often extending "feet" into the vasculature (Fig. 8, E-E'') as they moved (Supplementary Video 5). Thus, copper induced damage to the developing OOs initiated neutrophil migration (Fig. 8, F, blue), which occurred along the medial NV (Fig. 8, F green) at early stages, and later included the ventral lateral OO associated with lyve1b:DsRed positive LV branch (Fig. 3, G).

Migration route

Because the nasal artery/nasal veins are the primary routes for neutrophil migration to the OOs during early development and the classification as a vein or artery is unclear in the literature, we further analyzed the direction of blood flow in 5 dpf larvae. In *Tg(fli1a:EGFP);Tg(gata1a:DsRed);Tg(mpx:GFP)* triple transgenic larvae we observed movement of erythrocytes (Fig. 9, A, red, arrows) in the nasal vein and with a net direction from ventral to dorsal. Analysis of videos taken with transmitted light of whole mount larvae *in vivo* confirmed the net direction as ventral to dorsal or "away" from the OO (Fig. 9, B, arrow).

Furthermore using *Tg(fli1a:EGFP);Tg(lyve1b:DsRed)* double transgenic 15 dpf larvae we confirmed that the nasal lymphatic branch (Fig. 9, D, NL, arrow, lyve1b:DsRed+) appeared in association with the nasal blood vasculature (Fig. 9, D, NV, arrow, fli1a:EGFP+ and lyve1b:DsRed+).

Discussion

In this study we examined the population of the developing olfactory organ by myeloid immune cells (neutrophils/macrophages) and their response to copper induced damage. Key findings include (1) both local and non-local neutrophils and macrophages are present in the developing OOs, where the local immune cells may play a role in the lifelong neurogenesis of the olfactory epithelia, (2) the appearance of the immune cells is correlated with the developing blood and lymphatic vasculature of the OOs, (3) copper induced damage triggers rapid but distinct responses from neutrophils and macrophages. Further studies are needed to determine the origin(s) of neutrophils and macrophages as well as their different functions in developing and adult animals.

Phagocytic cell populations in th developing olfactory organ

Neutrophils are essential players in the innate immune system as they are the first cells that respond to tissue damage and infection by rapidly migrating to the site of injury (swarming) [40]. We first detected neutrophils in the OO at 3 dpf, well after the 30 hpf when functional macrophages and neutrophils are present [8; 9]. Perhaps consistent with the necessity of a strong immune defense, the OO had significantly greater number of neutrophils than the mouth or ear (the eye had no neutrophils). In contrast to the neutrophils, macrophage populations in the developing olfactory OO and the eye were much larger than the other sensory systems and there was no significant difference in numbers of macrophages found in the OOs and eyes. While little is known about macrophages in the larval retina, damage to the adult retina in zebrafish triggers the rapid accumulation of immune cells including local microglia, and extra-retinally derived macrophages [41]. Microglia appear to play a role in the regulation of neurogenesis [42] and macrophages may play a critical role in regeneration of sensory organs [43]. At this time we cannot determine whether the macrophage population we have described in the OOs also includes precursors of microglia that, in zebrafish, arise from the primitive macrophages [44].

The finding that both the eyes and the OOs have large macrophage populations, coupled with their anatomically unique peripheral extension of the meninges which contain a diverse array of immune cells [45], supports a model we proposed where the olfactory epithelia are more like the retina of the eye than placodal-derived structures [46; 47; 48]. The presence of microglia in the peripheral olfactory sensory system would argue that the olfactory organ shares more characteristics with the CNS than peripheral nervous system, and we are currently investigating macrophage and microglia populations in the adult olfactory system.

Neurogenic response of olfactory organ

Unlike mammals, fish have the unique ability to maintain neurogenesis of sensory neurons throughout life. The exception to this difference is the olfactory epithelia where all vertebrates share the characteristic of ongoing sensory cell replacement [49]. Copper, a heavy metal and pervasive environmental contaminant [50] is known to damage the olfactory sensory epithelia of fish, leading to loss of olfactory-driven behaviors [51] [26] [52] and to alter expression of genes involved in the olfactory signal transduction pathway in adult zebrafish [53]. Here we confirmed in larval zebrafish that exposure to copper resulted in OSN death [54] [37] and the rapid recovery of the OSNs was accompanied by the influx of both neutrophils and macrophages.

Neutrophil movements we observed in the OOs are consistent with earlier studies in juvenile zebrafish, where damage triggers a rapid mobilization of neutrophils, and directed chemotaxis contributes to the migration of more neutrophils to the site of damage [13]. Moreover, it has also been shown that in response to wounding induced inflammation neutrophils move rapidly (15 μm/min) toward the wound whereas macrophage migration velocity was significantly slower [25] [55]. Here we found similar results where neutrophils increased their velocity in response to damage while macrophages showed a slower response. In contrast to wound healing responses induced by tail cutting, here we found that the OOs contain populations of local neutrophils and macrophages who were joined by non-local neutrophils and wandering macrophages in response

to damage. This difference is most likely due to the unusual characteristics of the olfactory sensory neurons. In contrast to the tail wounding where the response is an inflammatory response in a tissue capable of regeneration, the olfactory organ is a tissue that has ongoing sensory neurogenesis over which is imposed neural damage induced by copper. Recent studies suggest that macrophages are involved in the repair of different neural tissue. In larval zebrafish, copper induced hair cell damage in both the lateral line [56] and spinal cord trans-section [57], resulted in the recruitment of neutrophils and macrophages to the injury site where macrophages were correlated with repair and regeneration of neural tissue. Because both macrophages and microglia are suggested to play a role in neurogenesis, as well as regeneration, the fixed or local macrophages we describe here (and potentially the local neutrophils) may play a role in the ongoing turnover of OSNs. Thus the presence of both local and non-local neutrophils and macrophages in the developing OOs suggests a dual response where the local immune cells protect against external challenges, and non-local immune cells arrive only once damage is detected.

Migration of neutrophils and macrophages

Studies in fish where a wounding response generated by tail and/or fin trans-section [25; 58] has elucidated the role of macrophages and neutrophils in inflammation. In the wounding response macrophages were found to patrol throughout the body yet neutrophils were motile only in the head region of the larvae [25; 59] [60]. While interstitial migration has been described for both neutrophils and macrophages [61] only neutrophils also use the blood-lymphatic vasculature to migrate [40] [62].

The lymphatic vasculature (LV) has recently been "re-discovered" in the central nervous system (CNS) of mammals [63; 64; 65; 66] and of zebrafish [32] [33] [34], yet little is known about the development of the LV in the brain of vertebrates. Lymphatic endothelial cells are thought to arise from the blood vasculature system [67; 68], yet to date there are no detailed descriptions of

the development of the blood vasculature (BV) and the LV in the olfactory sensory system. The development of the BV preceded the development of the LV in the OOs and the primary route of neutrophil migration to the OOs was via the nasal veins whose development coincides with the first appearance of myeloid cells in the peripheral olfactory sensory system.

A fascinating question, brought to the fore by the current SARS-CoV2 pandemic, is how viruses gain access to the nervous system and it is now apparent that the olfactory system is used by COVID-19 as an entry point to the nervous system [69; 70]. The study of the peripheral olfactory sensory system and the associated immune cells will allow us to better understand not only the rapid immune response to damage caused by toxic and infectious agents, but also how this neural immune interface may act as a host defense niche protecting the central nervous system.

Conclusions

During early development, at all times assayed, the olfactory organs contain local populations of both neutrophils and macrophages, reminiscent of a potential host-defense niche described in other tissues where neutrophils are marginated [4] [71] [72] (Fig. 10 A, blue). In response to damage non-local populations join local populations of neutrophils and macrophages as they mount a rapid immune response (Fig. 10 A, blue, pink). Neutrophils use the developing blood vasculature system (Fig. 10, B, green) to access the olfactory organs and this may account for their greater velocity relative to macrophages.

Figures & Figure Legends

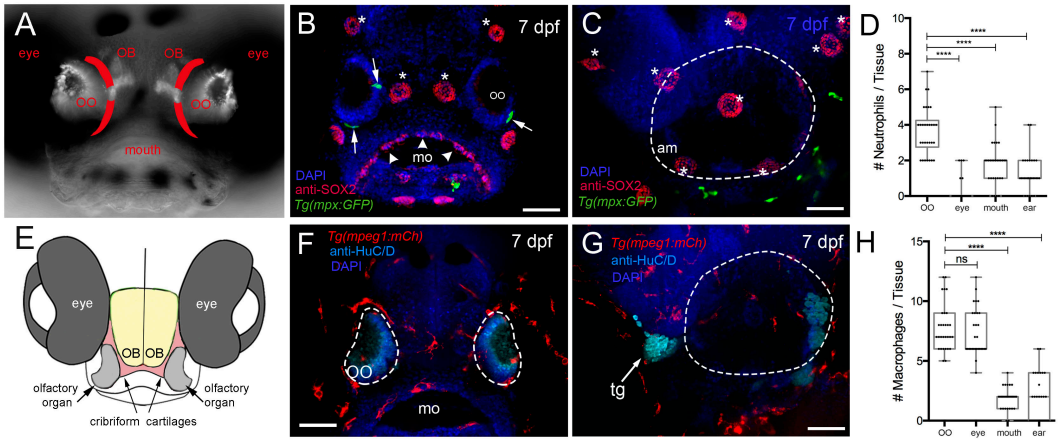

Figure 1

Figure 1. Neutrophils and macrophages are found in developing sensory systems.

(A) Frontal view of 7 dpf larvae. Brightfield/fluorescent image in wholemount larvae with OMP:RFP+ OSNs. Lines in red indicate the future adult cribriform plate. (B) Frontal view, wholemount 7 dpf *Tg(mpx:GFP)* larva, anti-Sox2 positive taste buds (red, arrowheads) and neuromasts (red, asterisks), neutrophils (green). (C) Lateral view, whole mount 7 dpf larva. Neutrophils (green) associated with border of the ear (dashed line), (am: ampulla). (D) Neutrophils are highly represented in the olfactory organ (OO) with fewer neutrophils associated wit the gustatory and auditory systems. No neutrophils were observed in the retina (*n*=30 animals, 1-way ANOVA, Tukey test, $p < 0.0001$). (E) Diagram of head of larva showing generalized position of the cartilages (red) giving rise to the cribriform plate in the adult animal. (F) Frontal view, wholemount 7 dpf *Tg(mpeg1:mCh)* larvae, anti-HuC/D positive neurons in the OO (pale blue), macrophages (red). (G) Lateral view, whole mount 7 dpf. Macrophages (red) associated with border of the ear (dashed line). (H) The olfactory organ (OO) and the eye have the most macrophages, with fewer neutrophils associated with gustatory (mo) and auditory (ear) systems. (*n*=30 animals, 1-way ANOVA, Tukey test, $p < 0.001$, ns= non significant). DAPI: blue, mo: mouth, tg: trigeminal ganglia . Scale bars: (A, B, D, E) = 100 μm.

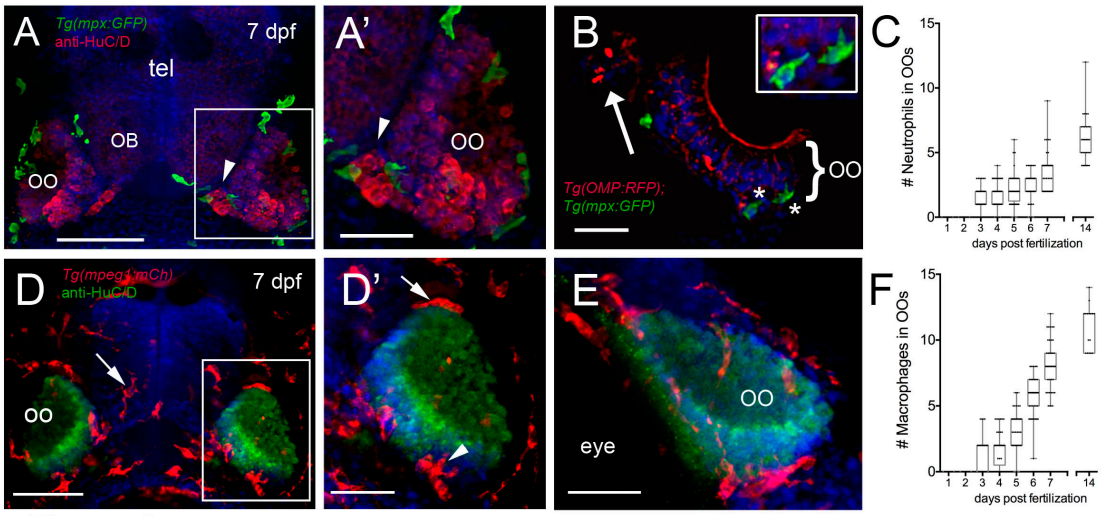
A
Tg(mpx:GFP)
anti-HuC/D
7 dpf
tel
OB
OO
A'
OO
B
Tg(OMP:RFP);
Tg(mpx:GFP)
OO
C
Neutrophils in OOs
days post fertilization
D
Tg(mpeg1:mCh)
anti-HuC/D
7 dpf
oo
D'
E
OO
eye
F
Macrophages in OOs
days post fertilization

Figure 2

Figure 2. Neutrophils and macrophages populate the olfactory system of juvenile animals.

(A) Frontal view of *Tg(mpx:GFP)* 7dpf larva with anti-HuC/D positive (red) neurons in the olfactory organ (OO) adjacent to the olfactory bulb (OB). (A') Image of OO (boxed area in A) with neutrophils (green). (B) 25 μm cryosection of a 7 dpf *Tg(OMP:RFP);Tg(mpx:GFP)* larva neutrophils (green, asterisks) localized within the OO margin and adjacent to OSNs (red, see inset). (C) Average number (± SEM) of neutrophils in OOs of *Tg(mpx:GFP)* during the first 2 weeks post fertilization (*n*=45 larvae). (D) Frontal view of *Tg(mpeg1:mCh)* 7 dpf larva. Anti-HuC/D positive (green) neurons populate the olfactory organs (OO). D'. Image of OO (boxed area in D) with macrophages (red) adjacent to the OO (arrow) and within the OO (arrowhead). (E) Lateral oblique view of OO at 7 dpf. (G) Average number (± SEM) of macrophages in OOs of *Tg(mpeg1:mCh)* during the first 2 weeks post fertilization (n=45 larvae). Scale Bars: (A, D)= 100 μm; (A', D', E) = 50 μm; C= 25 μm.

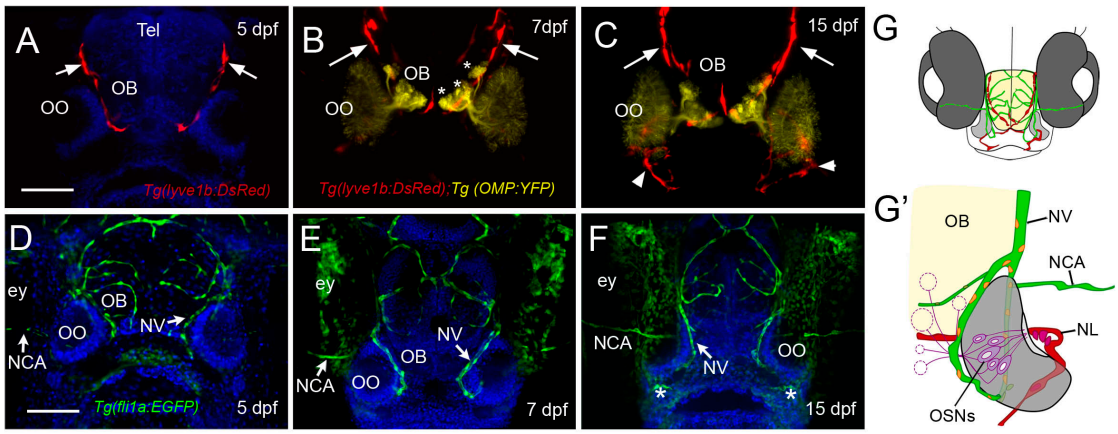
A
Tel
5 dpf
OB
OO
Tg(lyve1b:DsRed)
B
7dpf
OB
OO
Tg(lyve1b:DsRed),Tg (OMP:YFP)
C
15 dpf
OB
OO
G
G'
OB
NV
NCA
NL
OSNs
D
ey
OB
OO
NV
NCA
Tg(fli1a:EGFP)
5 dpf
E
ey
NV
OB
NCA
OO
7 dpf
F
ey
NCA
NV
OO
15 dpf

Figure 3

Figure 3. The developing olfactory organs have an extensive blood-lymphatic system

Lyve1b:DsRed+ lymphatic vessels (red) at 5 dpf (A), 7 dpf (B) and 15 dpf (C). (A-C) Lyve1b:DsRed+ lymphatic vasculature (red, arrows) extends from the dorsal brain toward the olfactory organs (OO). (B, C) Lymphatic vessels extend to region of olfactory sensory neurons (OMP:YFP+), yellow, asterisks) in olfactory bulb (OB). (C) At 15 hpf nasal lymphatic vasculature (red, arrowheads) is now visible wrapping around the posterior OO and associating with the ventral lateral OOs (G). Fli1a:EGFP+ blood vasculature (green) at 5 dpf (D), 7 dpf (E) and 15 dpf (F). Blood vessels (green) forming nasal vein (NV), NCA: nasal ciliary artery (NCA) are present at 5 dpf. The NV extends ventrally (E) encircling the OO (F). (G) Diagram of head of 15 dpf larva showing telencephalon (green) and olfactory organs (grey). (G') Olfactory organ (grey) summarizing blood (green) and lymphatic (red) vasculature. Nuclei of NV (orange) are positive for both lyve1b:DsRed and fli1a:EGFP. A, B, E, AND F: DAPI (blue). OO: olfactory organ, OB: olfactory bulb, ey: eyes. Scale Bars: (A-C) = 200 μm, (D-F) = 200 μm.

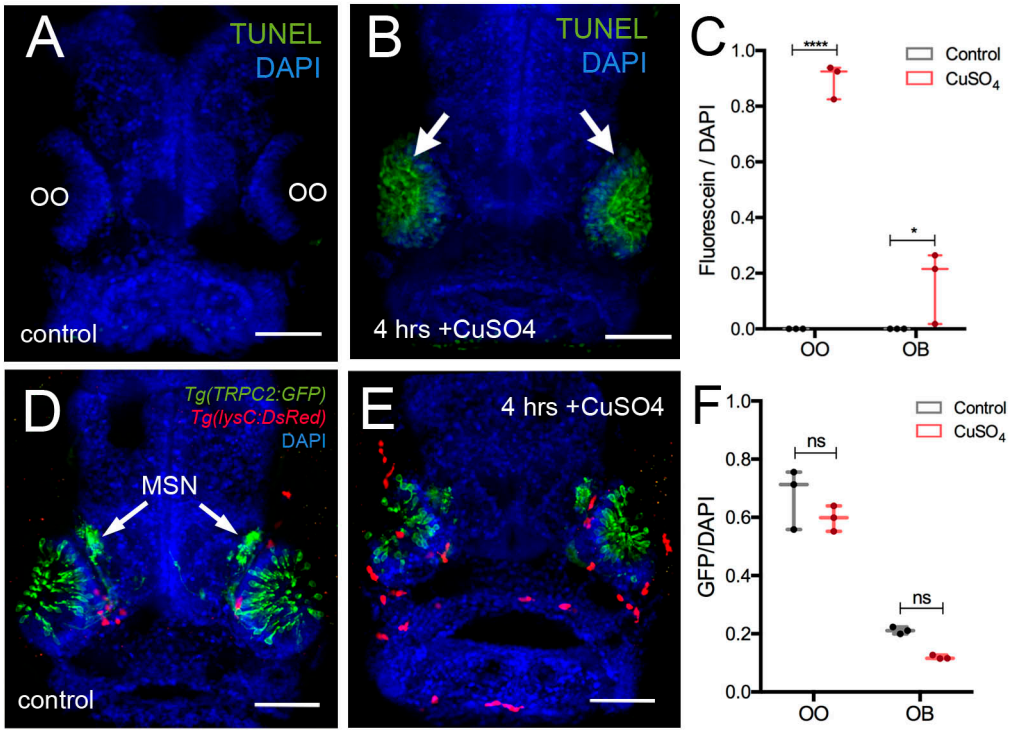
A
TUNEL
DAPI
OO
OO
control
B
TUNEL
DAPI
4 hrs +CuSO4
C
Control
CuSO4
Fluorescein / DAPI
1.0
0.8
0.6
0.4
0.2
0.0
****
*
OO
OB
D
Tg(TRPC2:GFP)
Tg(lysC:DsRed)
DAPI
MSN
control
E
4 hrs +CuSO4
F
Control
CuSO4
GFP/DAPI
1.0
0.8
0.6
0.4
0.2
0.0
ns
ns
OO
OB

Figure 4

Figure 4. Copper exposure induces cell death and subsequent regeneration in the olfactory sensory system.

(A, B) TUNEL Assay for copper induced damage to olfactory organ (OO). Whole mount, 5 dpf larva. (A) Control fish showed no cell death. (B) Only the OO were positive for TUNEL, green, arrows, DAPI (blue). (C) Quantification of TUNEL fluorescence control and treated animals. (D, E) Frontal view of *Tg(trpc2:GFP):Tg(lysC:DsRed)* with microvillous sensory neurons (MSN, green) extending into OB in control animals (D) and 4 hrs post treatment (E). Neutrophils (red) in the OO, but unlike OSNs, microvillous OSNs were largely unaffected. (F) Quantification of microvillous OSNs (green, fluorescence) in control (grey) and copper-treated animals (red); no significant decrease in Trpc2:GFP fluorescence was observed. All fluorescence was normalized using DAPI (n=3 larvae, Two-way ANOVA, Tukey multiple comparison test, ****, a= $P < 0.0001$, b= $P < 0.01$). All scale bars=100 μm.

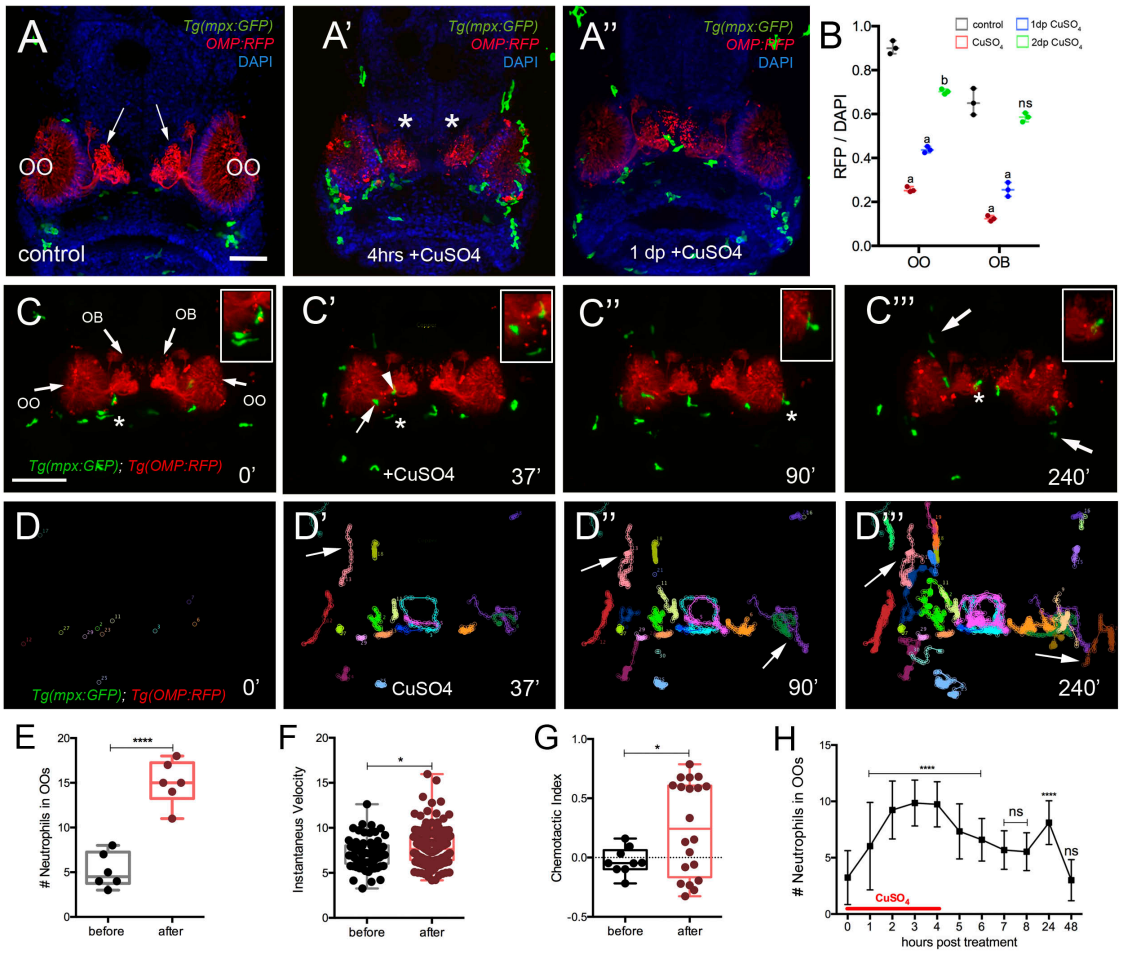
A
Tg(mpx:GFP)
OMP:RFP
DAPI
OO
OO
control
A'
4hrs +CuSO4
A''
1 dp +CuSO4
B
control
1dp CuSO4
CuSO4
2dp CuSO4
RFP / DAPI
ns
OO
OB
C
OB
OB
OO
OO
Tg(mpx:GFP); Tg(OMP:RFP)
0'
C'
+CuSO4
37'
C''
90'
C'''
240'
D
Tg(mpx:GFP); Tg(OMP:RFP)
0'
D'
CuSO4
37'
D''
90'
D'''
240'
E
Neutrophils in OOs
****
before
after
F
Instantaneus Velocity
*
before
after
G
Chemotactic Index
*
before
after
H
Neutrophils in OOs
****
ns
****
ns
CuSO4
hours post treatment

Figure 5

Figure 5. Exposure to copper induces migration of neutrophils.

(A-A'') Frontal view of *Tg(mpx:GFP);Tg(OMP:RFP)* larva with OSNs (red) extending into OB. (A) Control. (A') At 4 hrs post copper exposure neutrophils (green) swarmed to the OO and OSNs have degenerated (red, asterisk). (B) Quantification of OSN (red fluorescence) in control (grey), copper-treated animals (red), 1-day (green bar) and 2 days post treatment (blue bar). All fluorescence was normalized using DAPI (n=3 larvae, Two-way ANOVA, Tukey multiple comparison test, ****, a= $P < 0.0001$, b= $P < 0.01$). All scale bars=100 μm. (C-C'''). 5 dpf *Tg(mpx: GFP);Tg(OMP:RFP)* larva, frontal view. Imaging was initiated at time 0'. At 37' (C') larvae were exposed to 10 μM of $CuSO_4$ and imaging continued at times indicated (see Supplementary Video 1 for sequence taken every minute). Boxed areas: Neutrophils (green, asterisks) associated with olfactory organ (OO, C-C") and OMP:RFP+ OSNs in olfactory bulb (red, asterisk, C'''). (C", C''') Arrows in (C''') non-local neutrophils that do not enter the OO near the ON (see Supplementary Video 4). (D-D''') Individual 2D-cell tracking of neutrophils before, during, and after copper exposure. Each color represents a different neutrophil. (E) Number of neutrophils within the OO before and after copper exposure: analysis of six videos from different animals. Unpaired t test, $P < 0.0001$). (F) Speed of neutrophils before and after copper exposure (*n*=30 neutrophils; Unpaired t test, $P < 0.05$). (G) Chemotactic index of neutrophils before and after copper exposure (*n*=20 neutrophils; Unpaired t test, $p < 0.05$). (H) Time course of neutrophil movement to the OO (*n*=48 larvae. ANOVA, Kruskall-Wallis test, $P < 0.0001$). Scale bar C-C''' = 150 μm. Tracking was done using the ImageJ plugin, MTrackJ.

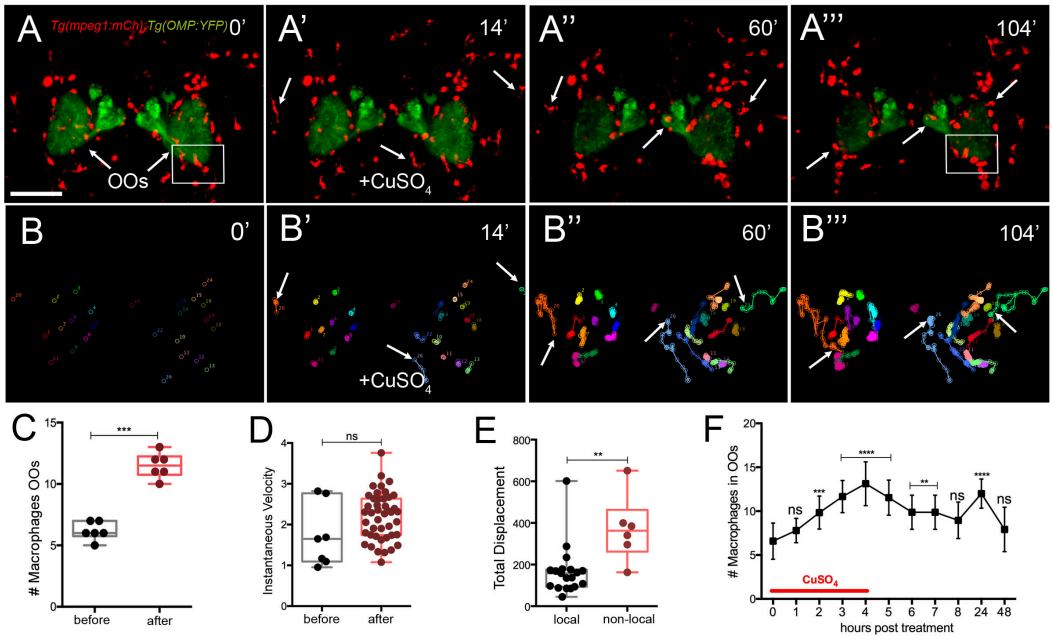
A
Tg(mpeg1:mCh);Tg(OMP:YFP) 0'
OOs
A'
14'
+CuSO4
A''
60'
A'''
104'
B
0'
B'
14'
+CuSO4
B''
60'
B'''
104'
C
Macrophages OOs
***
before
after
D
Instantaneous Velocity
ns
before
after
E
Total Displacement
**
local
non-local
F
Macrophages in OOs
ns
***
****
**
ns
****
ns
CuSO4
hours post treatment

Figure 6

Figure 6. Exposure to copper induces migration response of macrophages in the olfactory organ.

(A-A’’’) 5 dpf *Tg(mpeg1:mCh);Tg(OMP:YFP)* larva frontal view. Imaging was initiated at time 0’. At 14’ (A’) larvae were exposed to 10 μM of $CuSO_4$ and imaging continued at times indicated (see Supplementary Video 2 for sequences taken every two minutes). (A”, A’’’). Arrows in (A’’’): non-local macrophages that enter the OO (see Supplementary Video 2). (B-B’’’) Individual 2D-cell tracking of macrophages associated with the OOs before, during, and after copper exposure. Each color represents a different macrophage. (C) Number of macrophages within the OO before and after copper exposure: analysis of three independent videos. Unpaired t test, $p < 0.05$). (D) Speed of macrophages before and after copper exposure (*n*=50 macrophages, 1 time lapse; Unpaired t test, $P < 0.001$). (E) Total displacement of local and non-local macrophages (Supplementary Video 2) during a two-hour time lapse (*n*=51 macrophages, 16 local, 35 non-local; Unpaired t test, $P < 0.0001$). Scale bars= A = 150 μm,. Tracking was done using the ImageJ plugin, MTrackJ. (F) Time course of macrophage movement to the OO (*n*=24 larvae. ANOVA, Kruskall-Wallis test, $P < 0.0001$).

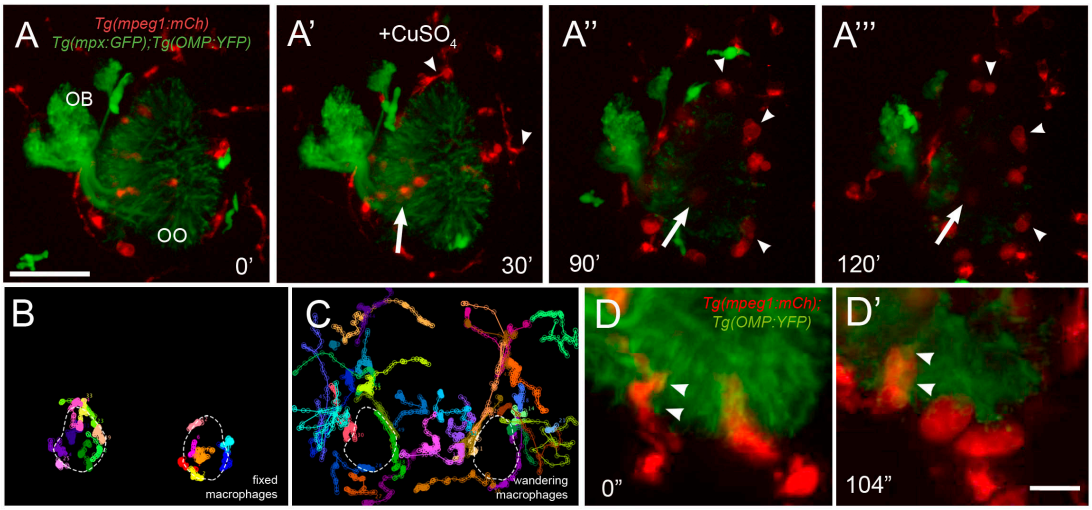
A
Tg(mpeg1:mCh)
Tg(mpx:GFP);Tg(OMP:YFP)
OB
OO
0'
A'
+CuSO4
30'
A''
90'
A'''
120'
B
fixed
macrophages
C
wandering
macrophages
D
Tg(mpeg1:mCh);
Tg(OMP:YFP)
0"
D'
104"

Figure 7

Figure 7. Exposure to copper reveales distinct clases of macrophages.

(A-A’’’) 5 dpf *Tg(mpeg1:mCh);Tg(mpx:GFP);Tg(OMP:YFP)* olfactory organ (OO) and imaging continued at times indicated (see Supplementary Video 3 for sequence taken every minute). (A) Imaging was initiated at time 0’. (A’) larvae were exposed to 10 μM of $CuSO_4$ at 30’. Individual cell tracking reveals the presence of (B) fixed and (C) wandering macrophages. (D) Before copper exposure (from boxed are in A) macrophages (red) are found associated with OSNs (green) in the ventral OO. (D’) After exposure to copper (from boxed are in Fig. 6, A’’’) macrophages (mpeg1:mCh+, red) accumulate at the ventral-basal OO, in close association with degenerating OSNs (green, OMP:YFP+). Arrowheads indicate places where macrophages appeared to engulf degenerating OSNs (mpeg1:mCh+ and OMP:YFP+). Scale bars*:* A-A’’’ = 75 μm, D = 25 μm

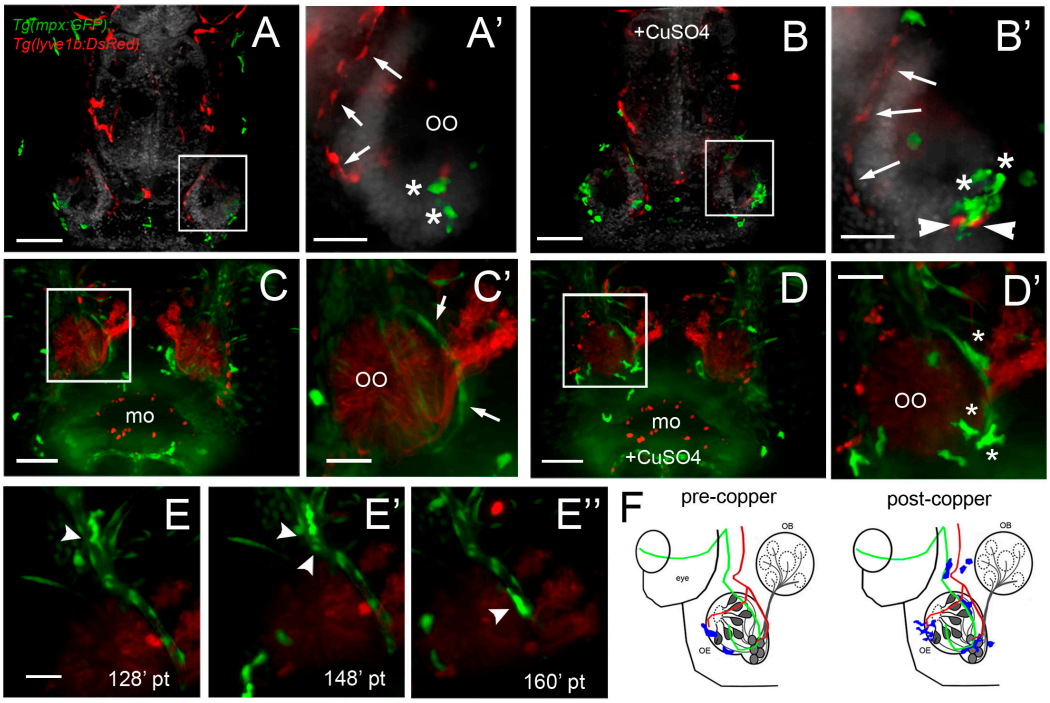
Tg(mpx:GFP)
Tg(lyve1b:DsRed)
A
A'
OO
B
+CuSO4
B'
C
mo
C'
OO
D
mo
+CuSO4
D'
OO
E
128' pt
E'
148' pt
E''
160' pt
F
pre-copper
post-copper
OB
eye
OE

Figure 8

Figure 8. During copper exposure neutrophils migrate in association with blood vasculature to reach to the developing olfactory organ.

(A) Frontal view of *Tg(mpx:gfp);Tg(lyve1b:DsRed)* 7 dpf larva. Boxed area (A') with nasal LV (arrows, red) and neutrophils (green, asterisks). (B) Frontal view of *Tg(mpx:GFP);Tg(lyve1b:DsRed)* 7 dpf larva after 4 hours of copper exposure, neutrophils (green, asterisks) associate with LV in ventral-lateral OO (arrowheads, red). Boxed area (B') indicates cluster of neutrophils (asterisks, green). (C-D') Images from Supplementary Video 4, *Tg(fli1a:EGFP)*;Tg(*gata1a:DeRed);Tg(mpx: GFP);Tg(OMP:RFP(* quadruple transgenic larva of 5dpf, showing OSN and erythrocytes in red; and neutrophils and endothelial vasculature in green. (C) Before copper exposure. Boxed area is magnified in (C'). Arrows indicate fli1a:EGFP+ branches that enclose the OO (see Fig. 2 G', NV, green). (D) After exposure to copper more neutrophils are associated with the OO. (D') Image from boxed area in (D). Asterisks indicate neutrophils that have migrated to the OO on the BV (NV) and clustered around the medial edge of the OO. (E-E'') A polarized neutrophil crawling (arrowhead) along the NV to finally enter the OO near the ventral basal ON (E" see Supplementary Video 5). Minutes are post treatment (pt). (F) Summary: Schematic of nasal blood and lymphatic vasculature at 5 dpf pre and post exposure to copper. OO: olfactory organ, OB: olfactory bulb. fli1a:EGFP (green) and lyve1b:DsRed (red), neutrophils (blue) migrate in response to copper exposure using the NV (C'-D'), entering the OO near ventral ON exiting, and associating with ventral-lateral LV (A'-B'). Scale bars: (A-D)= 100 μm; (A'-D', E-E'') = 50 μm.

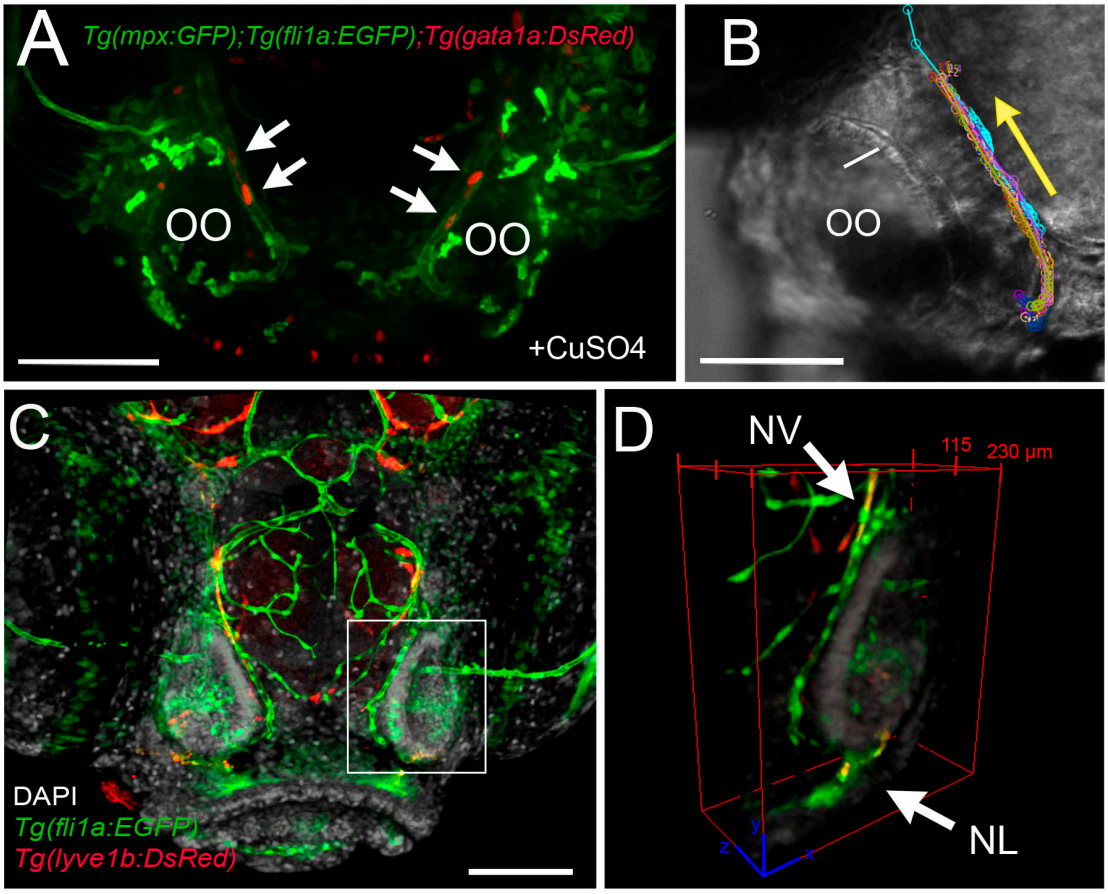
A
Tg(mpx:GFP);Tg(fli1a:EGFP);Tg(gata1a:DsRed)
OO
OO
+CuSO4
B
OO
C
DAPI
Tg(fli1a:EGFP)
Tg(lyve1b:DsRed)
D
NV
115
230 µm
NL

Figure 9

Figure 9. The nasal vein as the primary route to the olfactory organ during development.

(A) *Tg(fli1a:EGFP);Tg(gata1a:DsRed)*;*Tg(mpx:GFP)* larva at 5 dpf. Erythrocytes (gata1:DsRed^{+}, red, arrows) are observed within the nasal vein after copper exposure. (B) Tracking of blood flow of 10 erythrocytes circulating within the NV, whole mount preparation in transmitted light (video of 2 minutes). Each color represents a different erythrocyte. Direction of movement is represented as a yellow arrow. (C) Laser confocal maximum projection of a 15 dpf *Tg(fli1a:EGFP); Tg(lyve1b:DsRed)* larva, DAPI (grey). (**D**) 3D orthogonal view generated from optic sections (boxed area in C), showing the NV (Nasal Vein, arrow) positive for fli1a:EGFP and lyve1b:DsRed The NL (Nasal Lymphatics, arrow), is positive for lyve1b:DsRed and passes along the ventro-lateral region of the OO. Total depth: 230 μm, 2 μm spacing. Scale bars: (A, C)=100 μm, B= 50 μm.

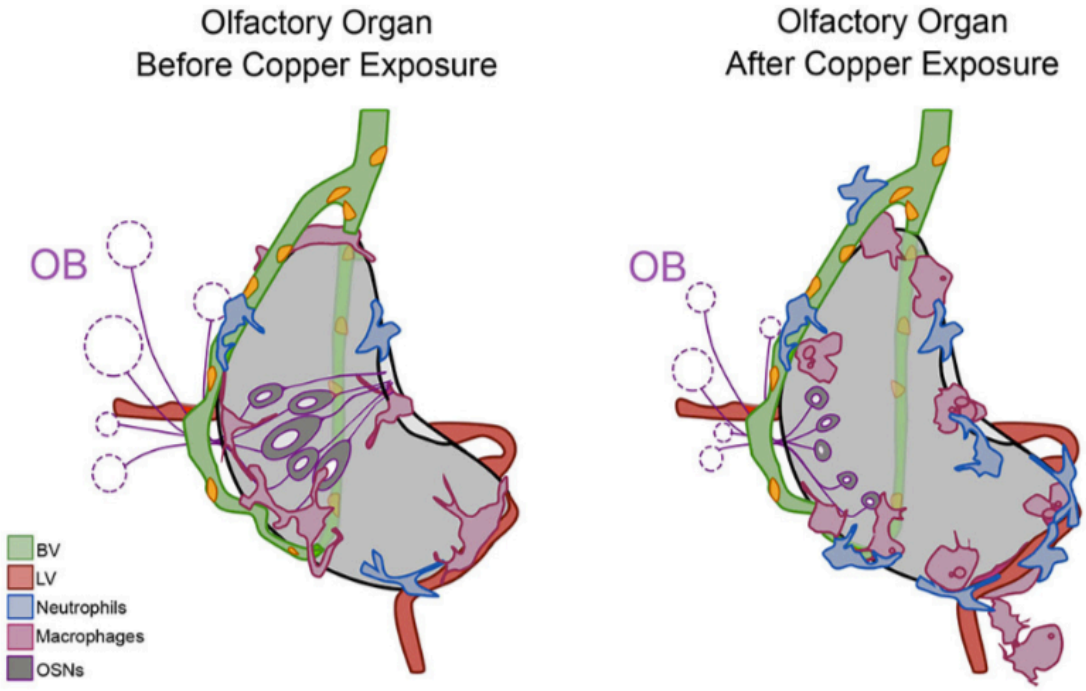

Figure 10. Summary of neutrophil and macrophage responses to copper induced damage in the larval olfactory organ (OO).

The blood vasculature (BV, green) wraps the olfactory organ (grey) and the lymphatic vasculature (LV, red) extends along the ventral posterior aspect. In untreated animals (before copper) there are local neutrophils (blue and macrophages (pink) associated with the OO. In response to damage (after copper exposure) of the olfactory sensory neurons (OSNs, dark grey), non-local neutrophils and macrophages migrated to the OO. Neutrophils migrated in association with the BV and both neutrophils and macrophages were seen associated with the LV. Macrophages changed to a more rounded morphology as they engulfed debris of dying OSNs.

Supplementary videos

Supplementary Video 1. Neutrophils mobilize in response to copper induced damage of the developing olfactory organ. Time lapse of *Tg(OMP:RFP0;Tg(mpx:GFP)* 5dpf larva, maximum projection of 150 μm depth (3 μm optical sections), taken every minute for 4 hours. A final concentration of 10 μM of $CuSO_4$ was added at minute 37 (Fig. 5). Scale bar= 150 μm. Time in minutes is indicated in upper left corner. Arrowheads indicate local neutrophils (green). After treatment neutrophils where observed to swarm, cluster and even divide, next to OSNs (red).

Supplementary Video 2. Local and non-local macrophages respond to copper-induced damage in the olfactory organ. Time lapse of *mpeg1:mCh;mpx:EGFP* 5 dpf transgenic larva, maximum projection of 150 μm depth (3 μm optical sections), taken every two minutes for 1.7 hours. A final concentration of 10 μM of $CuSO_4$ was added at minute 14 (Fig. 6). Scale bar= 150 μm. Time in minutes is indicated in upper left corner At the end of the time lapse macrophages are localized in the ventral and basal side of the olfactory organ, forming chain-like structures near branch of nasal lymphatics (Fig. 3; Fig. 7).

Supplementary Video 3. Macrophages respond differently to copper exposure. Time lapse of *Tg(mpeg1:mCh);Tg(mpx:EGFP);Tg(OMP:YFP)* in 5 dpf larva, maximum projection of 150 μm depth (3 μm optical sections), taken every minute for 2 hours. A final concentration of 10 μM of $CuSO_4$ was added at minute 30 (Fig. 7). Scale bar= 50 μm. Time in minutes is indicated in upper left corner. Local (or fixed) macrophages do not move, but displayed a swollen morphology after copper-induced damage.

Supplementary Video 4. Neutrophils move on the BV during early development. Time lapse of *Tg(fli1a:EGFP;Tg(gata1:DsRed);Tg(mpx:GFP);Tg(OMP:RFP)* quadruple transgenic larva at

5dpf, maximum projection of 300 μm depth with optical sections of 3 μm, taken every minute for 3.5 hours. OSNs and erythrocytes in red; neutrophils and endothelial vasculature in green. A final concentration of 10μM of $CuSO_4$ was added at minute 37 (Fig. 8). After treatment, neutrophils crawl on (arrowheads), and cluster next to (arrows), the NV. Scale= 150 μm. Time in minutes is indicated in upper left corner.

Supplementary Video 5. The nasal vein as route for neutrophil migration to the olfactory organ. Magnified image of the olfactory organ in a time lapse (35 minutes extract) of a *Tg(fli1a:EGFP;Tg(gata1:DsRed);Tg(mpx:GFP);Tg(OMP:RFP)* quadruple transgenic larva at 5 dpf, during copper exposure. Maximum projection of 300 μm depth, taken every minute. Scale bar= 50 μm. Time in minutes is indicated in upper left corner.

References

[1] H. Sakano, Neural map formation in the mouse olfactory system. Neuron. 67 (2010) 530-42. doi: 10.1016/j.neuron.2010.07.003.

[2] K.E. Whitlock, The loss of scents: Do defects in olfactory sensory neuron development underlie human disease? Birth Defects Res C Embryo Today. 105 (2015) 114-25. doi: 10.1002/bdrc.21094. Epub 2015 Jun 25.

[3] D. Pägelow, C. Chhatbar, A. Beineke, X. Liu, A. Nerlich, K. van Vorst, M. Rohde, U. Kalinke, R. Förster, S. Halle, P. Valentin-Weigand, M.W. Hornef, and M. Fulde, The olfactory epithelium as a port of entry in neonatal neurolisteriosis. Nat Commun. 9 (2018) 4269. doi: 10.1038/s41467-018-06668-2.

[4] B.G. Yipp, J.H. Kim, R. Lima, L.D. Zbytnuik, B. Petri, N. Swanlund, M. Ho, V.G. Szeto, T. Tak, L. Koenderman, P. Pickkers, A.T.J. Tool, T.W. Kuijpers, T.K. van den Berg, M.R. Looney, M.F. Krummel, and P. Kubes, The Lung is a Host Defense Niche for Immediate Neutrophil-Mediated Vascular Protection. Sci Immunol. 2 (2017) eaam8929. doi: 10.1126/sciimmunol.aam8929.

[5] L. Tacchi, R. Musharrafieh, E.T. Larragoite, K. Crossey, E.B. Erhardt, S.A.M. Martin, S.E. LaPatra, and I. Salinas, Nasal immunity is an ancient arm of the mucosal immune system of vertebrates. Nat Commun. 5:5205. (2014) 10.1038/ncomms6205.

[6] A.J. Davidson, and L.I. Zon, The 'definitive' (and 'primitive') guide to zebrafish hematopoiesis. Oncogene. 23 (2004) 7233-46. doi: 10.1038/sj.onc.1207943.

[7] G.J. Lieschke, A.C. Oates, B.H. Paw, M.A. Thompson, N.E. Hall, A.C. Ward, R.K. Ho, L.I. Zon, and J.E. Layton, Zebrafish SPI-1 (PU.1) marks a site of myeloid development independent of primitive erythropoiesis: implications for axial patterning. Dev Biol. 246 (2002) 274-95. doi: 10.1006/dbio.2002.0657.

[8] P. Herbomel, B. Thisse, and C. Thisse, Ontogeny and behaviour of early macrophages in the zebrafish embryo. Development. 126 (1999) 3735-45.

[9] D. Le Guyader, M.J. Redd, E. Colucci-Guyon, E. Murayama, K. Kissa, V. Briolat, E. Mordelet, A. Zapata, H. Shinomiya, and P. Herbomel, Origins and unconventional behavior of neutrophils in developing zebrafish. Blood. 111 (2008) 132-41. doi: 10.1182/blood-2007-06-095398. Epub 2007 Sep 17.

[10] J. Xu, L. Zhu, S. He, Y. Wu, W. Jin, T. Yu, J.Y. Qu, and Z. Wen, Temporal-Spatial Resolution Fate Mapping Reveals Distinct Origins for Embryonic and Adult Microglia in Zebrafish. Dev Cell. 34 (2015) 632-41. doi: 10.1016/j.devcel.2015.08.018.

[11] P. Herbomel, B. Thisse, and C. Thisse, Zebrafish early macrophages colonize cephalic mesenchyme and developing brain, retina, and epidermis through a M-CSF receptor-dependent invasive process. Dev Biol. 238 (2001) 274-88. doi: 10.1006/dbio.2001.0393.

[12] S.A. Renshaw, C.A. Loynes, D.M. Trushell, S. Elworthy, P.W. Ingham, and M.K. Whyte, A transgenic zebrafish model of neutrophilic inflammation. Blood. 108 (2006) 3976-8. doi: 10.1182/blood-2006-05-024075. Epub 2006 Aug 22.

[13] J.R. Mathias, B.J. Perrin, T.X. Liu, J. Kanki, A.T. Look, and A. Huttenlocher, Resolution of inflammation by retrograde chemotaxis of neutrophils in transgenic zebrafish. J Leukoc Biol. 80 (2006) 1281-8. doi: 10.1189/jlb.0506346. Epub 2006 Sep 8.

[14] C. Hall, M.V. Flores, T. Storm, K. Crosier, and P. Crosier, The zebrafish lysozyme C promoter drives myeloid-specific expression in transgenic fish. BMC Dev Biol. 7:42. (2007) 10.1186/1471-213X-7-42.

[15] A.L. Mescher, A.W. Neff, and M.W. King, Inflammation and immunity in organ regeneration. Dev Comp Immunol. 66:98-110. (2017) 10.1016/j.dci.2016.02.015. Epub 2016 Feb 16.

[16] M.V. Harden, L.A. Newton, R.C. Lloyd, and K.E. Whitlock, Olfactory imprinting is correlated with changes in gene expression in the olfactory epithelia of the zebrafish. Journal of Neurobiology 66 (2006) 1452-66.

[17] C. Calfun, C. Dominguez, T. Perez-Acle, and K.E. Whitlock, Changes in Olfactory Receptor Expression Are Correlated With Odor Exposure During Early Development in the zebrafish (Danio rerio). Chem Senses. 41 (2016) 301-12. doi: 10.1093/chemse/bjw002. Epub 2016 Feb 17.

[18] S. Masud, V. Torraca, and A.H. Meijer, Modeling Infectious Diseases in the Context of a Developing Immune System. Curr Top Dev Biol 124:277-329. (2017) 10.1016/bs.ctdb.2016.10.006. Epub 2016 Dec 19.

[19] M. Westerfield, The zebrafish book: A guide for the laboratory use of zebrafih (Danio rerio). University of Oregon Press, Eugene OR USA, 2007.

[20] C.B. Kimmel, W.W. Ballard, S.R. Kimmel, B. Ullmann, and T.F. Schilling, Stages of embryonic development of the zebrafish. Dev Dyn 203 (1995) 253-310.

[21] N.D. Lawson, and B.M. Weinstein, In vivo imaging of embryonic vascular development using transgenic zebrafish. Dev Biol. 248 (2002) 307-18. doi: 10.1006/dbio.2002.0711.

[22] K.S. Okuda, J.W. Astin, J.P. Misa, M.V. Flores, K.E. Crosier, and P.S. Crosier, lyve1 expression reveals novel lymphatic vessels and new mechanisms for lymphatic vessel development in zebrafish. Development. 139 (2012) 2381-91. doi: 10.1242/dev.077701. Epub 2012 May 23.

[23] D. Traver, B.H. Paw, K.D. Poss, W.T. Penberthy, S. Lin, and L.I. Zon, Transplantation and in vivo imaging of multilineage engraftment in zebrafish bloodless mutants. Nat Immunol. 4 (2003) 1238-46. doi: 10.1038/ni1007. Epub 2003 Nov 9.

[24] Y. Sato, N. Miyasaka, and Y. Yoshihara, Mutually exclusive glomerular innervation by two distinct types of olfactory sensory neurons revealed in transgenic zebrafish. J Neurosci 25 (2005) 4889-97.

[25] F. Ellett, L. Pase, J.W. Hayman, A. Andrianopoulos, and G.J. Lieschke, mpeg1 promoter transgenes direct macrophage-lineage expression in zebrafish. Blood. 117 (2011) e49-56. doi: 10.1182/blood-2010-10-314120. Epub 2010 Nov 17.

[26] D.H. Baldwin, J.F. Sandahl, J.S. Labenia, and N.L. Scholz, Sublethal effects of copper on coho salmon: impacts on nonoverlapping receptor pathways in the peripheral olfactory nervous system. Environ Toxicol Chem. 22 (2003) 2266-74. doi: 10.1897/02-428.

[27] P.P. Hernandez, C. Undurraga, V.E. Gallardo, N. Mackenzie, M.L. Allende, and A.E. Reyes, Sublethal concentrations of waterborne copper induce cellular stress and cell death in zebrafish embryos and larvae. Biol Res. 44 (2011) 7-15. doi: 10.4067/S0716-97602011000100002. Epub 2011 May 11.

[28] C.A. d'Alençon, O.A. Peña, C. Wittmann, V.E. Gallardo, R.A. Jones, F. Loosli, U. Liebel, C. Grabher, and M.L. Allende, A high-throughput chemically induced inflammation assay in zebrafish. BMC Biol. 8:151. (2010) 10.1186/1741-7007-8-151.

[29] J. Schindelin, I. Arganda-Carreras, E. Frise, V. Kaynig, M. Longair, T. Pietzsch, S. Preibisch, C. Rueden, S. Saalfeld, B. Schmid, J.Y. Tinevez, D.J. White, V. Hartenstein, K. Eliceiri, P. Tomancak, and A. Cardona, Fiji: an open-source platform for biological-image analysis. Nat Methods. 9 (2012) 676-82. doi: 10.1038/nmeth.2019.

[30] C. McQuin, A. Goodman, V. Chernyshev, L. Kamentsky, B.A. Cimini, K.W. Karhohs, M. Doan, L. Ding, S.M. Rafelski, D. Thirstrup, W. Wiegraebe, S. Singh, T. Becker, J.C. Caicedo, and A.E. Carpenter, CellProfiler 3.0: Next-generation image processing for biology. PLoS Biol. 16 (2018) e2005970. doi: 10.1371/journal.pbio.2005970. eCollection 2018 Jul.

[31] T. Lämmermann, P.V. Afonso, B.R. Angermann, J.M. Wang, W. Kastenmüller, C.A. Parent, and R.N. Germain, Neutrophil swarms require LTB4 and integrins at sites of cell death in vivo. Nature. 498 (2013) 371-5. doi: 10.1038/nature12175. Epub 2013 May 26.

[32] N.I. Bower, K. Koltowska, C. Pichol-Thievend, I. Virshup, S. Paterson, A.K. Lagendijk, W. Wang, B.W. Lindsey, S.J. Bent, S. Baek, M. Rondon-Galeano, D.G. Hurley, N. Mochizuki, C. Simons, M. Francois, C.A. Wells, J. Kaslin, and B.M. Hogan, Mural lymphatic endothelial cells regulate meningeal angiogenesis in the zebrafish. Nat Neurosci. 20 (2017) 774-783. doi: 10.1038/nn.4558. Epub 2017 May 1.

[33] N.I. Bower, and B.M. Hogan, Brain drains: new insights into brain clearance pathways from lymphatic biology. J Mol Med (Berl). 96 (2018) 383-390. doi: 10.1007/s00109-018-1634-9. Epub 2018 Apr 2.

[34] M. van Lessen, S. Shibata-Germanos, A. van Impel, T.A. Hawkins, J. Rihel, and S. Schulte-Merker, Intracellular uptake of macromolecules by brain lymphatic endothelial cells during zebrafish embryonic development. Elife. 6:e25932. (2017) 10.7554/eLife.25932.

[35] S. Isogai, M. Horiguchi, and B.M. Weinstein, The vascular anatomy of the developing zebrafish: an atlas of embryonic and early larval development. Dev Biol. 230 (2001) 278-301. doi: 10.1006/dbio.2000.9995.

[36] K.B. Tierney, D.H. Baldwin, T.J. Hara, P.S. Ross, N.L. Scholz, and C.J. Kennedy, Olfactory toxicity in fishes. Aquat Toxicol. 96 (2010) 2-26. doi: 10.1016/j.aquatox.2009.09.019. Epub 2009 Oct 30.

[37] E.Y. Ma, K. Heffern, J. Cheresh, and E.P. Gallagher, Differential copper-induced death and regeneration of olfactory sensory neuron populations and neurobehavioral function in larval zebrafish. Neurotoxicology. 69:141-151. (2018) 10.1016/j.neuro.2018.10.002. Epub 2018 Oct 4.

[38] K.B. Walters, J.M. Green, J.C. Surfus, S.K. Yoo, and A. Huttenlocher, Live imaging of neutrophil motility in a zebrafish model of WHIM syndrome. Blood. 116 (2010) 2803-11. doi: 10.1182/blood-2010-03-276972. Epub 2010 Jun 30.

[39] F. Peri, and C. Nusslein-Volhard, Live imaging of neuronal degradation by microglia reveals a role for v0-ATPase a1 in phagosomal fusion in vivo. Cell. 133 (2008) 916-27. doi: 10.1016/j.cell.2008.04.037.

[40] S. de Oliveira, E.E. Rosowski, and A. Huttenlocher, Neutrophil migration in infection and wound repair: going forward in reverse. Nat Rev Immunol. 16 (2016) 378-91. doi: 10.1038/nri.2016.49.

[41] D.M. Mitchell, A.G. Lovel, and D.L. Stenkamp, Dynamic changes in microglial and macrophage characteristics during degeneration and regeneration of the zebrafish retina. J Neuroinflammation. 15 (2018) 163. doi: 10.1186/s12974-018-1185-6.

[42] M.W. Salter, and S. Beggs, Sublime microglia: expanding roles for the guardians of the CNS. Cell. 158 (2014) 15-24. doi: 10.1016/j.cell.2014.06.008.

[43] N. Denans, S. Baek, and T. Piotrowski, Comparing Sensory Organs to Define the Path for Hair Cell Regeneration. Annu Rev Cell Dev Biol. 35:567-589. (2019) 10.1146/annurev-cellbio-100818-125503. Epub 2019 Sep 25.

[44] G. Ferrero, C.B. Mahony, E. Dupuis, L. Yvernogeau, E. Di Ruggiero, M. Miserocchi, M. Caron, C. Robin, D. Traver, J.Y. Bertrand, and V. Wittamer, Embryonic Microglia Derive from Primitive Macrophages and Are Replaced by cmyb-Dependent Definitive Microglia in Zebrafish. Cell Rep. 24 (2018) 130-141. doi: 10.1016/j.celrep.2018.05.066.

[45] R. Rua, and D.B. McGavern, Advances in Meningeal Immunity. Trends Mol Med. 24 (2018) 542-559. doi: 10.1016/j.molmed.2018.04.003. Epub 2018 May 3.

[46] K.E. Whitlock, Developing a sense of scents: plasticity in olfactory placode formation. Brain Res Bull. 75 (2008) 340-7. doi: 10.1016/j.brainresbull.2007.10.054. Epub 2007 Nov 21.

[47] J. Torres-Paz, and K.E. Whitlock, Olfactory sensory system develops from coordinated movements within the neural plate. Dev Dyn. 243 (2014) 1619-31. doi: 10.1002/dvdy.24194. Epub 2014 Oct 18.

[48] J. Torres-Paz, E.M. Tine, and K. Whitlock, Dissecting the neural divide: A continuous neurectoderm gives rise to both the olfactory placode and olfactory bulb. International Journal of Developmental Biology in press (2020).

[49] O. Bermingham-McDonogh, and T.A. Reh, Regulated reprogramming in the regeneration of sensory receptor cells. Neuron. 71 (2011) 389-405. doi: 10.1016/j.neuron.2011.07.015.

[50] J. Soller, J. Stephenson, K. Olivieri, J. Downing, and A.W. Olivieri, Evaluation of seasonal scale first flush pollutant loading and implications for urban runoff management. J Environ Manage. 76 (2005) 309-18. doi: 10.1016/j.jenvman.2004.12.007.

[51] F.W. Sunderman, Jr., Nasal toxicity, carcinogenicity, and olfactory uptake of metals. Ann Clin Lab Sci. 31 (2001) 3-24.

[52] C.J. Matz, and P.H. Krone, Cell death, stress-responsive transgene activation, and deficits in the olfactory system of larval zebrafish following cadmium exposure. Environ Sci Technol. 41 (2007) 5143-8. doi: 10.1021/es070452c.

[53] F. Tilton, S.C. Tilton, T.K. Bammler, R. Beyer, F. Farin, P.L. Stapleton, and E.P. Gallagher, Transcriptional biomarkers and mechanisms of copper-induced olfactory injury in zebrafish. Environ Sci Technol. 42 (2008) 9404-11. doi: 10.1021/es801636v.

[54] M. Lazzari, S. Bettini, L. Milani, M.G. Maurizii, and V. Franceschini, Differential response of olfactory sensory neuron populations to copper ion exposure in zebrafish. Aquat Toxicol. 183:54-62. (2017) 10.1016/j.aquatox.2016.12.012. Epub 2016 Dec 14.

[55] M. Dudek, A. Rosowski, M. Kozanecki, M. Jaszczak, W. Szymański, M. Sharp, and A. Karczemska, Microstructures Manufactured in Diamond by Use of Laser Micromachining. Materials (Basel). 13 (2020) 1199. doi: 10.3390/ma13051199.

[56] S.A. Carrillo, C. Anguita-Salinas, O.A. Peña, R.A. Morales, S. Muñoz-Sánchez, C. Muñoz-Montecinos, S. Paredes-Zúñiga, K. Tapia, and M.L. Allende, Macrophage Recruitment Contributes to Regeneration of Mechanosensory Hair Cells in the Zebrafish Lateral Line. J Cell Biochem. 117 (2016) 1880-9. doi: 10.1002/jcb.25487. Epub 2016 Jan 21.

[57] T.M. Tsarouchas, D. Wehner, L. Cavone, T. Munir, M. Keatinge, M. Lambertus, A. Underhill, T. Barrett, E. Kassapis, N. Ogryzko, Y. Feng, T.J. van Ham, T. Becker, and C.G. Becker, Dynamic control of proinflammatory cytokines Il-1β and Tnf-α by macrophages in zebrafish spinal cord regeneration. Nat Commun. 9 (2018) 4670. doi: 10.1038/s41467-018-07036-w.

[58] J. Xu, L. Du, and Z. Wen, Myelopoiesis during zebrafish early development. J Genet Genomics. 39 (2012) 435-42. doi: 10.1016/j.jgg.2012.06.005. Epub 2012 Aug 4.

[59] J.R. Mathias, M.E. Dodd, K.B. Walters, S.K. Yoo, E.A. Ranheim, and A. Huttenlocher, Characterization of zebrafish larval inflammatory macrophages. Dev Comp Immunol. 33 (2009) 1212-7. doi: 10.1016/j.dci.2009.07.003. Epub 2009 Jul 29.

[60] Q. Deng, S.K. Yoo, P.J. Cavnar, J.M. Green, and A. Huttenlocher, Dual roles for Rac2 in neutrophil motility and active retention in zebrafish hematopoietic tissue. Dev Cell. 21 (2011) 735-45. doi: 10.1016/j.devcel.2011.07.013.

[61] F. Barros-Becker, P.Y. Lam, R. Fisher, and A. Huttenlocher, Live imaging reveals distinct modes of neutrophil and macrophage migration within interstitial tissues. J Cell Sci. 130 (2017) 3801-3808. doi: 10.1242/jcs.206128. Epub 2017 Sep 28.

[62] S.K. Yoo, Q. Deng, P.J. Cavnar, Y.I. Wu, K.M. Hahn, and A. Huttenlocher, Differential regulation of protrusion and polarity by PI3K during neutrophil motility in live zebrafish. Dev Cell. 18 (2010) 226-36. doi: 10.1016/j.devcel.2009.11.015.

[63] A. Aspelund, S. Antila, S.T. Proulx, T.V. Karlsen, S. Karaman, M. Detmar, H. Wiig, and K. Alitalo, A dural lymphatic vascular system that drains brain interstitial fluid and macromolecules. J Exp Med. 212 (2015) 991-9. doi: 10.1084/jem.20142290. Epub 2015 Jun 15.

[64] A. Louveau, I. Smirnov, T.J. Keyes, J.D. Eccles, S.J. Rouhani, J.D. Peske, N.C. Derecki, D. Castle, J.W. Mandell, K.S. Lee, T.H. Harris, and J. Kipnis, Structural and functional features of central nervous system lymphatic vessels. Nature. 523 (2015) 337-41. doi: 10.1038/nature14432. Epub 2015 Jun 1.

[65] S. Da Mesquita, Z. Fu, and J. Kipnis, The Meningeal Lymphatic System: A New Player in Neurophysiology. Neuron. 100 (2018) 375-388. doi: 10.1016/j.neuron.2018.09.022.

[66] E. Dolgin, Brain's drain. Nat Biotechnol. 38 (2020) 258-262. doi: 10.1038/s41587-020-0443-1.

[67] H.M. Jung, D. Castranova, M.R. Swift, V.N. Pham, M. Venero Galanternik, S. Isogai, M.G. Butler, T.S. Mulligan, and B.M. Weinstein, Development of the larval lymphatic system in zebrafish. Development. 144 (2017) 2070-2081. doi: 10.1242/dev.145755. Epub 2017 May 15.

[68] Y. Padberg, S. Schulte-Merker, and A. van Impel, The lymphatic vasculature revisited-new developments in the zebrafish. Methods Cell Biol 138:221-238. (2017) 10.1016/bs.mcb.2016.11.001. Epub 2016 Dec 29.

[69] M. Desai, and J. Oppenheimer, "The Importance of Considering Olfactory Dysfunction During the COVID-19 Pandemic and in Clinical Practice". J Allergy Clin Immunol Pract 28 (2020) 31188-0.

[70] A.A. Divani, S. Andalib, J. Biller, D.M. Napoli, N. Moghimi, C.A. Rubinos, C.O. Nobleza, P.N. Sylaja, M. Toledano, S. Lattanzi, L.D. McCullough, S. Cruz-Flores, M. Torbey, and M.R. Azarpazhooh, Central Nervous System Manifestations Associated with COVID-19. Curr Neurol Neurosci Rep. 20 (2020) 60. doi: 10.1007/s11910-020-01079-7.

[71] E. Granton, J.H. Kim, J. Podstawka, and B.G. Yipp, The Lung Microvasculature Is a Functional Immune Niche. Trends Immunol. 39 (2018) 890-899. doi: 10.1016/j.it.2018.09.002. Epub 2018 Sep 22.

[72] A. Hidalgo, E.R. Chilvers, C. Summers, and L. Koenderman, The Neutrophil Life Cycle. Trends Immunol. 40 (2019) 584-597. doi: 10.1016/j.it.2019.04.013. Epub 2019 May 29.

CHAPTER 3: THE OLFACTORY ORGAN: A RESERVOIR OF NEUTROPHILS IN THE ADULT BRAIN

The olfactory organ: a reservoir of neutrophils in the adult brain

M. Fernanda Palominos[1, 2], Danissa Candia[1, 2], Jorge Torres Paz[3] and Kathleen E. Whitlock[1, 2]

1. Centro Interdisciplinario de Neurociencia de Valparaíso (CINV)

Pasaje Harrington 287, Universidad de Valparaíso

2. Instituto de Neurociencia

Avenida Gran Bretaña 1111, Universidad de Valparaíso

Valparaíso, Chile

Teléfono: 56-32-299-5510, 56-32-250-8040

FAX: 56-32-250-8027

3. Université Paris-Saclay, CNRS, Institut des Neurosciences Paris-Saclay, 91190, Gif-sur-Yvette, France

Manuscript to be submitted.

Abstract

Until recently the brain was thought to be immune privileged, lacking an inflammatory immune response that could potentially damage the nervous system. It is now known that the brain has an extensive lymphatic vasculature associated with the meningeal coverings. These brain lymphatics are a second drainage route, the first being via the subarachnoid space across the cribriform plate to the nasal mucosa and cervical lymph nodes. Little is known about the potential role of the olfactory epithelia and associated lymphatics in the immune response. To better understand the immune architecture in the olfactory organ we characterized the blood-lymphatic vasculature and the neutrophils in the olfactory sensory system of adult zebrafish. Here we describe an extensive lymphatic vasculature within the olfactory epithelia, where one cell type is also shared with the central nervous system. Surprisingly, the olfactory organs contain a large population of resident neutrophils in contrast to the brain where no neutrophils were observed. Next, to characterize the inflammatory response in the olfactory sensory system a chemical agent was used to eliminate olfactory sensory neurons in adult animals. Damage to olfactory epithelia resulted a rapid increase in neutrophils within the olfactory organs as well as the appearance of neutrophils in the brain. Further analysis of cell division during and after chemical treatment showed an expected increase in BrdU labeling in the neurogenic olfactory sensory epithelia as neurons were replaced, as well as BrdU labeling in the respiratory epithelia, the associated epineurium, and a subset of neutrophils. Our results reveal the existence of a new population of local neutrophils found only in the olfactory organ of the adult brain, suggesting a dual olfactory-immune function for this unique sensory system.

Significance Statement

It has been over one hundred years since scientists first introduced dyes into the subarachnoid space of the brain and elucidated a unique connection to the nasal mucosa and cervical lymph nodes. But what is the role of fluid drainage through the nasal mucosa? Here we show that two types of lymphatic cells are associated with the olfactory system and that the olfactory organ serves as a unique reservoir of neutrophils in the adult brain. Damage to olfactory sensory neurons triggers a rapid mobilization of these neutrophils within the olfactory organ followed by the appearance of neutrophils in the central nervous system. Thus, the olfactory organ may act as a secondary lymphoid organ protecting the nervous system.

Introduction

The adult olfactory organ blood-lymphatic system

In vertebrates the olfactory sensory neurons (OSNs), a group of continually-renewing neuronal population located in the olfactory epithelium (OE), extend their axons across the cribriform plate where they make their first synapses in the olfactory bulb (OB) (1, 2). This connection between the OE and the OB is part of a complex neural and immune interface that includes flow of cerebral spinal fluid (CSF) and interstitial fluid (ISF) from the subarachnoid space toward the nasal mucosa. Evidence supporting a connection between the subarachnoid space of the brain and cervical lymph nodes via the nasal mucosa was first proposed over a century ago (for review see: (3, 4). Subsequent studies in mammals using labeled tracers confirmed a drainage route from the cranial subarachnoid space through the olfactory pathway leaving the nasal mucosa via terminal lymphatics or into blood capillaries (5). Thus, the potential for turnover of brain extracellular fluids, via drainage to blood and deep cervical lymph, presented a system whereby immunogenic material and immune cells from the central nervous system (CNS) could pass to immune organs outside the brain.

The lymphatic system of vertebrates, composed of lymphatic vessels, lymphoid organs/tissues and the circulating lymph fluid, is highly conserved at the functional level (6) and is suggested to have originated in teleost fishes where the heart provided the energy to propel lymph through vessels associated with the primary vasculature (7). Lymphocytes are generated in primary lymphoid organs (thymus and bone marrow: mammals / thymus and kidney; teleost fishes) and maintained in secondary lymphoid tissues (spleen and lymph nodes; mammals/spleen, nasopharynx and gill tissues: teleost fishes) (8). Of particular interest are the nasopharynx-associated lymphoid tissues (NALT), a term used in mammals to describe the network of lymphoid tissue in the pharynx and palate (tonsils). Teleost fish lack organized lymphoid

structures such as tonsils yet a recent study suggested the presence of a NALT-like diffuse network of lymphoid and myeloid cells scattered both intraepithelial and in the lamina propria of the fish olfactory organ (9).

More recently the "re-discovery" of lymphatic vasculature associated with the meninges in the central nervous system (CNS) of mammals (10);(11);(12);(13) and of zebrafish (14); (15) coupled with more recent studies indicating that the meninges contain a diverse array of immune cells (16) that can migrate via the sinus-associated meningeal lymphatic vessels (17) and/or via cribriform plate and nasal lymphatics into cervical lymph nodes (18), have led to a renewed interest in immune trafficking in the nervous system. To date, in spite of over a century of reports on "brain drainage" through the olfactory system/nasal mucosa and the expanded knowledge of lymphatics in the vertebrate brain, there are no detailed descriptions of the lymphatic vasculature (LV) in the olfactory organ.

Neutrophils and the Nervous System

Neutrophils, the most abundant type of white blood cells, are normally found in the blood stream where they are rapidly recruited to a site of injury or infection and perform a critical role in inflammation and pathogen clearance. Neutrophils have been shown to interact with and regulate not only the innate but also the adaptive immune cells where they can rapidly migrate via afferent lymphatics of inflamed tissues to lymph nodes (19) (20) (21, 22). Thus, neutrophils migrate not only on the blood vasculature and interstitial tissues, but can migrate into the lymphoid system and are in the unique position to participate in the very early stages of both innate and adaptive immune responses. Under normal conditions, neutrophils are scarce in the central nervous system (CNS) where the brain–blood barrier (BBB) prevents their migration into the brain parenchyma and cerebrospinal fluid. Conditions of neuroinflammation and injury-induced damage to the BBB are associated with the infiltration of the CNS by neutrophils (23-25).

Previously, we performed both microarray and RNAseq analyses (26) (27) of adult OE zebrafish looking for differentially expressed genes involved in the formation of olfactory memory (28). In addition to known genes expressed in the OE, we found genes specific to both the innate and the adaptive immune systems (29), prompting us to investigate the potential "immune architecture" of the OE.

We have shown that neutrophils populate the developing olfactory organ and use the blood vasculature to migrate to the olfactory organ in response to injury (30). Inspired by the recent re-discovery of the CNS lymphatics in mammals and zebrafish (11, 15), we examined the extent of lymphatic vasculature in the adult olfactory organ and its association with blood vasculature. Neutrophils, known to play a key role in both the innate and the adaptive immune response (31);(32);(33)), are always found in the olfactory organ of adult zebrafish under both normal and damaged conditions. In fishes, the olfactory bulb may be involved in immune responses where activation of olfactory bulb results from peripheral neuronal signals. (34). Our results suggest that the olfactory organ has the potential to respond quickly to damage via a local population of neutrophils located in both the neuronal and non-neuronal tissues of the olfactory organ.

Material and Methods

Animals

Zebrafish were maintained in a re-circulating system (Aquatic Habitats Inc, Apopka, FL) at 28°C on a light-dark cycle of 14 and 10 hours respectively. All fish were maintained in the Whitlock Fish Facility at the Universidad de Valparaiso. Wild-type (WT) fish of the Cornell strain (derived from Oregon AB) were used. All protocols and procedures employed were reviewed and approved by the Institutional Committee of Bioethics for Research with Experimental Animals, University of Valparaiso (#BA084-2016).

Adults were around 1 year old. Transgenic lines were used to visualize specific cell types. *Tg(BACmpx:gfp)*^{i114}, *Tg(mpx:GFP) (61)*; (*Tg(fli1a:EGFP)*^{y1} *(fli1a:EGFP*; (62); *Tg(−5.2lyve1b:DsRed)*^{nz101},*((2lyve1b:DsRed) Tg(−5.2lyve1b:EGFP)*^{nz151} (*lyve1b:EGFP*), *(63); Tg(gata1a:DsRed)*^{sd2} (*gata1a:DsRed*) (64), *Tg(pOMP*^{2k}*:gap-YFP)*^{rw032a}, (OMP:YFP); *Tg(pOMP*^{2k}*:lyn-mRFP)*^{rw035a} *Tg(OMP:RFP*); and *Tg(pTRPC*$^{4.5k}$*:gap-Venus)*^{rw037a} (65); *Tg(six4b:mCh)*, (66).

Copper Exposure

Initial dose response analysis was performed based on previous work in zebrafish and salmon (67); (68). A stock solution of 10 mM $CuSO_4$ was diluted in filtered embryo medium (69) to a final concentration of 10 uM $CuSO_4$. Adult animals were exposed to the same concentration of copper, but dissolved in system water.

Immunocytochemistry and Cell Labeling

Staged larvae and dissected adult brains were fixed in 4% PFA in 0.1M phosphate buffer 0.4M pH 7.3), or 1X phosphate-buffered saline PBS pH 7.4). Larvae were rinsed three times in phosphate buffer or PBS, permeabilized in acetone at -20 ºC for 10 minutes then incubated for two hours in blocking solution (10 mg/ml BSA, 1% DMSO, 0.5% Triton X-100 (Sigma) and 4% normal goat serum in 0.1M phosphate buffer or 1X PBS). Primary antibodies used were anti-

RFP (rabbit 1:250, Life Technologies), anti-GFP (mouse 1:500, Life Technologies), anti-GFP (rabbit 1:500, Invitrogen), anti-SOX2 (mouse 1:250, Abcam), anti-Acetylated tubulin (rabbit 1:500, Abcam), anti-DsRed (mouse 1:500, Santa Cruz Biotechnology), anti-HuC/D (rabbit 1:500, Invitrogen) and anti-BrdU (rabbit 1:250,Invitrogen). Adult brains were incubated in primary antibodies for up to a week. After washes, tissues were incubated overnight in any of the following secondary antibodies, as appropriate: Dylight 488 conjugated anti-mouse antibody (goat 1:500, Jackson Immuno Research), Alexa Fluor 488 conjugated anti-rabbit antibody (goat 1:1000, Molecular Probes), Alexa Fluor 568 conjugated anti-rabbit antibody (goat 1:1000, Molecular Probes), Alexa Fluor 568 conjugated anti-mouse antibody (goat 1:1000, Molecular Probes), Dylight 650 conjugated anti-rabbit antibody (goat 1:500, Jackson Immuno Research), Alexa Fluor 350 conjugated anti-rabbit antibody (goat 1:1000, Molecular Probes). Tissues were then rinsed in 0.1M phosphate buffer or 1X PBS with 1% DMSO, stained for DAPI (1 µg/ml, Sigma), washed in 0.1M phosphate buffer or 1X PBS and mounted in 1.5 % low melting temperature agarose (Sigma) in an Attofluor Chamber for subsequent imaging (see below).

Cryosectioning. Adult fish were sacrificed, then fixed and embedded in 5% sucrose/ 1.5 % agarose in mqH_2O. Blocks were then submerged in 30% sucrose for 2-3 days and then stored covered by O.C.T. Compound (Tissue-Tek®) in cryomolds at -20ºC. Twenty-five µm cryosections were cut and processed for immunofluorescense as described above; primary and secondary antibodies were incubated overnight. Non-fluorescent labeling was done using Vectastain ABC Kit (Mouse IgG, Vector Laboratories) and ImmPACT DAB peroxidase substrate kit (Vector Laboratories) following manufacturer recommendations.

For flat mounting, olfactory rosettes were dissected after immunohistochemistry or staining, and caudal-mounted in Poly-L-Lysine coated slides between triple 22x22 coverslip bridges and covered in VECTASHIELD® Antifade Mounting Media (Vector laboratories).

BrdU Labeling

Fish were selected and placed overnight in 10 mM BrdU in system water. Fish were placed in 1.5-liter tanks with system water (control) and tanks with system water containing 10 μM $CuSO_4$, and allowed to swim freely (4 hours). All control and half of Cu-exposed fish were then anesthetized, sacrificed, and heads fixed overnight in 4% PFA/1X PBS. The other half of the fish exposed to copper were transferred to a clean 1.5-liter tank, filled with system water, and allowed to recover. The next day, these fish were anesthetized, sacrificed, and fixed as described above. After fixation, heads were incubated in EDTA (0.2 M, pH 7.5) for three days at 4 ºC and brains dissected in sterile 1X PBS and pre-treated in 2 M HCl for 30 minutes at 37 ºC. Immunocytochemistry was performed as described in Immunocytochemistry & Staining section. For imaging, whole adult brain were mounted on 2% low melting temperature agarose, and the OEs mounted between coverslips, as described above. (The removal of brains from the skull with the OO still attached is a difficult dissection because the OSN axons pass through the cribriform plate to arrive in the OB. Therefore it was not always possible to have a preparation with both OE still connected to the brain.)

Cryosectioning

Fish were euthanized and heads were fixed overnight in 4% PFA at 4 ºC and decalcified in EDTA (0.2 M, pH 7.6) for 3 days, and embedded in 1.5% agarose/ 5% sucrose blocks and submerged in 30% sucrose for 2 days at 4 ºC. Blocks were frozen (-20 ºC) with O.C.T. Compound (Tissue Tek®) and sectioned (20 μm) using a cryostat.

Imaging and Image analysis

Microscopy: Fluorescent images were taken using a Spinning Disc microscope Olympus BX-DSU (Olympus Corporation, Shinjuku-ku, Tokyo, Japan) and acquired with ORCA IR2 Hamamatsu camera (Hamamatsu Photonics, Higashi-ku, Hamamatsu City, Japan). Images were acquired using the Olympus CellR software (Olympus Soft Imaging Solutions, Munich, Germany). Some images were also obtained using a confocal laser scanning microscope (Nikon

C1 Plus; Nikon, Tokyo, Japan). Images were then deconvoluted in AutoQuantX 2.2.2 (Media Cybernetics, Bethesda, MD, USA) and processed using FIJI (National Institute of Health, Bethesda, Maryland, USA; (70) and CellProfiler (71).

Live imaging: Images were captured using a Spinning disc confocal microscope (Olympus) with a 20X 0.95 NA water immersion LUMPlanFL/IR objective. Temperature was maintained at 26-28ºC during this time.

Image Analyses

Neutrophils: Only neutrophils within the boundaries of the sensory tissue in adults were counted and the values were given as the average of total number of mpx:GFP positive with standard deviation. Values given for paired sensory structure are a sum of the values for the individual sensory tissues. For time-lapse videos all counts of neutrophils in the two olfactory organs were combined for each animal and the mean/SEM calculated for each time point.

To analyze the distribution of mpx:GFP positive neutrophils from both whole adult brains and flat-mounted olfactory rosettes, images were filtered by size (6-30 μm) and pixel intensity, and then counted using CellProfiler available Pipelines (71). For quantification of neutrophils in different regions of the OE, sensory (ss) versus non-sensory (ns) regions were separated using *Tg(OMP:RFP)* animals or anti-HuC/D labeling as neuronal markers. We grouped the ns region with the epineurial extensions (EN) wrapping the OE. The percent of total neutrophils is the number of GFP cells in ss or ns regions, divided by total (sum of all GFP positive cells in ss, ns and EN). BrdU nuclei were detected by filtering size between 2-5 μm and co-localization between BrdU and neutrophils was done using "Co-localization" Pipeline in CellProfiler (71).

The circularity index of each neutrophil was calculated using Analyze Particles in FIJI (National Institute of Health, Bethesda, Maryland, USA; (70). Neutrophils were size-filtered and values were graphed according frequency of distribution.

*BV/LV vessel density***.** Density is defined by the ratio of the area positive for fli1a:EGFP (BV) and lyve1b:DsRed (LV) over the total dorsal telencephalic or the olfactory system area (which includes both the OE and OB). Protocol adapted from Zhao et al., 2016. *Scientific Reports*.

Statistics. Data are presented as means ± standard deviations. Statistical analysis were done using Prism 9 (Graphpad), and are indicated in each figure legend. Unpaired Student's t-tests were performed unless otherwise indicated. P values are indicated as follows: *P, 0.05, **P, 0.01, ***P, 0.001.

Acknowledgements

Grants/Fellowships Fondo Nacional de Desarrollo Científico y Tecnológico (FONDECYT) 1160076 (KEW); ICM-ANID Instituto Milenio Centro Interdisciplinario de Neurociencias de Valparaíso PO9-022-F, supported by the Millennium Scientific Initiative of the Ministerio de Ciencia (K.E.W; MFP) and Graduate Fellowship (CONICYT) 21161437 (MFP).

Results

The Adult Olfactory Sensory System has Extensive Lymphatic Vasculature

Previously, we have shown that the lymphatic vasculature (LV) associated with the developing olfactory organs is evident at 14 days post fertilization (dpf) initiating in the ventrolateral side of the organ (30). To better understand the LV system in the olfactory sensory system of the adult we dissected brains, with olfactory organs attached, from *Tg(lyve1b:EGFP;OMP:RFP)* animals (Fig. 1). The olfactory organs (OO) are made up of sensory epithelia containing the OMP:RFP positive sensory neurons (Fig. 1 *A-D*, *F*, red) and respiratory epithelia, surrounded by what appears to be an extension of the epineurium (EN) of the olfactory nerve (Fig 1, *A-D*, EN). At this point it is not clear where the meningeal membranes fuse with the epineurium after crossing the cribriform plate (3). Viewed from the dorsal side, lyve1b:EGFP positive LV were found in the OO (Fig 1, *A*, OO, green, *B*, green, arrowheads), olfactory bulb (Fig 1, *A*, OB, green, arrow) and diencephalon (Fig. 1 *A*, TeO, green, arrow), but not the telencephalon. In the dorsal OO the lyve1b:EGFP positive cells (Fig. 1 *B*, green, arrowheads) line the lamellae of the OE (Fig. 1 *B*, LOE). In contrast, when viewed from ventral there was an apparently continuous network of LV extending from the OO to the OB and along ventral telencephalon (Fig. 1 *C*, *D*, green). The lyve1b:EGFP positive cells were also evident in the ventral OO associated with the olfactory nerve (Fig. 1 *D*, ON, red). Two morphologically distinct lymphatic cell types were observed. In the OO thick tubular cells associated with the LOE (Fig. 1 *B*, *D*, arrowheads) occur, which resemble the High Endothelial Venules (HEV-like, HEV-L; Fig. 1, *E*) that control lymphocyte trafficking in mammals (35). To date these cells have not been described in the peripheral olfactory sensory system. In the OB, we observed smaller lyve1b:EGFP positive cells covering the dorsal OB and ventral telencephalon, apparently connected by fine processes and resembling Mural Lymphatic Endothelial Cells (muLEC-L) after Bower (14) (Fig. 1 *D*, arrows, green, *F*, muLEC-L, green). This cell type was also observed in the OO (Figs. S1, S2). In contrast to the

cells described by Bower, the muLEC-L appeared to be connected by fine processes (Fig. 1, *F*, arrows) and not occur as separate cells like the BV-associated muLECs (14). At this time it is not clear whether these connections have a lumen. Thus, in adult zebrafish there is an extensive LV system associated with the olfactory sensory system (Fig. 1) that wraps the OE (HEV-L), encompassing the olfactory bulb (muLEC-L) with apparently continuous connections along the ventral telencephalon (Fig. 1 *C*).

To investigate the association between the lymphatic vasculature (LV) and the blood vasculature (BV) in the OOs, *Tg(lyve1b:DsRed;fli1a:EGFP)* animals were used to visualize the LV (red) and BV (green) (Fig. S1). We found extensive BV (fli1a:EGFP-positive) surrounding the OE associated with the EN in both the dorsal (Fig S1 *A*, green) and ventral (Fig S1 *B*, green) OO and OB. The BV (Supp. Fig S1 *A*, *B*, green) and LV (Supp. Fig. 1 *A*, *B*, red) form an extensive network extending along the lamellae of the dorsal and ventral OE. In comparing the density of BV and LV in the dorsal brain, the OE/OB have a richer BV and LV density than the telencephalon (Fig. S1 *C*) as the BV and LV are intimately associated within the OO/OB (*lyveb1:DsRed: Tg(fli1a:EGFP)*. The BV and LV extended along the EN that surrounds the LOE (Fig. S1 *D*). In the *Tg(lyve1b:DsRed;fli1a:EGFP)* animals (Fig. S1 *E*, *F*) the LV (red) and BV (green) meet at the tips of the LOE where muLEC-L like cells were observed. Thus, the extensive BV/LV associated with the EN connects with the BV of the olfactory epithelia in the distal lamellae.

In mammals, the olfactory lymphatic route crosses the cribriform plate separating the OBs and OOs, draining cerebral spinal fluid (CSF) through the perineural space surrounding olfactory nerve (18), connecting to nasal lymphatics and carrying lymphatic endothelial cells T, B lymphocytes and antigen presenting cells (APCs) toward cervical lymph nodes (36). To characterize the LV structure crossing the cribriform plate we sectioned intact, decalcified heads from *Tg(lyve1b:DsRed;fli1a:EGFP)* animals to determine whether the muLEC-L cells or HEV-

L cells extended across the cribriform plate (Fig. S2, CP). Dorsal to, and at the site of, ON crossing (Fig. S2, *A*, *B*) the OE was populated primarily by fli1a:EGFP-positive BV. Leaving the ON and advancing ventrally (Fig. S2, *C*, *D,* arrows) extensive lyve1b:DsRed-positive LV was observed in the OE and associated with fli1a:EGFP-positive BV crossing the cribriform plate (Fig. S2, *E,* arrows*)*. We never observed HEV-L cells (Fig 1, *E*) crossing the CP or on the intra-cranial side of the ethmoid bone. Thus the muLEC-L cells associated with the BV were found wrapping the exterior surface of the OB (Fig. 1), crossing the CP (Supp. Fig. S2) and extending along the EN (Fig. S1) where they were associated with the HEV-L LV (Fig. S2, *F*).

Neutrophil population in the adult olfactory organ

Neutrophils, the most abundant leukocyte sub-types in adult zebrafish, are essential players in the innate immune system and more recently have been shown to migrate not only on BV but also LV. We used the *Tg(OMP:RFP);Tg(mpx:GFP*) animals to visualize olfactory sensory neurons (red) and neutrophils (green), in fixed whole mount brains. Surprisingly, we observed neutrophils only in the OO of adult brains (Fig. 2 *A*, *B* green). Neutrophils were localized in the fingerlike lamellae of the OE predominantly associated with the EN wrapping around the OE (Fig S1, *A, B*). The OMP:RFP positive OSNs (Fig. 2 *A*, *B*, red, ss, red) are in the central OE (ss) and peripheral regions of the lamellae are non-sensory epithelia (Fig. 2, *B*, ns). The tips of the LOE are connected to the EN (Fig. 2 *B*, EN, LOE, blue; Fig. S1). Analysis of the distribution of GFP-positive neutrophils revealed that they were located primarily in the ns epithelia and EN with many fewer neutrophils in the ss epithelia (Fig. 2, *C*, *D*, *D1*, *E, F*). Within the OE/EN there were three morphologically distinct mpx:GFP-positive cells (Fig. 2 rounded, *C*; amoeboid, *D*; columnar, *D1; F*). Neutrophils with rounded shape (Fig. 2, *C*, green, nt1) were associated with the basal OE, while neutrophils with amoeboid like morphology (Fig. 2 *C*, green, nt2, *D*, ci=0.7) were present in the tips of the LOE and EN, although this distribution changed in response to damage of the OE (see below). In sectioned OE tissue the columnar shaped mpx:GFP-positive

cells (Fig. 2, *D1*, green) were morphologically similar to sustentacular cells of the OE visualized with the *Tg(six4b:mCh)* reporter line ((37); Fig. S3 *A, B* red). These cells lie at the interface of the ss and ns epithelia (Fig. S3 *C*) and further studies are needed to carefully characterize this class of GFP-expressing cells. To confirm that the neutrophils observed in the whole mount OE (Fig. 2, *G*, green) were within and not on the surface of the OE, a z-stack analysis was performed (Fig. 2, *H*) showing that the mpx:GFP-positive cells are in the OE tissue. Thus the adult OOs are unique because they are the only regions of the adult brain where resident neutrophils are found under normal conditions.

Neutrophil response to damage in the adult olfactory sensory system

In order to investigate the neutrophil response to damage of the OE, we exposed *Tg(mpx:GFP);Tg(OMP:RFP*) adult fish to 10 μM CuSO4. Because of the challenges of live imaging in the whole mount adult brain, we sacrificed adults at different times after copper exposure to follow the dynamics of neutrophil response over time. In untreated control animals, and consistent with previous results, neutrophils were observed only in the OO (Fig. 3 *A*, arrowhead, A') and were absent in the brain (Fig. 3 *A*). After four hours of copper exposure, an increase in neutrophils was observed in the OO (Fig. 3 *B*, green, arrowhead, *B'*, *B''*). Within the OO the ns and ss OE as well as the EN (Fig. S4) showed an increase in neutrophils in response to damage. Additionally neutrophils were observed in the ventromedial OB, along the telencephalic ventricle (Fig. 3, *B*, OB, V) and in the ventral telencephalon (Fig. 3 *B*, green, arrows). Fish left to recover for one day post-treatment still showed elevated numbers of neutrophils in the ventral OB (Fig. 3, *C*, green, arrows, *D*) and the OO (Fig. 3, *C'*, green). The increased numbers of neutrophils in the OO and subsequent appearance of neutrophils in the ventral OB and ventral telencephalon (Fig. 3, *D*, *E*, vCNS), suggests that neutrophils may move from the OO into the ventral CNS in response to peripheral damage.

Damage induced changes in cell cycle dynamics in the olfactory sensory system

To further investigate the cellular dynamics of the neutrophil response to copper-induced damage in the adult, we repeated the experiments with copper using *Tg(mpx:GFP)* animals in the presence of BrdU. When viewed in flattened whole mount preparations (Fig 4, *A*-*C*), the OE of the adult is organized as a "rosette" with the central region midline raphe (mr) surrounded by ss and the outer regions of the rosette (tips of the lamellae) containing the ns or respiratory epithelia. In control animals (Fig. 4, *A*, viewed looking into the rosette) BrdU labeling consistent with the mitogenic nature of the olfactory system was observed (38, 39). After four hours of exposure to copper, BrdU labeling showed significant increases in the mr (Fig. 4, *B*, white, arrow), and in the ns epithelia extending to the EN. In contrast, one day post treatment (dpt) significant increases in BrdU labeling were observed in the ss epithelia (Fig. 4 *C*, *F*) consistent with the renewal of OSN in the OE after damage (40). Additionally, the neutrophils now lined LOE (Fig. 4, *C*, green), possibly in association with the BV (Fig. 4, *D*, green). The number of neutrophils showed significant increases at 4 hours post-treatment (hpt) and remained high in the ss epithelia one dpt (Fig, 4, *E*; 444.67 ± 31.39 and 373.33 ± 32.32 neutrophils in 4 hpt, red, and 1 dpt, green). Significant increases in BrdU labeling at both 4 hpt and 1 dpt were observed only in the ss epithelia (Fig. 4, *F*; 480 ± 241.76 and 786 ± 211.6, respectively). Analysis of cells expressing both mpx:GFP and BrdU showed a significant increase compared to control animals (Fig. 4 *G*, control: 9 ± 1, 4 hpt: 26 ± 6, 1 dpt: 22 ± 5.29). The frequency of rounded (see Fig. 2 green, nt1; ci 0.7 or greater) and amoeboid-like neutrophils (see Fig. 2 green, nt2; ci 0.4-0.6), potentially representing "resting" and activated neutrophils, respectively, increased in the OE post-damage (Fig. 4, *H*). The columnar shaped cells (ci 0.1-0.3) increased in frequency at one dpt in the sensory region (Fig. 4, *H*, green, 0.2 -0.3 green bars) but remained as the least

common morphology. We found that damage to the OE resulted in an increased number of rounded neutrophils and a small but significant number were double labeled for BrdU, indicating that the majority of the increase in neutrophil number was likely due to migration as opposed to proliferation. Future work using photoconversion will allow us to determine the exact contribution of local vs. immigrant neutrophils in the response to damage in developing and adult fish brain.

Discussion

In this study we have shown that the olfactory sensory system has a unique "immune architecture" where neutrophils permanently populate the sensory organ in association with a complex network of BV-LV. These neutrophils mount a rapid response to copper-induced damage to the OE populating not only the tissues of the OE and associated EN, but also appearing in tracts extending posteriorly along the ventral CNS. These data demonstrate a role for resident neutrophils in the olfactory sensory system and suggest that the nasal lymphatic pathway may be a potential site of entry for immune cells into the CNS.

Lymphatic Vasculature

The olfactory/nasal lymphatic route first described using India ink to label CSF drainage pathways from the brain where particles moved from cranial subarachnoid space to lymphatic channels of the olfactory mucosa (3). Subsequently, it was shown that while the subarachnoid space of the optic nerves and cochlea region were labeled, the only direct connection between cranial CSF and lymphatics was the nasal route (41-43) passing through cribriform plate along perineural spaces near the olfactory nerves to the nasal mucosa and cervical lymph nodes (18). With the re-discovery of the brain lymphatics (11) the relative importance of the drainage of CSF via the meningeal LV versus olfactory/nasal LV is currently a subject of debate, (see for discussion (13).

In descriptions of the olfactory/nasal drainage in mammals, the LV is generally depicted with terminations at the extra-cranial side of the cribriform plate. Here we found two types of lyve1b:EGFP positive LV: one having muLEC like structure where the cells line the BV (14, 15), appeared to be connected, and were found on both the intracranial and extra cranial side of

the cribriform plate; and a second with morphology similar to HEVs that were found in association with the OE/EN on the extra-cranial side of the cribriform plate.

The muLEC-like LV wrap the dorsal and ventral surfaces of the olfactory bulbs extending posteriorly along the ventral telencephalon and anteriorly through the cribriform plate with the BV. Within the muLEC-like cells there were two populations: one positive only for lyvel1b and a second positive for both lyve1b and fli1a. During development, muLECS have been shown to form from local blood vessels by (14) and these forming cells are positive for fli1a and lyve1b. Thus, the lyve1b+/fli1a+ population may represent adult progenitors of LV important in restructuring the OE after extensive damage. The muLEC-like cells appear to be connected, yet future studies are needed to confirm that these cells are from the non-lumenized mural lineage (44).

Lymph node equivalent in fish

In mammals the nasal lymphatic route that drains into the cervical lymph nodes through the cribriform plate, carry immune cells such as monocytes, dendritic cells, and T cells (45, 46). In addition, mammals have Nasal-Associated Lymphoid Tissue (NALT) also referred to as Waldeyer's lymphatic ring, surrounding the naso/oropharynx. This tissue contains lymphatic vessels and HEVs, which are specialized post-capillary venous swellings, enable lymphocytes circulating in the blood to directly enter a lymph node (by crossing through the HEV). Recently, tissue described as NALT has been reported in fish (34, 47), yet fish do not have lymph nodes. Thus a distinction is made between “organized” NALT and “diffuse NALT” (47) or NALT versus non-NALT (for murine nasal dendritic cells (48) where teleost fish have diffuse-NALT/non-NALT in the olfactory organs. Here we found that the OE/EN has an extensive blood vasculature associated with lyve1b:EGFP positive lymphatic endothelial cells resembling high endothelial venules (HEVs) of the lymph nodes in mammals (Fig. 5, olfactory rosette, upper, HEV-like). The HEV-like cells were localized to the tips of the LOE extending on the

external side of the EN to the base, terminating in the region where the meningeal membranes fuse on the extra-cranial side of the cribriform plate. At the tips of the LOE, on the internal side, the BV is associated with the HEV-like cells and in this region we identified lyve1b/fli1a positive cells similar to those seen in the OB although not on the BV. This cell type was also observed lining the cribriform plate in the region of the meninges (Fig. S2). The structures observed raise the possibility that, in spite of lacking lymph nodes, the zebrafish OO shows similarities to mammalian lymph node organization thus suggesting the existence of an organized secondary lymphoid tissue in the OO.

Neutrophils

It has recently been shown that neutrophils, in addition to their role as the first line of defense in the innate immune response, also transport antigens and populate lymph nodes via HEVs where they coordinate early adaptive immune responses (22, 49, 50). Neutrophils are found in many tissues and these subpopulations of neutrophils perform many functions (51) such as in the lung, which is known to retain neutrophils as a host defense niche (52, 53). In mammals the OE is reported to have B lymphocytes, lactoferrin and lysozyme, in the Bowman's glands (54) and neutrophils in the non-sensory epithelium of the vomeronasal organ (55). In teleosts, limited morphological studies have shown scattered myeloid and lymphoid cells within the OE and lamina propria (9, 56) (57)). Most recently, in the OO, in response to inflammation neutrophils infiltrate and later express neurogenesis-related genes suggesting a potential role for neutrophils in the ongoing neurogenesis of the OE (58).

The neutrophils we observed in the OO were striking not only in their number but also their limited distribution: they were found only in the OO of the adult brain under normal conditions. After copper exposure there was a large increase in the number of neutrophils in the OE/EN and subsequently neutrophils appeared in the CNS, initially in the ON and ventral lateral OB, and then extending posteriorly along the ventral telencephalon although far fewer neutrophils were

observed in the CNS. This ventral tract from OO contains a rich network of LV (Fig. 1), and has previously been suggested as a route for immune cell influx through the basal forebrain in mice (59) and mesenchymal stem cell migration cell from the periphery to the OB (60). Thus, the pattern of neutrophils observed is suggestive of neutrophil movement from the periphery along the ON, ventral OB, and ventral telencephalon. While it is tempting to propose that these neutrophils enter from the OE into the CNS, more experiments are needed to better understand the source of the CNS neutrophils.

In summary, in mammals the olfactory/nasal brain lymphatic drainage system is assumed to function in water homeostasis and pressure regulation and the meningeal lymphatic system in immune responses and surveillance (18). Yet, here we have shown that the OO has an extensive blood lymphatic vasculature (including HEV-like structures) enveloping the OE, a large resident neutrophil population and, furthermore, that damage induced in the olfactory sensory epithelia is correlated with the appearance of neutrophils in the brain. Whether the presence of these neutrophils is related to the regenerative properties of the OE as the OSNs undergo constant replacement, represents a special population secondary lymphoid tissue capable of mounting a rapid immune response, or both, remains to be determined.

Figures & Figure legends

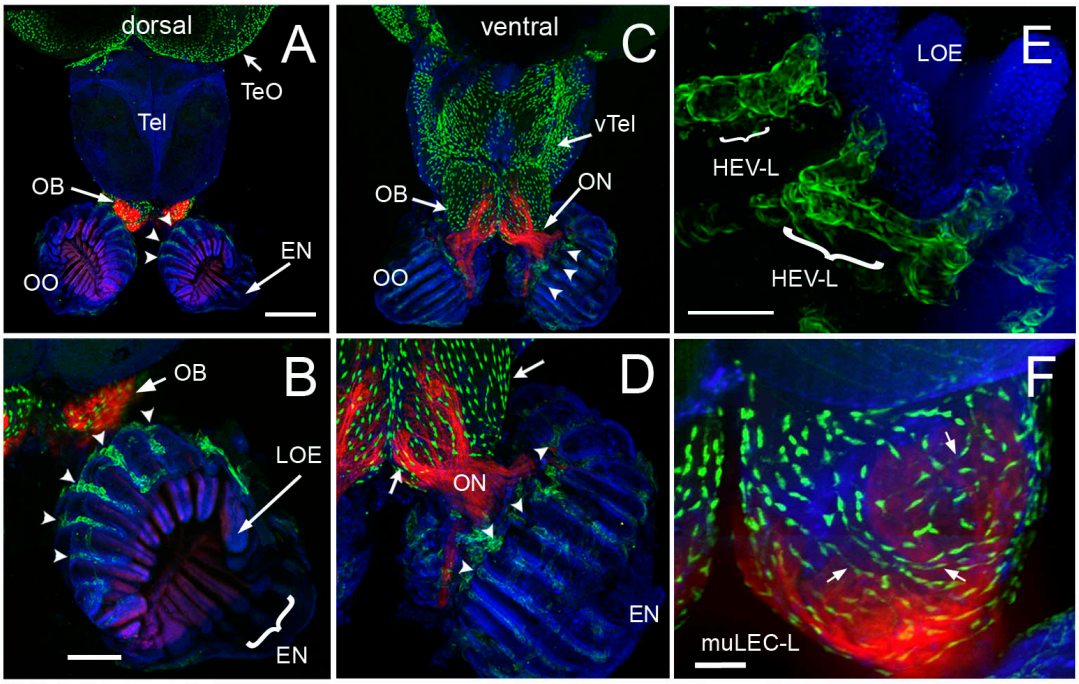

Figure 1

Figure 1. The adult olfactory organ have an extensive blood-lymphatic system

(A-F). Whole mount brains of adult *lyve1b:EGFP;OMP:RFP* animals with OSN (red) and lymphatic vasculture (green). (*A*) The OE and OBs have extensive lymphatic vasculature (LV, green) but not dorsal the telencephalon (Tel). (*B*) Higher magnification of OO in *A* with meningeal extension (EN, arrow) wrapping around outer surface of lamella of the OE (LOE). Lymphatic cells are found in OO (arrowheads) and OB. (*C*) The LV extends centrally from the OO/OB along the ventral telencephalon (vTel) posteriorly to the ventral diencephalon. (*D*) Higher magnification of OO in *B*. LV (arrowheads) is associated with olfactory nerve (ON, red) and covers ventral surface of OB (green, arrows). (*E*) Lyve1b:EGFP positive cells in tips of LOE resemble High Endothelial Venules (HEVs). (*F*) Putative Mural lymphatic endothelial cells (MuLECs) wrap the OB (arrows). Representative images selected from detailed analysis of 9 brains. DAPI (blue). A, C**,** = 200 μm; B, D = 100 μm; C, F = 50 μm.

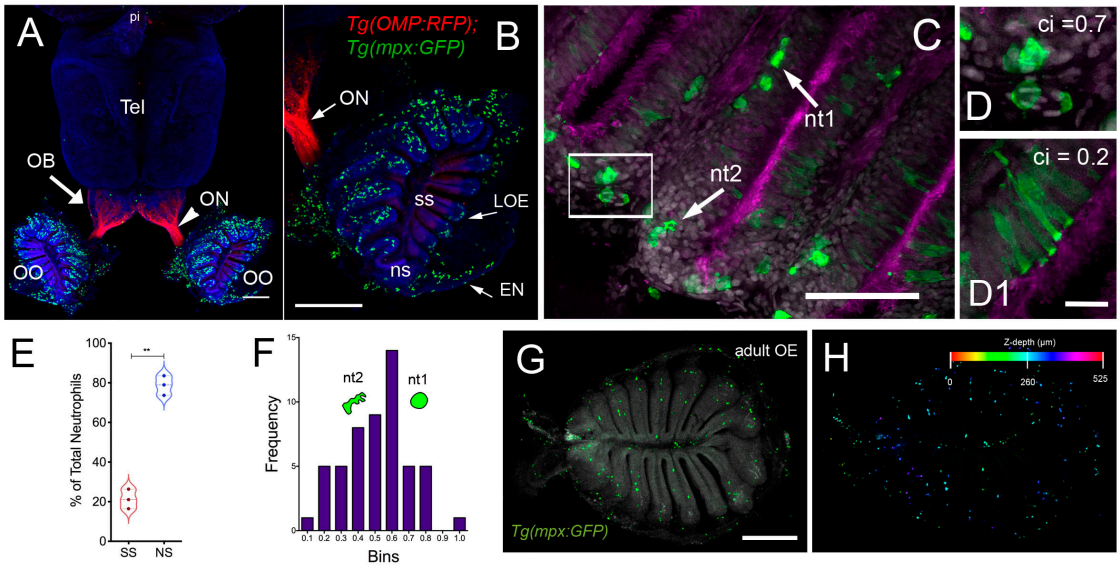
A
pi
Tel
OB
ON
OO
OO
B
Tg(OMP:RFP);
Tg(mpx:GFP)
ON
ss
LOE
ns
EN
C
nt1
nt2
D
ci =0.7
D1
ci = 0.2
E
% of Total Neutrophils
100
80
60
40
20
0
SS
NS
F
Frequency
15
10
5
0
nt2
nt1
0.1 0.2 0.3 0.4 0.5 0.6 0.7 0.8 0.9 1.0
Bins
G
adult OE
Tg(mpx:GFP)
H
Z-depth (µm)
0
260
525

Figure 2

Figure 2. Neutrophils are found only in the olfactory organ of the adult brain.

(*A*) Wholemount brain of *Tg(OMP:RFP);Tg(mpx:GFP)* adult: neutrophils (green) are only present in the OO (OE/EN), telencephalon (tel), pineal (pi). (*B*) OO (from A) contains a large population of neutrophils (green, *n*=487 neutrophils). OMP:RFP positive OSNs are located only in sensory epithelia (ss, red) not in non-sensory epithelia (ns), olfactory nerve (ON). (*C*) Neutrophils with a rounded shape, (*C*, nt1, arrow) with a circularity index 0.7 or greater (*D*, *F*) were observed in the LOE. Amoeboid neutrophils, (*C*, nt2, arrow) with a circularity index of 0.4-0.6 (F), were located throughout the OE and EN. Sustentacular-like cells (*D1*), circularity index 0.2 (*F*), lie at ointerface of ns-ss epithelia (Fig. S3). (*E*) Total number of neutrophils in the OO. The non-sensory (ns) tissues (respiratory epithelia + NE, blue) have more neutrophils than sensory epithelia (ss, red), n=3 adult fish, 6 OE. (*F*) Frequency distribution of nt1 and nt2 cells (*n*= 53 neutrophils). (*G*) Maximal projection of whole mount *Tg(mpx:GFP)* adult OE: Neutrophils (green); autofluorescence (gray). (*H*) Neutrophils (from *G*) were color-coded based on (H) Z-stack depth. Total depth= 550µm. Scale bars A, B = 200 µm; C = 60 µm; D, D1=20 µm; G, H =100 µm.

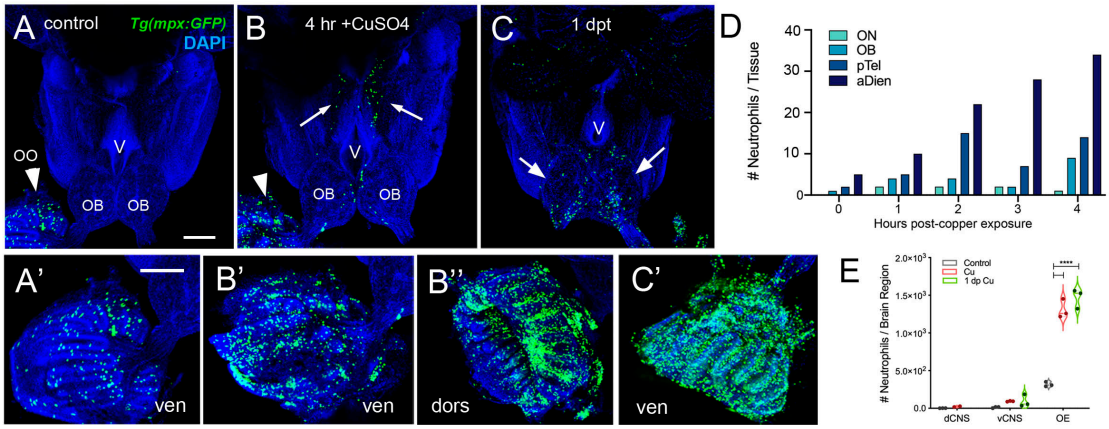
A control
Tg(mpx:GFP)
DAPI
OO
V
OB
OB
B 4 hr +CuSO4
V
OB
OB
C 1 dpt
V
D
Neutrophils / Tissue
ON
OB
pTel
aDien
Hours post-copper exposure
A'
ven
B'
ven
B''
dors
C'
ven
E
Neutrophils / Brain Region
Control
Cu
1 dp Cu
dCNS
vCNS
OE

Figure 3

Figure 3. Exposure to copper is correlated with incerased neutrophils in the peripheral and central nervous system.

(*A-C*) Ventral views of whole mount adult brains from *Tg(mpx:GFP)*. (*A, A'*). Control with neutrophils found only in OO (arrowhead; A'). (*B*) After four-hour exposure to copper, there is an increase in the number of neutrophils in the OO (*B*, arrowhead, *B'*, *B*"). Neutrophils were observed in the ventral OB, along the ventricle (V) and in the ventral telencephalon (*B*, arrows). (*C*) One day post treatment neutrophils are still present in OO (*C'*), OB (arrows) and ventral telencephalon. (*D*) Neutrophils appear over time in an anterior to posterior spatial pattern in the CNS. OO is not plotted because number (average ~1,500) is out of range (see E). (*E*) Copper exposure was correlated with increased neutrophils in OE and ventral CNS. For all experiments at least 6 brains were examined. Preparations were selected for imaging based on whether they were intact and the signal to noise of the labeling. Scale bars: A-C; A'-C'= 100 μm.

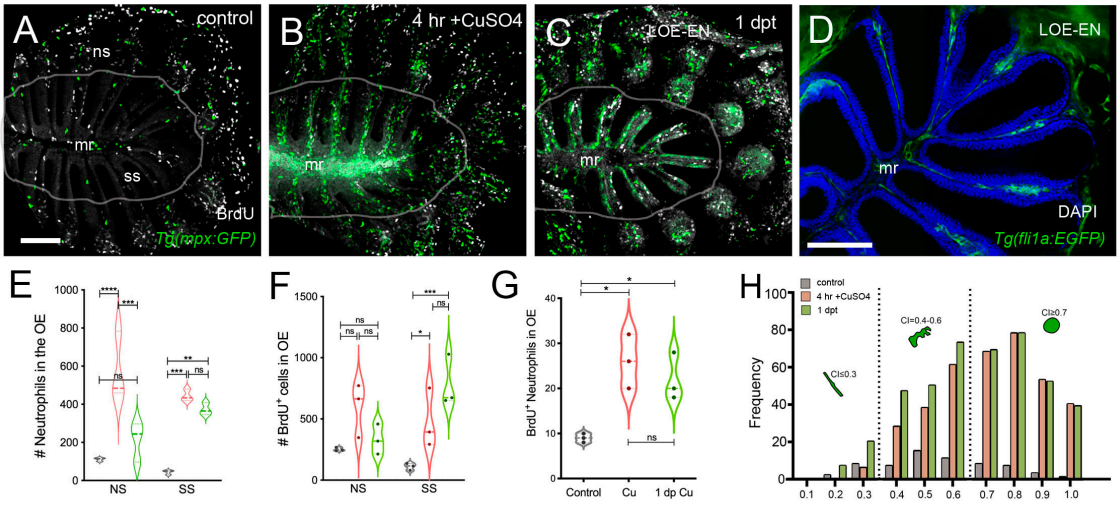
A
control
ns
mr
ss
BrdU
Tg(mpx:GFP)
B
4 hr +CuSO4
mr
C
LOE-EN
1 dpt
mr
D
LOE-EN
mr
DAPI
Tg(fli1a:EGFP)
E
Neutrophils in the OE
NS
SS
F
BrdU+ cells in OE
NS
SS
G
BrdU+ Neutrophils in OE
Control
Cu
1 dp Cu
H
control
4 hr +CuSO4
1 dpt
Frequency
Cl≤0.3
Cl=0.4-0.6
Cl≥0.7

Figure 4

Figure 4. Damage induces changes in cell división of OSN and neutrophil precursors in the adult olfactory organ.

(*A-C*) BrdU labeled cells (white), neutrophils (green) in whole mount OO of adult fish. (*A*) Prior to copper exposure BrdU labeling and scattered neutrophils were observed in the medial raphe (mr), sensory (ss), and non-sensory (ns) epithelia. (*B*) After four hours of exposure to copper intense BrdU labeling was observed in the mr. (*C*) One day post recovery neutrophils lined the lamellae and intense BrdU labeling was observed in ss and LOE-EN. (*D*) Section of *Tg(fli1a:EGFP)* adult OE showing extensions of blood vasculature (green) within the OE. (*E*) Significant increases in neutrophil number were observed after 4 hour copper exposure (red) in both the ns and ss epithelia when compared to control (grey). At one dpt (green) only the ss remained significantly greater than controls. (*F*) Damage induced changes in BrdU positive cells have were significant in the ss epithelia but not the ns at 4 hour copper exposure (red) and one dpt (green). (*G*) There was a small but significant increase in mpx:GFP positive cells double labeled for BrdU scored in the OE. (E-F, *n*=3 adult OE from different fish; Two-way ANOVA, Tukey multiple comparison test, $p < 0.05$). (*P , 0.05, **P , 0.01, ***P , 0.001). (*H*) Four hours of copper exposure (orange) and one day post-treatment (green) resulted in an increase in rounded neutrophils (nt1; circularity index 0.7 or greater see Fig. 1) and amoeboid neutrophils (nt2; circularity index 0.4-0.6) when compared to controls that had few rounded neutrophils. Scale bars: (*A-C)*= 50 μm. D = 100 μm.

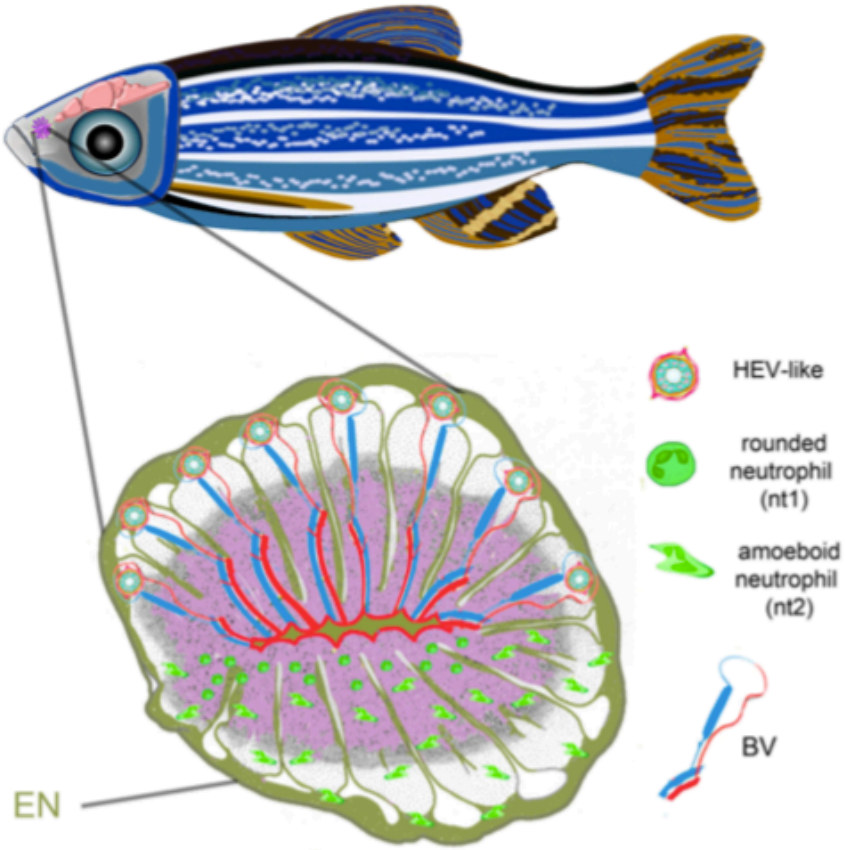
HEV-like
rounded neutrophil (nt1)
amoeboid neutrophil (nt2)
BV
EN
olfactory rosette

Figure 5

Figure 5. The olfactory organ is a neural-immune interface.

Schematic of olfactory organ (olfactory rosette) of adult zebrafish. The BV-LV and neutrophils are shown in different halves of the olfactory rosette for clarity. Upper half of olfactory rosette is proposed connections of Blood-Vasculature (BV) with LV via HEV-like cells that may also contact the meningeal immune system via vasculature associated with the EN. Lower half of olfactory rosette depicts resident neutrophils found only in the OE.

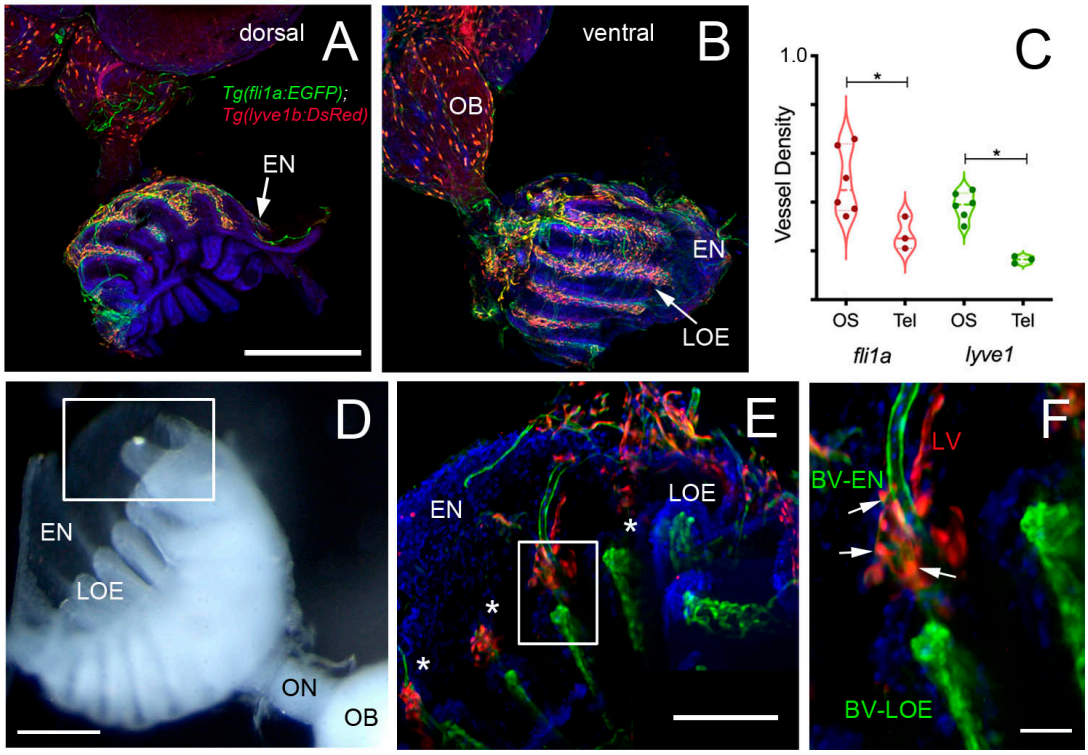

Supp Figure 1

Figure S1. The adult olfactory organs (OO) have extensive and interconnected Blood (BV) and Lymphatic Vasculature (LV).

(*A, B)* Whole mount *fli1a:EGFP;lyve1b:DsRed* adult OO connected to OB with BV (*fli1a:EGFP,* green) and LV *(lyve1b:DsRed*, red). Dorsal (*A*) and ventral (*B*) views; DAPI (blue). (*C*) BV (red) and LV (green) density is greater (SE, P-value <0.05, unpaired t-test) in olfactory system (OS = OE and OB) than telencephalon (Tel), *n* = 3 adult brains. One-way ANOVA, Tukey multiple comparison test, P < 0.05. Representative images selected from detailed analysis of least 6 brains. (*D*) Transmitted light image of fixed whole mount OO. Boxed area represent where LOE connect with EN. (*E*) At the distal tips of each lamellae (asterisks) the LV (red) meet the BV (green) (*E*, boxed area). (*F*) In this region cells express both lyve1b:DsRed and fli1a:EGFP (arrows). Scale Bars: A, B = 200 μm; *D, E* = 100 μm, F = 25 μm.

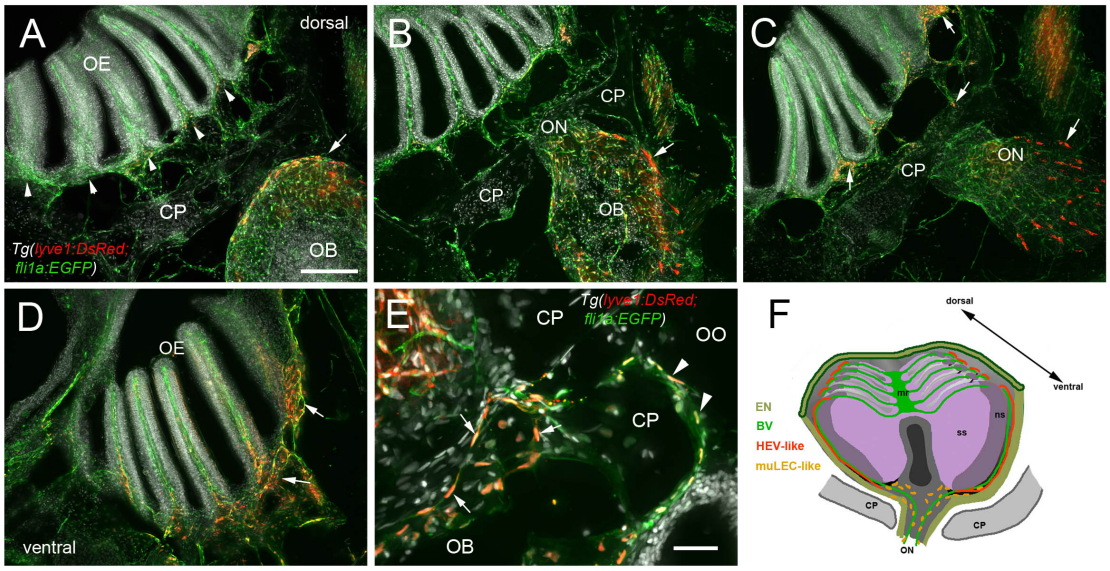

Supp Figure 2

Figure S2. Blood vasculature extends through cribriform plate with muLEC-like lymphatic cells.

(*A-E*). Sections from *Tg(lyve1b:DsRed;fli1a:EGFP)* adult brains. (*A*) In dorsal sections the OB is separated from the OE by the cribriform plate (CP). The OB has extensive BV (green) extending into the lamellae of the OE and muLEC-like cells (red) on the surface of the OB (arrow). (*B*) The ON passes through the CP accompanied by extensive BV (green). muLEC-like cells are on the medial surface (red, arrow) of the OB. (*C*) The muLEC-like cells (red, arrow) line the most ventral aspect of the ON. (*D*) muLEC-like cells line the basal OE (red, arrows) in the most ventral region of the OO. (*E*) muLEC-like cells on the BV extending across the CP and many are positive for both lyvel1:DsRed and fli1a:EGFP (arrows). (*F*) Diagram depicting olfactory organ with sensory (ss) and non-sensory (ns) epithelia that have extensive BV (green). The lamella of the OE contain HEV-like LV (red) that do not extend across the cribriform plate (CP). muLEC-like cells (orange) line the BV and extend from the olfactory bulb across the CP to the basal OE. Scale bars: A-D = 100 μm, E = 50 μm.

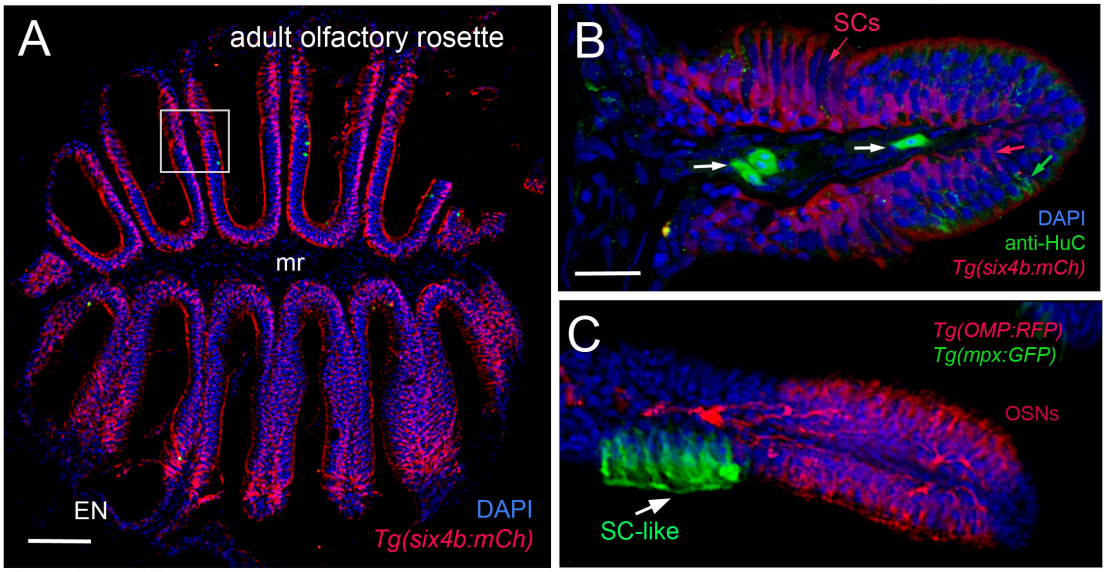

Supp Figure 3

Figure S3. Sustentacullar cells in the olfactory epithelium are associated with markers for neutrophils.

Cryosections of adult olfactory epithelia. (*A*) low magnification of adult olfactory rosette (OE) from *Tg(six4b:mCh)* line showing sustentacular cells (SCs, red) that are distributed within the lamellae of the OE where some areas have denser clusters (boxed area). (*B*) lamellae of OE with Six4b:mCh positive SCs (red) and anti-HuC positive neurons (green).(*C*) mpx:GFP positive cells (green, arrow) lie in clusters adjacent to OSN (red) and are similar to SCs (SC-like, see *B*, red). Scale bars: *A* = 100 μm; *B, C* = 25 μm

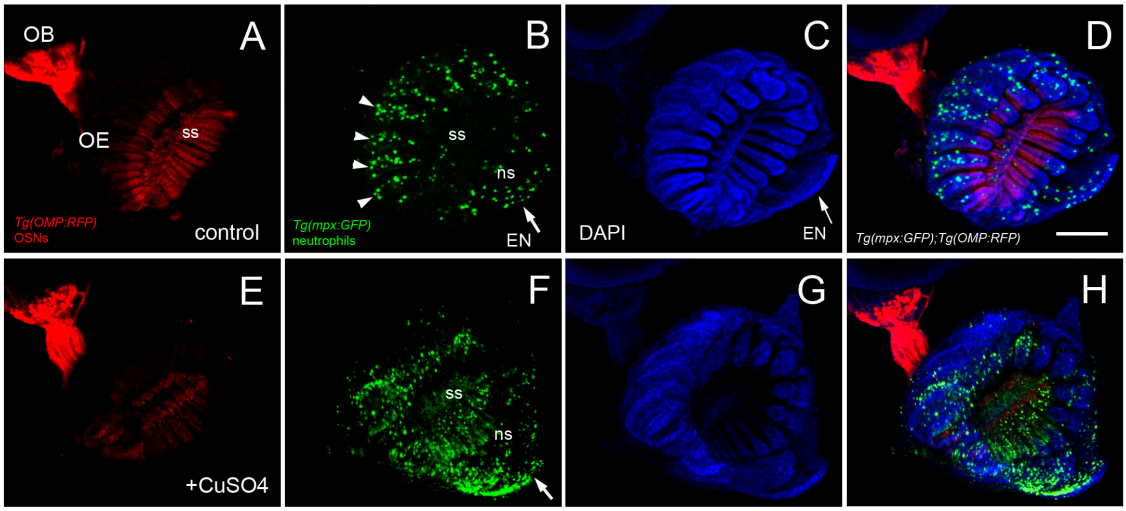

Supp Figure 4

Figure S4. Copper exposure induces rapid incerase in neutrophils in the OO.

(*A-D*) Control. (*A*) OSNs (red) populate the sensory epithelia of the OE. (*B*) neutrophils extend up the lamellae and are found in the EN (arrow). (*C*) DAPI labeling. (*D*) Merge of A-C. (*E-H*) OO from copper exposed animals. (*E*) Reduced OMP:RFP exxpression as neurons die. (*F*) increased neutrophils in sensory epithelia (ss), non-sensory epithelia (ns) and EN (arrow). (*G*) DAPI. (*H*) Merge of *E-G*. Scale bar = 100 μm

References

1. Sakano H (2010) Neural map formation in the mouse olfactory system. *Neuron.* 67(4):530-542. doi: 510.1016/j.neuron.2010.1007.1003.
2. Whitlock KE (2015) The loss of scents: Do defects in olfactory sensory neuron development underlie human disease? *Birth Defects Res C Embryo Today.* 105(2):114-125. doi: 110.1002/bdrc.21094. Epub 22015 Jun 2015.
3. Jackson RT, Tigges J, & Arnold W (1979) Subarachnoid space of the CNS, nasal mucosa, and lymphatic system. *Arch Otolaryngol.* 105(4):180-184. doi: 110.1001/archotol.1979.00790160014003.
4. Faber WM (1937) The nasal mucosa and the subarachnoid space. *American Journal of Anatomy* Vol. 6(No. 1):121-148.
5. Cserr HF, Harling-Berg CJ, & Knopf PM (1992) Drainage of brain extracellular fluid into blood and deep cervical lymph and its immunological significance. *Brain Pathol.* 2(4):269-276. doi: 210.1111/j.1750-3639.1992.tb00703.x.
6. Boehm T, Hess I, & Swann JB (2012) Evolution of lymphoid tissues. *Trends Immunol.* 33(6):315-321. doi: 310.1016/j.it.2012.1002.1005. Epub 2012 Apr 1016.
7. Hedrick MS, Hillman SS, Drewes RC, & Withers PC (2013) Lymphatic regulation in nonmammalian vertebrates. *1985).* 115(3):297-308. doi: 210.1152/japplphysiol.00201.02013. Epub 02013 May 00202.
8. Bjørgen H & Koppang EO (2021) Anatomy of teleost fish immune structures and organs. *Immunogenetics.* 73(1):53-63. doi: 10.1007/s00251-00020-01196-00250. Epub 02021 Jan 00211.
9. Tacchi L*, et al.* (2014) Nasal immunity is an ancient arm of the mucosal immune system of vertebrates. *Nat Commun.* 5:5205.(doi):10.1038/ncomms6205.

10. Aspelund A, *et al.* (2015) A dural lymphatic vascular system that drains brain interstitial fluid and macromolecules. *J Exp Med.* 212(7):991-999. doi: 910.1084/jem.20142290. Epub 20142015 Jun 20142215.

11. Louveau A, *et al.* (2015) Structural and functional features of central nervous system lymphatic vessels. *Nature.* 523(7560):337-341. doi: 310.1038/nature14432. Epub 12015 Jun 14431.

12. Da Mesquita S, Fu Z, & Kipnis J (2018) The Meningeal Lymphatic System: A New Player in Neurophysiology. *Neuron.* 100(2):375-388. doi: 310.1016/j.neuron.2018.1009.1022.

13. Dolgin E (2020) Brain's drain. *Nat Biotechnol.* 38(3):258-262. doi: 210.1038/s41587-41020-40443-41581.

14. Bower NI, *et al.* (2017) Mural lymphatic endothelial cells regulate meningeal angiogenesis in the zebrafish. *Nat Neurosci.* 20(6):774-783. doi: 710.1038/nn.4558. Epub 2017 May 1031.

15. Bower NI & Hogan BM (2018) Brain drains: new insights into brain clearance pathways from lymphatic biology. *J Mol Med (Berl).* 96(5):383-390. doi: 310.1007/s00109-00018-01634-00109. Epub 02018 Apr 00102.

16. Rua R & McGavern DB (2018) Advances in Meningeal Immunity. *Trends Mol Med.* 24(6):542-559. doi: 510.1016/j.molmed.2018.1004.1003. Epub 2018 May 1013.

17. Rustenhoven J, *et al.* (2021) Functional characterization of the dural sinuses as a neuroimmune interface. *Cell.* 184(4):1000-1016.e1027. doi: 1010.1016/j.cell.2020.1012.1040. Epub 2021 Jan 1027.

18. Sun BL, *et al.* (2018) Lymphatic drainage system of the brain: A novel target for intervention of neurological diseases. *Prog Neurobiol.* 163-164:118-143.(doi):10.1016/j.pneurobio.2017.1008.1007. Epub 2017 Sep 1010.

19. Voisin MB & Nourshargh S (2019) Neutrophil trafficking to lymphoid tissues: physiological and pathological implications. *J Pathol.* 247(5):662-671. doi: 610.1002/path.5227. Epub 2019 Feb 1004.

20. Beauvillain C*, et al.* (2011) CCR7 is involved in the migration of neutrophils to lymph nodes. *Blood.* 117(4):1196-1204. doi: 1110.1182/blood-2009-1111-254490. Epub 252010 Nov 254494.

21. Maletto BA*, et al.* (2006) Presence of neutrophil-bearing antigen in lymphoid organs of immune mice. *Blood.* 108(9):3094-3102. doi: 3010.1182/blood-2006-3004-016659. Epub 012006 Jul 016611.

22. Hampton HR, Bailey J, Tomura M, Brink R, & Chtanova T (2015) Microbe-dependent lymphatic migration of neutrophils modulates lymphocyte proliferation in lymph nodes. *Nat Commun.* 6:7139.(doi):10.1038/ncomms8139.

23. Harrison-Brown M, Liu GJ, & Banati R (2016) Checkpoints to the Brain: Directing Myeloid Cell Migration to the Central Nervous System. *Int J Mol Sci.* 17(12):2030. doi: 2010.3390/ijms17122030.

24. Manda-Handzlik A & Demkow U (2019) The Brain Entangled: The Contribution of Neutrophil Extracellular Traps to the Diseases of the Central Nervous System. *Cells.* 8(12):1477. doi: 1410.3390/cells8121477.

25. Khorooshi R*, et al.* (2020) Innate signaling within the central nervous system recruits protective neutrophils. *Acta Neuropathol Commun.* 8(1):2. doi: 10.1186/s40478-40019-40876-40472.

26. Harden MV, Newton LA, Lloyd RC, & Whitlock KE (2006) Olfactory imprinting is correlated with changes in gene expression in the olfactory epithelia of the zebrafish. *Journal of Neurobiology* 66(13):1452-1466.

27. Calfun C, Dominguez C, Perez-Acle T, & Whitlock KE (2016) Changes in Olfactory Receptor Expression Are Correlated With Odor Exposure During Early Development in the zebrafish (Danio rerio). *Chem Senses.* 41(4):301-312. doi: 310.1093/chemse/bjw1002. Epub 2016 Feb 1017.

28. Whitlock KE (2006) The sense of scents: olfactory behaviors in the zebrafish. *Zebrafish* 3(2):203-213.

29. Calfún C (2017) "Genomic Plasticity in the Olfactory Epithelium mediated by Odorant Exposure in Zebrafish (Danio rerio)". PhD (Universidad de Valparaiso).

30. Palominos MF & Whitlock KE (2020) The Olfactory Organ Is Populated by Neutrophils and Macrophages During Early Development. *Front Cell Dev Biol.* 8:604030.(doi):10.3389/fcell.2020.604030. eCollection 602020.

31. Odobasic D, Kitching AR, & Holdsworth SR (2016) Neutrophil-Mediated Regulation of Innate and Adaptive Immunity: The Role of Myeloperoxidase. *J Immunol Res* 2016:2349817.(doi):10.1155/2016/2349817. Epub 2342016 Jan 2349820.

32. Meinderts SM*, et al.* (2019) Neutrophils acquire antigen-presenting cell features after phagocytosis of IgG-opsonized erythrocytes. *Blood Adv.* 3(11):1761-1773. doi: 1710.1182/bloodadvances.2018028753.

33. Yang CW, Strong BS, Miller MJ, & Unanue ER (2010) Neutrophils influence the level of antigen presentation during the immune response to protein antigens in adjuvants. *J Immunol.* 185(5):2927-2934. doi: 2910.4049/jimmunol.1001289. Epub 1002010 Aug 1001282.

34. Das PK & Salinas I (2020) Fish nasal immunity: From mucosal vaccines to neuroimmunology. *Fish Shellfish Immunol.* 104:165-171.(doi):10.1016/j.fsi.2020.1005.1076. Epub 2020 Jun 1011.

35. Ager A (2017) High Endothelial Venules and Other Blood Vessels: Critical Regulators of Lymphoid Organ Development and Function. *Front Immunol.* 8:45.(doi):10.3389/fimmu.2017.00045. eCollection 02017.

36. Kaminski M*, et al.* (2012) Migration of monocytes after intracerebral injection at entorhinal cortex lesion site. *J Leukoc Biol.* 92(1):31-39. doi: 10.1189/jlb.0511241. Epub 0512012 Jan 0511230.

37. Torres-Paz J & Whitlock KE (2014) Olfactory sensory system develops from coordinated movements within the neural plate. *Dev Dyn.* 243(12):1619-1631. doi: 1610.1002/dvdy.24194. Epub 22014 Oct 24118.

38. Brann JH & Firestein SJ (2014) A lifetime of neurogenesis in the olfactory system. *Front Neurosci.* 8:182.(doi):10.3389/fnins.2014.00182. eCollection 02014.

39. Bayramli X, Kocagöz Y, Sakizli U, & Fuss SH (2017) Patterned Arrangements of Olfactory Receptor Gene Expression in Zebrafish are Established by Radial Movement of Specified Olfactory Sensory Neurons. *Sci Rep.* 7(1):5572. doi: 5510.1038/s41598-41017-06041-41591.

40. Iqbal T & Byrd-Jacobs C (2010) Rapid degeneration and regeneration of the zebrafish olfactory epithelium after triton X-100 application. *Chem Senses.* 35(5):351-361. doi: 310.1093/chemse/bjq1019. Epub 2010 Mar 1012.

41. Kida S, Pantazis A, & Weller RO (1993) CSF drains directly from the subarachnoid space into nasal lymphatics in the rat. Anatomy, histology and immunological significance. *Neuropathol Appl Neurobiol.* 19(6):480-488. doi: 410.1111/j.1365-2990.1993.tb00476.x.

42. Kida S, Weller RO, Zhang ET, Phillips MJ, & Iannotti F (1995) Anatomical pathways for lymphatic drainage of the brain and their pathological significance. *Neuropathol Appl Neurobiol.* 21(3):181-184. doi: 110.1111/j.1365-2990.1995.tb01048.x.

43. Koh L, Zakharov A, & Johnston M (2005) Integration of the subarachnoid space and lymphatics: is it time to embrace a new concept of cerebrospinal fluid absorption? *Cerebrospinal Fluid Res.* 2:6.(doi):10.1186/1743-8454-1182-1186.

44. Okuda KS & Hogan BM (2020) Endothelial Cell Dynamics in Vascular Development: Insights From Live-Imaging in Zebrafish. *Front Physiol.* 11:842.(doi):10.3389/fphys.2020.00842. eCollection 02020.

45. Goldmann J*, et al.* (2006) T cells traffic from brain to cervical lymph nodes via the cribroid plate and the nasal mucosa. *J Leukoc Biol.* 80(4):797-801. doi: 710.1189/jlb.0306176. Epub 0302006 Aug 0306172.

46. Hsu M*, et al.* (2019) Neuroinflammation-induced lymphangiogenesis near the cribriform plate contributes to drainage of CNS-derived antigens and immune cells. *Nat Commun.* 10(1):229. doi: 210.1038/s41467-41018-08163-41460.

47. Sepahi A & Salinas I (2016) The evolution of nasal immune systems in vertebrates. *Mol Immunol.* 69:131-8.(doi):10.1016/j.molimm.2015.1009.1008. Epub 2015 Sep 1019.

48. Lee H*, et al.* (2015) Phenotype and function of nasal dendritic cells. *Mucosal Immunol.* 8(5):1083-1098. doi: 1010.1038/mi.2014.1135. Epub 2015 Feb 1011.

49. Hampton HR & Chtanova T (2016) The lymph node neutrophil. *Semin Immunol.* 28(2):129-136. doi: 110.1016/j.smim.2016.1003.1008. Epub 2016 Mar 1026.

50. Li Y*, et al.* (2019) The regulatory roles of neutrophils in adaptive immunity. *Cell Commun Signal.* 17(1):147. doi: 110.1186/s12964-12019-10471-y.

51. Rosales C (2018) Neutrophil: A Cell with Many Roles in Inflammation or Several Cell Types? *Front Physiol.* 9:113.(doi):10.3389/fphys.2018.00113. eCollection 02018.

52. Yipp BG*, et al.* (2017) The Lung is a Host Defense Niche for Immediate Neutrophil-Mediated Vascular Protection. *Sci Immunol.* 2(10):eaam8929. doi: 8910.1126/sciimmunol.aam8929.

53. Kubes P (2018) The enigmatic neutrophil: what we do not know. *Cell Tissue Res.* 371(3):399-406. doi: 310.1007/s00441-00018-02790-00445. Epub 02018 Feb 00445.

54. Mellert TK, Getchell ML, Sparks L, & Getchell TV (1992) Characterization of the immune barrier in human olfactory mucosa. *Otolaryngol Head Neck Surg.* 106(2):181-188.

55. Getchell ML & Kulkarni AP (1995) Identification of neutrophils in the nonsensory epithelium of the vomeronasal organ in virus-antibody-free rats. *Cell Tissue Res.* 280(1):139-151. doi: 110.1007/BF00304519.

56. Dong F*, et al.* (2020) IgT Plays a Predominant Role in the Antibacterial Immunity of Rainbow Trout Olfactory Organs. *Front Immunol.* 11:583740.(doi):10.3389/fimmu.2020.583740. eCollection 582020.

57. Yu YY*, et al.* (2018) Mucosal immunoglobulins protect the olfactory organ of teleost fish against parasitic infection. *PLoS Pathog.* 14(11):e1007251. doi: 1007210.1001371/journal.ppat.1007251. eCollection 1002018 Nov.

58. Ogawa K*, et al.* (2021) Frontline Science: Conversion of neutrophils into atypical Ly6G(+) SiglecF(+) immune cells with neurosupportive potential in olfactory neuroepithelium. *J Leukoc Biol.* 109(3):481-496. doi: 410.1002/JLB.1001HI0620-1190RR. Epub 2020 Jul 1029.

59. Pägelow D*, et al.* (2018) The olfactory epithelium as a port of entry in neonatal neurolisteriosis. *Nat Commun.* 9(1):4269. doi: 4210.1038/s41467-41018-06668-41462.

60. Galeano C*, et al.* (2018) The Route by Which Intranasally Delivered Stem Cells Enter the Central Nervous System. *Cell Transplant.* 27(3):501-514. doi: 510.1177/0963689718754561. Epub 0963689718752018 May 0963689718754514.

61. Renshaw SA, *et al.* (2006) A transgenic zebrafish model of neutrophilic inflammation. *Blood.* 108(13):3976-3978. doi: 3910.1182/blood-2006-3905-024075. Epub 022006 Aug 024022.

62. Lawson ND & Weinstein BM (2002) In vivo imaging of embryonic vascular development using transgenic zebrafish. *Dev Biol.* 248(2):307-318. doi: 310.1006/dbio.2002.0711.

63. Okuda KS, *et al.* (2012) lyve1 expression reveals novel lymphatic vessels and new mechanisms for lymphatic vessel development in zebrafish. *Development.* 139(13):2381-2391. doi: 2310.1242/dev.077701. Epub 072012 May 077723.

64. Traver D, *et al.* (2003) Transplantation and in vivo imaging of multilineage engraftment in zebrafish bloodless mutants. *Nat Immunol.* 4(12):1238-1246. doi: 1210.1038/ni1007. Epub 2003 Nov 1239.

65. Sato Y, Miyasaka N, & Yoshihara Y (2005) Mutually exclusive glomerular innervation by two distinct types of olfactory sensory neurons revealed in transgenic zebrafish. *J Neurosci* 25(20):4889-4897.

66. Harden MV, *et al.* (2012) Close association of olfactory placode precursors and cranial neural crest cells does not predestine cell mixing. *Developmental Dynamics* 241(7):1143-1154.

67. Baldwin DH, Sandahl JF, Labenia JS, & Scholz NL (2003) Sublethal effects of copper on coho salmon: impacts on nonoverlapping receptor pathways in the peripheral olfactory nervous system. *Environ Toxicol Chem.* 22(10):2266-2274. doi: 2210.1897/2202-2428.

68. Hernandez PP, *et al.* (2011) Sublethal concentrations of waterborne copper induce cellular stress and cell death in zebrafish embryos and larvae. *Biol Res.* 44(1):7-15. doi:

10.4067/S0716-97602011000100002. Epub 97602011000102011 May 97602011000100011.

69. Westerfield M (2007) *The zebrafish book: A guide for the laboratory use of zebrafih (Danio rerio)*. (University of Oregon Press, Eugene OR USA).

70. Schindelin J*, et al.* (2012) Fiji: an open-source platform for biological-image analysis. *Nat Methods.* 9(7):676-682. doi: 610.1038/nmeth.2019.

71. McQuin C*, et al.* (2018) CellProfiler 3.0: Next-generation image processing for biology. *PLoS Biol.* 16(7):e2005970. doi: 2005910.2001371/journal.pbio.2005970. eCollection 2002018 Jul.

CHAPTER 4: DAMAGE-INDUCED CALCIUM TRANSIENTS TRIGGER NEUTROPHIL RECRUITMENT IN THE DEVELOPING OLFACTORY ORGAN

Damage-induced calcium transients trigger neutrophil recruitment in the developing olfactory organ

M. Fernanda Palominos and Kathleen E. Whitlock

Introduction

Epithelial barriers protect against injury and infection. After damage, the coordination of cells and their secreted chemical cues allow for proper tissue restoration. The role of early chemotactic signals on immune cell recruitment is still not well understood despite the identification of transcriptional growth factors and chemokine cascades during tissue inflammation. Immediately after damage, the initial 'detection phase' in wound healing is orchestrated within minutes, with no new protein synthesis required. Initially, intrinsic Damage-associated Molecular Patterns (DAMPs, Venereau et al., 2015; De Oliveira et al., 2016) are leaked from lysing cells to generate the spatial transmission of biochemical signals (calcium, H_2O_2, ATP, or eicosanoids; Yoo et al., 2012; Razzell et al., 2013; Gadani et al., 2015; Niethammer, 2016; Rådmark et al., 2014; Penuela et al., 2013; Enyedi et al., 2013) to then trigger leukocyte recruitment and epithelial closure (as the earliest protective cellular responses). Later, (hours to days), amplification and resolution of the inflammatory response is coordinated by chemokine-, cytokine-, and growth factor-signaling cascades to produce protein synthesis, cell proliferation, and regeneration (Enyedi and Niethammer, 2015).

Calcium is not only the earliest regulator of inflammatory responses, but it is indispensable in the control of almost all physiological processes; its concentration and positional information are interpreted to produce, for example, either a controlled neurotransmitter liberation or an inflammatory response. In both *Drosophila* (Razzell et al., 2013) and zebrafish (Yoo et al., 2012), epithelial damage triggers rapid cytoplasmic Ca^{2+} signals extending outward from the point of wounding that are necessary for H_2O_2 production and to amplify the inflammation response.

Previous studies have shown that the exposure to non-lethal copper concentrations causes cell death and regeneration of ciliated olfactory sensory neurons (OSNs)(Ma et al., 2018). Subsequently, we have shown that damage induces recruitment of circulating neutrophils and

macrophages to the developing olfactory organs (OOs) of the zebrafish (Palominos and Whitlock, 2021). However, the initial damage signals from injured neurons after copper exposure and how they communicate to local and non-local immune cells remains unknown. The earliest phases of molecular inflammation includes the release of chemical signals such as calcium and Adenosine triphosphate (ATP), which then coordinate neutrophil arrival and inflammation resolution (Enyedi et al., 2013; Enyedi and Niethammer, 2015; Gadani et al., 2015). Cytosolic Ca^{2+} has also been shown to regulate leukocyte arrest and subsequent migration through release of calcium from internal stores and synergic external influx via Ca^{2+}-release activated channels (Niggli, 2003; Dixit and Simon, 2012). L-type calcium channels (LTCC) are voltage-gated channels particularly highly expressed in the olfactory sensory system of human (Solis-Chagoyan et al., 2016), mice (Berger and Bartsch, 2014; Darcy and Isaacson, 2009); rat (Jerome et al., 2012), and fish (Yoshida et al., 2009). In addition to calcium signaling, pannexin hemichannels have been identified as key mediators of ATP release during inflammation (Crespo Yanguas et al., 2016). Pannexin1 (Panx1) is abundantly expressed across different brain regions but enriched in the peripheral and central components of the olfactory (Ray et al., 2005; Kurtenbach et al., 2014) and visual (retina & lens; Ray et al., 2005; Vogt et al., 2005; Penuela et al., 2013; Dvoriantchikova et al., 2006) systems.

Here we hypothesized that damage-induced calcium transients in OSNs trigger the migration of neutrophils to the OOs and that these transients will affect post-synaptic interneurons in the OBs (mitral, Tufted) (Fuller et al., 2006; Friedrich, 2012; Kermen et al., 2012), therefore suggesting that any damage to the peripherally-located sensory neurons may cause secondary damage to the central nervous system if inflammation is not rapidly resolved. We used a genetically encoded calcium indicator to characterize damage-induced calcium transients in the developing OSNs. In wholemount *in vivo* preparations we showed that calcium transients are correlated with targeted migration of neutrophils to the OOs during copper-induced damage, as described previously

(Palominos and Whitlock, 2021). Blocking Panx1 hemichannels and LTCCs channels resulted in short term and long-term effects on neutrophil recruitment in response to damage. Therefore, our results suggest that neuronal calcium signaling is continuously needed for immune cell migration.

Materials and Methods

Animals: Zebrafish were maintained in a re-circulating system (Aquatic Habitats Inc, Apopka, FL) at 28º C on a light-dark cycle of 14 and 10 hours, respectively. All fish were maintained in the Whitlock Fish Facility at the Universidad de Valparaiso. All protocols and procedures employed were reviewed and approved by the Institutional Committee of Bioethics for Research with Experimental Animals, Universidad de Valparaiso (#BA084-2016). Embryos were obtained from natural spawnings under laboratory conditions and raised at 28.5º C in Embryo medium as previously described (Westerfield, 2007), and staging was done according to Kimmel et al., 1995. We carried out experiments in 3 and 5 dpf larvae of the following transgenic lines: Tg(*HuC:GCamP3*) (Panier et al., 2013); Tg(*mpx:mCherry*) (Varas et al., 2010); and Tg(*lysC:DsRED2*) (Hall et al., 2007).

Calcium imaging: Experimental procedure was done as described in Palominos and Whitlock (2021). Briefly, larvae were anesthetized (2% Tricaine, Sigma) and mounted in a cut tip plastic Pasteur pipette in 2% low temperature agarose (Sigma) in embryo medium. Larvae were imaged in frontal view using an Attofluor Chamber (Thermo Fisher Scientific) filled with embryo medium, and the agarose covering the olfactory system was removed. The temperature was maintained at 26º C, and images were acquired using a Spinning disc confocal microscope (Olympus) with a 20X 0.95 NA water immersion LUMPlanFL/IR objective.

Images were acquired in a single Z-stack, every 400 ms. For the simultaneously imaging of calcium and neutrophil recruitment, images were collected with 5 μm/optical sections in a total

depth of 25 μm depth. All data analysis was carried out using FIJI (National Institute of Health, Bethesda, Maryland, USA; Schindelin et al., 2012) calculating the mean fluorescence in each ROI (whether the OO or OB) and normalized by the basal fluorescence (F_0)

Copper and odorant exposure:

One ml of a stock solution of 1 mM taurocholic acid (TA; Taurocholyc acid, sodium salt hydrate, 97%, Sigma-Aldrich) was prepared and stored at 4º C. Baseline calcium dynamics were recorded for thirty minutes in Tg(*HuC:GCamP3*) animals in filtered embryo medium (EM) with 2% Tricaine. The EM/2% Tricaine solution was later replaced by EM and followed by 10 μM TA + 2% Tricaine.To record calcium responses during copper exposure the TA solution was replaced by filtered EM followed by 10 μM $CuSO_4$ + 2% Tricaine (Palominos and Whitlock, 2021).

LTCC and Pannexin blockade during copper-induced damage:

The number of neutrophils in the OOs during copper exposure was counted as described in Palominos and Whitlock (2021) and quantified in individual larvae using a modified ChIn assay (d'Alençon et al., 2010). The L-Type Calcium Channel (LTCC) blocker, Furnidipine (kindly provided by Dr. Ana María Cárdenas, Universidad de Valparaíso), was diluted to 1 μM (from a 0.6 mM stock solution stored at -20º C) in 1% DMSO in embryo medium, as described for another LTCC blocker in zebrafish (Yoshida et al., 2009). Probenecid (water-soluble, Invitrogen), used as a Pannexin-1 (Silverman et al., 2008; Zhang et al., 2019) inhibitor, was diluted from to 2.5 μM working solution (from a 250 mM stock solution stored at -20º C) in embryo medium. The number of neutrophils in left and right olfactory organs was quantified every hour for 6 hours.

Statistics: Data are presented as means ± standard deviations. Statistical analysis were done using Prism 9 (Graphpad), and are indicated in each figure legend. Unpaired Student's t-tests were performed unless otherwise indicated. P values are indicated as follows: *: $P < 0.05$, **: P

< 0.01, ***: P < 0.001, ****: P < 0.0001.

Acknowledgments

We thank A. Moscoso, T. Ordenes and S. Alanis for care of the zebrafish, especially with the difficulties brought on by the pandemic. Funding: Fondo Nacional de Desarrollo Científico y Tecnológico (FONDECYT) 1160076 (KEW); Centro Interdisciplinario de Neurociencia de Valparaíso (CINV) ICM ANID Millennium Institute project code ICN09-022, CINV (KEW) and Graduate Fellowship (CONICYT) 21161437 (MFP).

Results

Copper exposure triggers rapid and long-lasting calcium responses in olfactory neurons

Previously, we have demonstrated that neutrophils patrol the OOs during normal zebrafish development, but that when exposed to damaging concentrations of copper, neutrophils and macrophages migrate to the OOs (Palominos and Whitlock, 2021). In order to visualize the calcium response in living animals we used the genetically encoded calcium indicator Tg*(HuC:GCaMP3*). The *HuC* promoter drives pan-neuronal expression of GCaMP3 thus allowing for *in vivo* recording of calcium dynamics in neurons from both peripheral and central components of the olfactory sensory system. To quantify neuronal responses under normal physiological and damage-induced conditions, we quantified calcium responses to 10 μM TA (a potent social odor; Vitebsky et al., 2005) and 10 μM CuSO4 (an OSN damaging agent, Palominos and Whitlock, 2021) in 3 day post-fertilization (dpf) fish. In the absence of added odorants there is little background activity (Fig. 1A). Exposure to TA transiently increases F/F0 signal in the OOs (Fig 1 A") and the OBs (Fig. 1, A', B left; Supplementary Video 1). In comparison with individual OSNs (Fig 1 A' arrowheads, C) the signal is amplified in the CNS by the convergence of the OSN axons on the post-synaptic sites in the OB (Fig 1 A', arrows, C)

with a time decay constant of 0.56 and 0.78 minutes for the OOs and OBs, respectively (Fig. 1, D, black, red).

In contrast to physiological response to odors represented by TA, the first 20 minutes of exposure to copper induced three consecutive calcium waves (>0.5 minutes, each) in both peripheral OOs and central OBs (Fig. 1, A", A'", B right; Supplementary Video 2), with a time decay of 5.31 and 4.37 minutes for the OOs and OBs (Fig. 1, D, gray, dark red), respectively (almost nine times slower than the response to TA). At 2 minutes post-administration, copper induced large responses in individual OSNs (Figure 1A''') relative to TA (Figure 1A'). In contrast very large increases in Ca^{2+} were observed in the OBs (Figure 1A''' arrowheads) suggesting that the calcium reponses observed in the OBs may reflect mechanisms independent of the OSNs damage-induced signaling. The mean change of GCaMP fluorescence after 20 minutes of exposure was consistently higher in the OBs than in the OOs, for both TA and copper treatments (Fig. 1, C). In contrast to TA, copper exposure triggered a distinct large-amplitude response in OOs (Fig. 1, C, black versus gray).

In order to analyze the coordination of peripheral and central calcium responses we calculated the Pearson correlation coefficient (r) between OOs and OBs during TA and copper-induced damage. We found that calcium transients between OOs and OBs were perfectly negatively correlated during odor exposure (Fig. 1, E, rTA=-0.977, see Fig. 1B, taurocholic acid). In contrast, damage-induced calcium responses showed no correlation between the OBs and OOs (Fig. 1, ErCu=0.181, see Fig. 1B, copper) suggesting that, as expected, the non-physiological responses triggered by copper exposure are distinct from those triggered by odors.

A central and peripheral delayed calcium wave correlates with neutrophil infiltration to the olfactory organs

Previously, we have shown that copper exposure triggers a rapid increase in neutrophil numbers in the developing OOs as early as 1-hour post copper exposure (Palominos and Whitlock, 2021).

In order to better understand the role of calcium in the response to OSN damage we next correlated calcium dynamics with neutrophil migration during copper exposure. To visualize *in vivo* the long-term effect of calcium dynamics on neutrophil migration, we used 5 dpf Tg(*HuC:GCaMP3*);Tg(*mpx:mCherry)* larvae (Supplementary Video 3) and collected serial images of 5 z-stacks every 30 seconds for 1.5 hours (Figure 2). Before copper exposure there were few neutrophils in the OO (Fig. 2 A, red, B, green) and Ca^{2+} levels in the OO and OB were steady (Figure 2 B, black, red). In response to 30 minutes of copper exposure neutrophils moved into the OO (Figure 2 A'). In the presence of copper (A', A'', A'''), OSNs with persistent increases in Ca^{2+} were continuously contacted by migrating neutrophils (Fig. 2, A', A'', A''', purple, arrows ; Supplementary Video 3). Degeneration of OSNs was observed (Fig, 2, A'', arrowhead) with apparent loss of OSN dendrites (Fig. 2, A'', white arrowhead). The increase of the neutrophils in the OO after copper correlated with the observed damage-induced Ca^{2+}increases in the OO (Fig 2B black) and OB (Fig 2 B red).

We then tested the long-term temporal correlation between calcium waves in the OOs and OBs with the number of neutrophils recruited to the OOs. During copper exposure, we found a higher positive correlation between long lasting copper-induced calcium waves in the OOs and OBs (Fig. 2, C, rOO/OB=0.814, 90 minutes recording) than we did between OB/OO during the first 20 minutes after damage (Fig. 1, E). This suggest that during damage Ca^{2+}-associated dynamics are synchronous between the peripheral and the central components of the olfactory sensory system, in contrast to the uncorrelated OO/OB waves observed after 20 minutes post damage (Fig. 1, B'', E).

We further quantified the correlation between the number of neutrophils and the calcium changes observed in the OO 90 minutes after copper exposure. We found a positive correlation between the numbers of neutrophils in the OO with the changes in OSN fluorescence 90 minutes

post damage (Fig. 2, C, dark gray) thus supporting the role of damage induced calcium transients in neutrophil migration.

L-type calcium channel blockade inhibits neutrophil migration to damaged olfactory organs

To test the potential role of calcium increases in neutrophil migration to the olfactory sensory system, we blocked L-type calcium channels (which mediate inward Ca^{2+} currents and trigger calcium release from the sarcoplasmic reticulum) using Furnidipine. Using 5 dpf Tg(*HuC:GCaMP3*);Tg(*mpx:mCherry)* larvae exposed to 10 mM Furnidipine, the number of neutrophils were scored every hour for the 4 hours of copper exposure, and 2 hours after its removal (Fig 2, D). Furnidipine completely inhibited neutrophil migration to the olfactory organ during and post copper exposure (Fig. 2, D, red).

To further test the potential role of calcium in neutrophil migration we used Probenecid, an inhibitor of Pannexin 1 (PANX1) channel that blocks the activation of the extracellular ATP release-induced purinergic pathway and inflammatory response (Silverman et al., 2008; Zhang et al., 2019). At concentrations of 1 mM (Fig 2, D light blue) and 10 mM (Fig 2, D dark blue) Probenecid inhibited neutrophil migration only during the first two hours of copper exposure, (Fig. 2, D, light blue, blue). These results suggest that the entry of Ca^{2+} through LTCC in olfactory neurons may be needed to initiate and maintain neutrophil migration. Furthermore, it suggests that the ATP-induced purigenic response in neutrophils is a short response that can be overcome by sustained calcium signaling.

Discussion

Exposure to copper during early development leads to death of ciliated OSN, (Lazzari et al., 2017; Ma et al., 2018), a continuously renewing cell population in vertebrates, as well as immune cell migration to the OOs (Palominos and Whitlock, 2021). Here we characterized damage-induced calcium transients in the developing olfactory sensory system using a neuronally-expressed genetically encoded calcium indicator (*HuC:GCaMP3*) and found that the copper-induced early and late Ca^{2+} responses accompanying cell death in the developing olfactory sensory epithelia are needed for neutrophil recruitment. Furthermore the blockage of L-type calcium channels (LTCCs) and Pannexin1 hemichannels eliminated or reduced neutrophil migration in the olfactory sensory system. Our results suggest that continuous calcium signaling in the OSNs is needed for immune cell migration and that the release of ATP by Pannexin1 channels is necessary only during the initial hours post-injury, but not for later damage amplification and resolution.

First minutes after damage

We have demonstrated that during the first minutes after copper exposure non-transient and long-lasting calcium waves occur in both the peripheral OOs and the central OBs (Fig. 1).

The observation that the OBs showed a rapid and very large calcium response suggests that additional non-HuC+ cell types may transmit damage signals centrally. Previous unpublished work from our (Whitlock) laboratory suggests the presence of cells that express oligodendrocyte marker Olig2+ in the OOs. Recent studies suggest the oligodendrocytes not only act as support cells but also have multiple roles in the brain such as metabolic exchangers with neurons and are a cellular interface with blood vessels (Dansu et al., 2020). Furthermore, our recent findings characterizing the extensive blood and lymphatic vasculature surrounding the olfactory epithelia and extending into the CNS (Palominos et al 2021, submitted) coupled with recent studies suggesting the BBI (Blood Brain Interface) allows for molecular cross talk between the nervous

and vascular systems (Segarra et al., 2019; Lenz et al 2020) support the idea that other types of cells in the OO may signal damage to the OB faster than do the OSNs.

At 3 dpf, the axon terminations of the olfactory sensory neurons segregate into three branches in the developing olfactory bulb: the medial, central, and lateral (Dynes and Ngai, 1998; Vitebsky et al., 2005). During TA exposure we primary observed the activation of the medial glomeruli (Fig. 1., A') most likely reflecting axon termination of the sensory neurons activated by TA. In contrast, copper exposure appeared to trigger calcium increases in all axon branches (Fig 1., A'', arrowheads), most likely reflecting the sustained calcium response of the ciliated OSN. Furthermore, after twenty minutes, calcium remained elevated only in neurons located in the central and medial glomeruli (Fig. 1., A'"). It is known that in adult zebrafish the lateral and central regions of the OB respond positively to aminoacids and nucleotides, whereas the medial subregion responds to bile acids (Friedrich and Korshing, 1998; Vitebsky et al., 2005; Yoshihara 2008; Koide et al., 2009). Thus, the activation of interneurons in the OBs suggests that the earliest neural responses to damage in the CNS are chemotopically unspecific and constitute a non-specific activation of Ca^{2+} pathways in OSN rather than a receptor-induced sensory response.

Ca^{2+} signaling and immune response to copper-induced damage

Calcium is a universal yet versatile regulator of many vital physiological processes, however changes in Ca^{2+} homeostatic concentrations can lead to cell stress, damage and death (Zhivotovsky and Orrenius, 2011). Immediatly after damage calcium controls the subsequent generation of chemical signals such as ROS, ATP, eicosanoids and chemokines (Razzell et al., 2013; Yoo et al., 2012; Niethammer, 2016). Our results are consistent with studies showing that calcium ions play a vital role in cell death pathways (Ludhiadch et al., 2021).

LTCCs are widely distributed, being found in skeletal, smooth and heart muscle as well as in OMP+ human olfactory sensory neurons (Solis-Chagoyan et al., 2016). In our studies the

blockade of LTCCs completely abolished neutrophil recruitment during and after damage, suggesting that neutrophil chemotaxis is dependent on the OSN influx of calcium. In addition to muscle and neural tissues, LTCCs are expressed in myeloid and lymphoid immune cells (Suzuki et al., 2010; Davenport et al., 2015; Fenninger et al., 2019; Ramirez-Moreno et al., 2020). Thus, the use of LTCCs blocker might also directly affect targeted neutrophil migration (Suzuki et al., 2010; De Oliveira et al., 2016). Ca^{2+} changes triggered by TA and copper were inhibited during Furnidipine treatment in the OOs thus showing that LTCC blockade affected both the sensory neurons as well as the migration of neutrophils. Further studies are needed to determine whether the effects of LTCCs blockers are at the level of the OSN, neutrophils or both.

In addition to calcium, we also blocked ATP released via activation of the Pannexin1 channel. This pathway leads to the release of interleukin-1β as one of earliest "find-me" signals secreted by dying cells (Chekeni et al., 2010; Chen et al., 2014; Shestopalov and Slepak, 2014; Crespo Yanguas et al., 2016; Niethammer, 2016) but had shown to be dispensable for olfactory signal transduction and odor perception (Kurtenbach et al., 2014). Here we showed that blocking Pannexin1 is associated with delayed initiation of neutrophil migration during the first hour post copper exposure, but subsequently the neutrophil migration returns to normal levels. Because Panx1 is expressed in OSN (Kurtenbach et al., 2014), vascular endothelium (Lohman et al., 2015), and leukocytes (Junger, 2011), we cannot discern whether the delayed migration of immune cells is caused by the response of neurons, immune cells or of other cell types. Here we have demonstrated that non-physiological increases in intracellular Ca^{2+} levels in OSNs are sufficient to coordinate early and sustained neutrophil migration to the OOs. Further studies are needed to determine the contributions of LTCCs and Pannexin hemichannels to the initial damage–response as well as on later healing and regeneration phases.

References

Alqadah, A., Hsieh, Y. W., Xiong, R., & Chuang, C. F. (2016). Stochastic left - Right neuronal asymmetry in caenorhabditis elegans. *Philosophical Transactions of the Royal Society B: Biological Sciences*, *371*(1710). https://doi.org/10.1098/rstb.2015.0407

Berger, S. M., & Bartsch, D. (2014). The role of L-type voltage-gated calcium channels Cav1.2 and Cav1.3 in normal and pathological brain function. *Cell and Tissue Research*, *357*(2), 463–476. https://doi.org/10.1007/s00441-014-1936-3

Chekeni, F. B., & Ravichandran, K. S. (2011). The role of nucleotides in apoptotic cell clearance: implications for disease pathogenesis. *Journal of Molecular Medicine*, *89*(1), 13–22. https://doi.org/10.1007/s00109-010-0673-7

Chen, J., Zhao, Y., & Liu, Y. (2014). The role of nucleotides and purinergic signaling in apoptotic cell clearance - implications for chronic inflammatory diseases. *Frontiers in Immunology*, *5*(DEC). https://doi.org/10.3389/fimmu.2014.00656

Cohen, Y., Putrino, D., & Wilson, D. A. (2015). Dynamic cortical lateralization during olfactory discrimination learning. *Journal of Physiology*, *593*(7), 1701–1714. https://doi.org/10.1113/jphysiol.2014.288381

Crespo Yanguas, S., Willebrords, J., Johnstone, S. R., Maes, M., Decrock, E., De Bock, M., Leybaert, L., Cogliati, B., & Vinken, M. (2017). Pannexin1 as mediator of inflammation and cell death. *Biochimica et Biophysica Acta - Molecular Cell Research*, *1864*(1), 51–61. https://doi.org/10.1016/j.bbamcr.2016.10.006

d'Alençon, C. A., Peña, O. A., Wittmann, C., Gallardo, V. E., Jones, R. A., Loosli, F., Liebel, U., Grabher, C., & Allende, M. L. (2010). A high-throughput chemically induced inflammation assay in zebrafish. *BMC Biology*, *8*(1), 151. https://doi.org/10.1186/1741-7007-8-151

Dansu, D. K., Sauma, S., & Casaccia, P. (2020). Oligodendrocyte progenitors as environmental biosensors. *Seminars in Cell and Developmental Biology*, *September*. https://doi.org/10.1016/j.semcdb.2020.09.012

Darcy, D. P., & Isaacson, J. S. (2009). L-type calcium channels govern calcium signaling in migrating newborn neurons in the postnatal olfactory bulb. *Journal of Neuroscience*, *29*(8), 2510–2518. https://doi.org/10.1523/JNEUROSCI.5333-08.2009

De Oliveira, S., Rosowski, E. E., & Huttenlocher, A. (2016). Neutrophil migration in infection and wound repair: Going forward in reverse. *Nature Reviews Immunology*, *16*(6), 378–391. https://doi.org/10.1038/nri.2016.49

Dreosti, E., Vendrell Llopis, N., Carl, M., Yaksi, E., & Wilson, S. W. (2014). Left-Right Asymmetry Is Required for the Habenulae to Respond to Both Visual and Olfactory Stimuli. *Current Biology*, *24*(4), 440–445. https://doi.org/10.1016/j.cub.2014.01.016

Dvoriantchikova, G., Ivanov, D., Pestova, A., & Shestopalov, V. (2006). Molecular charaterization of pannexins in the lens. *Molecular Vision*, *12*(November), 1417–1426.

Dynes, J. L., & Ngai, J. (1998). Pathfinding of olfactory neuron axons to stereotyped glomerular targets revealed by dynamic imaging in living zebrafish embryos. *Neuron*, *20*(6), 1081–1091. https://doi.org/10.1016/S0896-6273(00)80490-0

Enyedi, B., & Niethammer, P. (2015). Mechanisms of epithelial wound detection. *Trends in Cell Biology*, *25*(7), 398–407. https://doi.org/10.1016/j.tcb.2015.02.007

Enyedi, B., Kala, S., Nikolich-Zugich, T., & Niethammer, P. (2013). Tissue damage detection by osmotic surveillance. *Nature Cell Biology*, *15*(9), 1123–1130. https://doi.org/10.1038/ncb2818

Fuller, C. L., Yettaw, H. K., & Byrd, C. A. (2006). Mitral cells in the olfactory bulb of adult zebrafish (Danio rerio): Morphology and distribution. *The Journal of Comparative Neurology*, *499*(2), 218–230. https://doi.org/10.1002/cne.21091

Friedrich, R. W., & Korsching, S. I. (1997). Combinatorial and Chemotopic Odorant Coding in the Zebrafish Olfactory Bulb Visualized by Optical Imaging. *Neuron*, *18*(5), 737–752. https://doi.org/10.1016/S0896-6273(00)80314-1

Friedrich, R. W. (2013). Neuronal Computations in the Olfactory System of Zebrafish. *Annual Review of Neuroscience*, *36*(1), 383–402. https://doi.org/10.1146/annurev-neuro-062111-150504

Gadani, S. P., Walsh, J. T., Lukens, J. R., & Kipnis, J. (2015). Dealing with Danger in the CNS: The Response of the Immune System to Injury. In *Neuron* (Vol. 87, Issue 1, pp. 47–62). Elsevier Inc. https://doi.org/10.1016/j.neuron.2015.05.019

Hall, C., Flores, M., Storm, T., Crosier, K., & Crosier, P. (2007). The zebrafish lysozyme C promoter drives myeloid-specific expression in transgenic fish. *BMC Developmental Biology*, *7*(1), 42. https://doi.org/10.1186/1471-213X-7-42

Jerome, D., Hou, Q., & Yuan, Q. (2012). Interaction of NMDA receptors and L-type calcium channels during early odor preference learning in rats. *European Journal of Neuroscience*, *36*(8), 3134–3141. https://doi.org/10.1111/j.1460-9568.2012.08210.x

Junger, W. G. (2011). Immune cell regulation by autocrine purinergic signalling. *Nature Reviews Immunology*, *11*(3), 201–212. https://doi.org/10.1038/nri2938

Kermen, F., Franco, L. M., Wyatt, C., & Yaksi, E. (2013). Neural circuits mediating olfactory-driven behavior in fish. *Frontiers in Neural Circuits*, *7*(April), 62. https://doi.org/10.3389/fncir.2013.00062

Koide, T., Miyasaka, N., Morimoto, K., Asakawa, K., Urasaki, A., Kawakami, K., & Yoshihara, Y. (2009). Olfactory neural circuitry for attraction to amino acids revealed by transposon-mediated gene trap approach in zebrafish. *Proceedings of the National Academy of Sciences of the United States of America*, *106*(24), 9884–9889. https://doi.org/10.1073/pnas.0900470106

Kurtenbach, S., Whyte-Fagundes, P., Gelis, L., Kurtenbach, S., Brazil, É., Zoidl, C., Hatt, H., Shestopalov, V. I., & Zoidl, G. (2014). Investigation of olfactory function in a Panx1 knock out

mouse model. *Frontiers in Cellular Neuroscience*, *8*(September), 1–8. https://doi.org/10.3389/fncel.2014.00266

Lämmermann, T., Afonso, P. V., Angermann, B. R., Wang, J. M., Kastenmüller, W., Parent, C. A., & Germain, R. N. (2013). Neutrophil swarms require LTB4 and integrins at sites of cell death in vivo. *Nature*, *498*(7454), 371–375. https://doi.org/10.1038/nature12175

Lazzari, M., Bettini, S., Milani, L., Maurizii, M. G., & Franceschini, V. (2017). Differential response of olfactory sensory neuron populations to copper ion exposure in zebrafish. *Aquatic Toxicology*, *183*, 54–62. https://doi.org/10.1016/j.aquatox.2016.12.012

Lenz, M., Eichler, A., & Vlachos, A. (2021). Monitoring and modulating inflammation‐associated alterations in synaptic plasticity: Role of brain stimulation and the blood‐brain interface. *Biomolecules*, *11*(3), 1‐9. https://doi.org/10.3390/biom11030359

Lohman, A. W., Leskov, I. L., Butcher, J. T., Johnstone, S. R., Stokes, T. a., Begandt, D., DeLalio, L. J., Best, A. K., Penuela, S., Leitinger, N., Ravichandran, K. S., Stokes, K. Y., & Isakson, B. E. (2015). Pannexin 1 channels regulate leukocyte emigration through the venous endothelium during acute inflammation. *Nature Communications*, *6*, 7965. https://doi.org/10.1038/ncomms8965

Ma, E. Y., Heffern, K., Cheresh, J., & Gallagher, E. P. (2018). Differential copper-induced death and regeneration of olfactory sensory neuron populations and neurobehavioral function in larval zebrafish. *NeuroToxicology*. https://doi.org/10.1016/j.neuro.2018.10.002

Niethammer, P. (2016). The early wound signals. *Current Opinion in Genetics and Development*, *40*, 17–22. https://doi.org/10.1016/j.gde.2016.05.001

Panier, T., Romano, S. a., Olive, R., Pietri, T., Sumbre, G., Candelier, R., & Debrégeas, G. (2013). Fast functional imaging of multiple brain regions in intact zebrafish larvae using

Selective Plane Illumination Microscopy. *Frontiers in Neural Circuits*, *7*(April), 1–11. https://doi.org/10.3389/fncir.2013.00065

Palominos, M. F., & Whitlock, K. E. (2021). The Olfactory Organ Is Populated by Neutrophils and Macrophages During Early Development. *Frontiers in Cell and Developmental Biology*, *8*(January), 1–15. https://doi.org/10.3389/fcell.2020.604030

Penuela, S., Gehi, R., & Laird, D. W. (2013). The biochemistry and function of pannexin channels. *Biochimica et Biophysica Acta - Biomembranes*, *1828*(1), 15–22. https://doi.org/10.1016/j.bbamem.2012.01.017

Rådmark, O., Werz, O., Steinhilber, D., & Samuelsson, B. (2015). 5-Lipoxygenase, a key enzyme for leukotriene biosynthesis in health and disease. *Biochimica et Biophysica Acta - Molecular and Cell Biology of Lipids*, *1851*(4), 331–339. https://doi.org/10.1016/j.bbalip.2014.08.012

Ray, A., Zoidl, G., Weickert, S., Wahle, P., & Dermietzel, R. (2005). Site-specific and developmental expression of pannexin1 in the mouse nervous system. *European Journal of Neuroscience*, *21*(12), 3277–3290. https://doi.org/10.1111/j.1460-9568.2005.04139.x

Razzell, W., Evans, I. R., Martin, P., & Wood, W. (2013). Calcium Flashes Orchestrate the Wound Inflammatory Response through DUOX Activation and Hydrogen Peroxide Release. *Current Biology*, *23*(5), 424–429. https://doi.org/10.1016/j.cub.2013.01.058

Schindelin, J., Arganda-Carreras, I., Frise, E., Kaynig, V., Longair, M., Pietzsch, T., Preibisch, S., Rueden, C., Saalfeld, S., Schmid, B., Tinevez, J. Y., White, D. J., Hartenstein, V., Eliceiri, K., Tomancak, P., & Cardona, A. (2012). Fiji: An open-source platform for biological-image analysis. *Nature Methods*, *9*(7), 676–682. https://doi.org/10.1038/nmeth.2019

Segarra, M., Aburto, M. R., Hefendehl, J., & Acker-Palmer, A. (2019). Neurovascular interactions in the nervous system. *Annual Review of Cell and Developmental Biology*, *35*, 615–635. https://doi.org/10.1146/annurev-cellbio-100818-125142

Shestopalov, V. I., & Slepak, V. Z. (2014). Molecular pathways of pannexin1-mediated neurotoxicity. *Frontiers in Physiology*, *5 FEB*(February), 1–8. https://doi.org/10.3389/fphys.2014.00023

Silverman, W., Locovei, S., & Dahl, G. (2008). Probenecid, a gout remedy, inhibits pannexin 1 channels. *American Journal of Physiology - Cell Physiology*, *295*(3), 761–767. https://doi.org/10.1152/ajpcell.00227.2008

Solís-Chagoyán, H., Flores-Soto, E., Reyes-García, J., Valdés-Tovar, M., Calixto, E., Montaño, L., & Benítez-King, G. (2016). Voltage-Activated Calcium Channels as Functional Markers of Mature Neurons in Human Olfactory Neuroepithelial Cells: Implications for the Study of Neurodevelopment in Neuropsychiatric Disorders. *International Journal of Molecular Sciences*, *17*(6), 941. https://doi.org/10.3390/ijms17060941

Suzuki, Y., Inoue, T., & Ra, C. (2010). L-type Ca2+ channels: A new player in the regulation of Ca2+ signaling, cell activation and cell survival in immune cells. *Molecular Immunology*, *47*(4), 640–648. https://doi.org/10.1016/j.molimm.2009.10.013

Varas, M., Ortíz-Severín, J., Marcoleta, A. E., Díaz-Pascual, F., Allende, M. L., Santiviago, C. A., & Chávez, F. P. (2017). Salmonella Typhimurium induces cloacitis-like symptomsin zebrafish larvae. *Microbial Pathogenesis*, *107*, 317–320. https://doi.org/10.1016/j.micpath.2017.04.010

Vénéreau, E., Ceriotti, C., & Bianchi, M. E. (2015). DAMPs from cell death to new life. *Frontiers in Immunology*, *6*(AUG), 1–11. https://doi.org/10.3389/fimmu.2015.00422

Vitebsky, a., Reyes, R., Sanderson, M. J., Michel, W. C., & Whitlock, K. E. (2005). Isolation and characterization of the laure olfactory behavioral mutant in the zebrafish, Danio rerio. *Developmental Dynamics*, *234*(1), 229–242. https://doi.org/10.1002/dvdy.20530

Vogt, A., Hormuzdi, S. G., & Monyer, H. (2005). Pannexin1 and Pannexin2 expression in the developing and mature rat brain. *Molecular Brain Research*, *141*(1), 113–120. https://doi.org/10.1016/j.molbrainres.2005.08.002

Yoo, S. K., Freisinger, C. M., LeBert, D. C., & Huttenlocher, A. (2012). Early redox, Src family kinase, and calcium signaling integrate wound responses and tissue regeneration in zebrafish. *Journal of Cell Biology*, *199*(2), 225–234. https://doi.org/10.1083/jcb.201203154

Yoshida, T., Uchida, S., & Mishina, M. (2009). Regulation of synaptic vesicle accumulation and axon terminal remodeling during synapse formation by distinct Ca2+signaling. *Journal of Neurochemistry*, *111*(1), 160–170. https://doi.org/10.1111/j.1471-4159.2009.06309.x

Yoshihara, Y. (2009). Molecular genetic dissection of the zebrafish olfactory system. *Results and Problems in Cell Differentiation*, *47*, 97–120. https://doi.org/10.1007/400_2008_1

Zhang, Z., Lei, Y., Yan, C., Mei, X., Jiang, T., Ma, Z., & Wang, Q. (2019). Probenecid Relieves Cerebral Dysfunction of Sepsis by Inhibiting Pannexin 1-Dependent ATP Release. *Inflammation*, *42*(3), 1082–1092. https://doi.org/10.1007/s10753-019-00969-4

Zhivotovsky, B., & Orrenius, S. (2011). Calcium and cell death mechanisms: A perspective from the cell death community. *Cell Calcium*, *50*(3), 211–221. https://doi.org/10.1016/j.ceca.2011.03.003

APPENDIX

Differential responses of the left and right sides of the olfactory sensory system

Left-right (L/R) asymmetry is a phenomenon involved in the patterning, development, and morphogenesis of tissues and body plans of vegetal and animal species of different sizes and scales. From the three main body axes (antero-posterior, A/P; dorso-ventral, D/V; and L/R), the L/R axis establishes functional correlates with olfactory discrimination in worms, fish, and mammals (Alqadah et al., 2016; Dreosti et al., 2014, Cohen et al., 2015). To identify damage-induced asymmetries in calcium signaling between the left and right olfactory sensory epithelia and their downstream target in the OBs we quantified calcium dynamics of left and right OO and OB of 5 dpf *HuC:GCaMP3* larvae exposed to copper over three-time scales: short (5 min), median (15 min) and long-term (2 hrs) responses.

Copper: As described in Chapter Three, copper exposure induces calcium increases that are non-transient in both the OO and the OB (Fig. 1, B'-B"; Fig. 2, B; Fig. 3, A-A"). No significant differences were found between left and right OO or OB in control and copper-exposed animals after 5 minutes (Fig. 3, B, 5 min, control, grey, copper, red). However, copper-induced calcium transients showed asymmetries between L/R OO at 15 minutes post exposure (Fig. 3, C, copper, red, asterisk) that were not observable at 2 hours post exposure (Fig. 3, D, 2 hrs, copper, red).

Taurocholic Acid: We found that the response of the left and right OO to TA differed in amplitude only after 5 min post-TA exposure (Fig. 3, B, 5 min, TA, green, asterisk), and we observed that TA-induced differences between left and right OO were transient, as they were not maintained past 15 minutes (Fig. 3, C, 5 min, TA, green).

In both short-term TA (Fig. 3, B, green, OO left= 1.13 ± 0.021 F/F0; OO right= 1.08 ± 0.021 F/F0) and mid-term Copper (Fig. 3, C, red, OO left= 1.40 ± 0.114 F/F0; OO right= 1.30 ± 0.084 F/F0) responses, the left OO had a higher mean amplitude than the right OO. These data suggest

that the response to either odorant or damaging agent (such as TA and copper, respectively) is lateralized, showing a higher response in the left OO.

We also explored the correlation between L/R OO and OB's responses to TA and copper during 5 minutes, 15 minutes, and 2 hour exposures. In control conditions, we observed a more significant correlation between the left OO and OB than between the right OO and OB (Fig. 3, B', control, underlined, r OO/OB left= 0.56, r OO/OB right= -0.25), suggesting that basal signaling of the olfactory sensory system is lateralized to the left (with a higher average response over the right side). However, 5 minute exposure to odorant/copper, the correlation of L/R in response to TA and copper changed drastically. In the short-term, the correlation of the OO/OB responses on the left side decreased while it is doubled on the right side. Copper exposure did not induce significant changes with 5 minutes of exposure, but with 15 minutes exposure responses showed significant changes in the correlation index in both left and right OO/OB in comparison with the control (Fig. 3, C', copper, r OO/OB left= -0.74, r OO/OB right= -0.09). Thus, after 15 minutes exposure, copper induced laterally coordinated calcium waves between the peripheral and central olfactory sensory system. However, these damage-induced calcium waves were not coordinated in the long-term.

Figures & Figure Legends

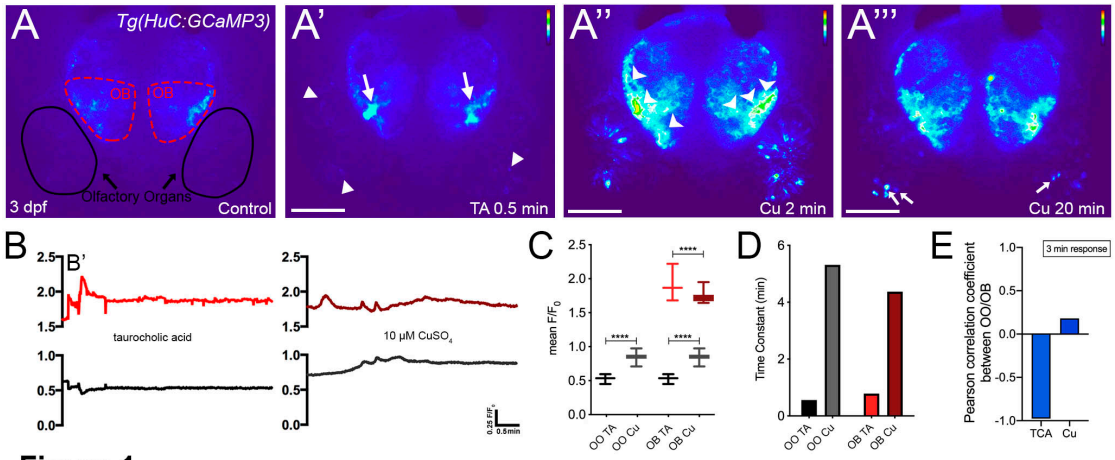

Figure 1

Figure 1. Exposure to non-lethal copper concentrations triggers early but long-lasting calcium responses in OSNs.

(A-A’’’) Frontal view of Tg(*HuC:GCaMP3*) 3 dpf larva response to 10 µM taurocholic acid and copper exposure. Fluorescence changes are coded in thermal scale. OOs are labeled with black circles, and OBs with red circles, respectively. Cu exposure induced a fast, strong calcium response in the OBs (A’’, arrowheads). After 20 minutes, calcium accumulated in OSNs, which became increasingly round (A’’’, arrows). Imaging was initiated at time 0 min. Time in A’-A’’’ are minutes post-TA or Cu administration. (B) F/F_0 values during 20 minutes of TA (B’, left), and Cu (B’’, right) administration. OO responses are represented by a black (TA) or gray (Cu) line; OB responses by a red (TA) and dark red (Cu) line. n=3 larvae. (C) Mean changes of F/F_0 of 3 2hole recordings (20 minutes each). 1-way ANOVA, Tukey test, $p < 0.005$. (D) Exponential decay ($F(x)=e^{\lambda X}$) of the greater response to TA (red, dark red) and Cu (black, gray) was used to calculate the time constant ($\tau=1/\lambda$) in every condition and olfactory region (organ or bulb). (E) Pearson correlation coefficient between OOs and OBs during TCA and Cu exposure. All scale bars= 100 µm.

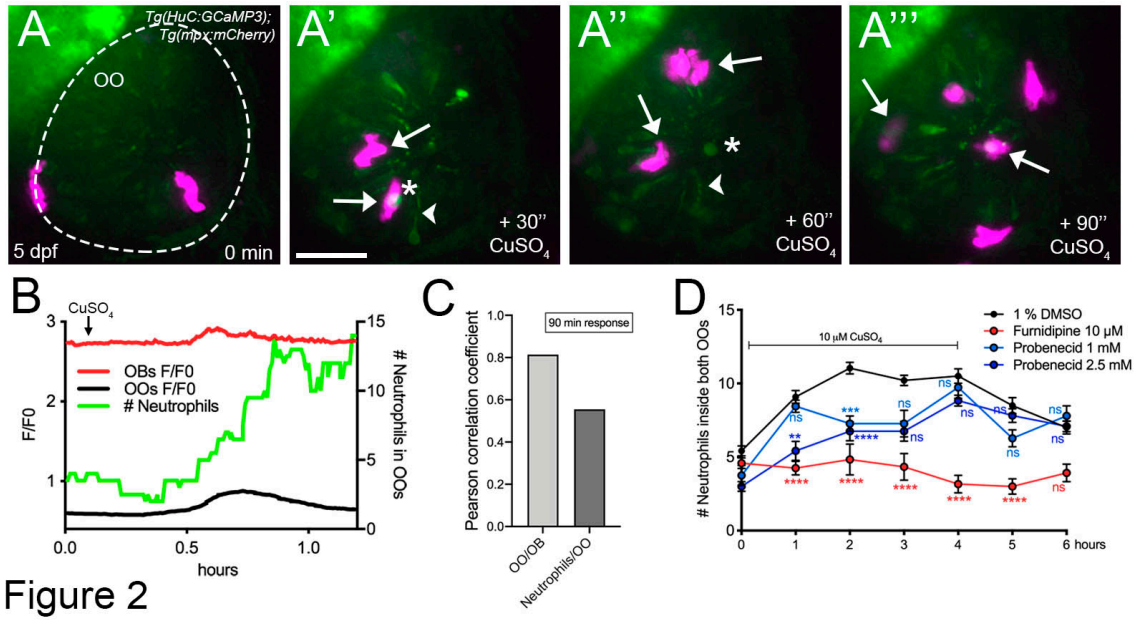
A
Tg(HuC:GCaMP3);
Tg(mpx:mCherry)
OO
5 dpf
0 min
A'
+ 30"
CuSO4
A''
+ 60"
CuSO4
A'''
+ 90"
CuSO4
B
CuSO4
OBs F/F0
OOs F/F0
Neutrophils
F/F0
Neutrophils in OOs
hours
C
90 min response
Pearson correlation coefficient
OO/OB
Neutrophils/OO
D
10 µM CuSO4
1 % DMSO
Furnidipine 10 µM
Probenecid 1 mM
Probenecid 2.5 mM
Neutrophils inside both OOs
6 hours

Figure 2

Figure 2. Neutrophil entry to the olfactory epithelia correlates with a delayed calcium increase in the olfactory organs through L-type Ca^{2+} channel.

(A-A’’’) Frontal view of an olfactory organ of a 5 dpf Tg(*huc:GCaMP3*); Tg(*mpx:mCherry*) and its response to copper. Imaging was initiated at time 0 min. Copper exposure started 15 minutes after imaging. Time in A’-A’’’ are minutes post-Cu administration. During copper exposure, neutrophils (purple) were constantly contacting OSNs (arrows), which lose their cilia (green, arrowheads) and became increasingly round (green, asterisks). All scale bars= 50 μm. (B) Copper induced long-term F/F_0 increases in the OO (black line) and OB (red line) that temporally correlated with the number of neutrophils recruited to the OO (green line) *in vivo*. n=5 Tg(*HuC:GCaMP3*); Tg(*mpx:mCherry*) 5 dpf larvae. (C) Pearson correlation coefficient between the number of neutrophils and the OOs and OB, and between OOs and OBs. (D) Neutrophil numbers in both OO during Cu exposure and 2 hours post-removal when co-exposed with LTCC blocker furnidipine (red line) or the Pannexin1 blocker, Probenecid (light blue and blue lines). Control animals were exposed to copper in 1% DMSO (vehicle). n=24 Tg(*HuC:GCaMP3*); Tg(*mpx:mCherry*) larvae, ANOVA Kruskall-Wallis test, $p < 0.05$. ns: no statistical significance.

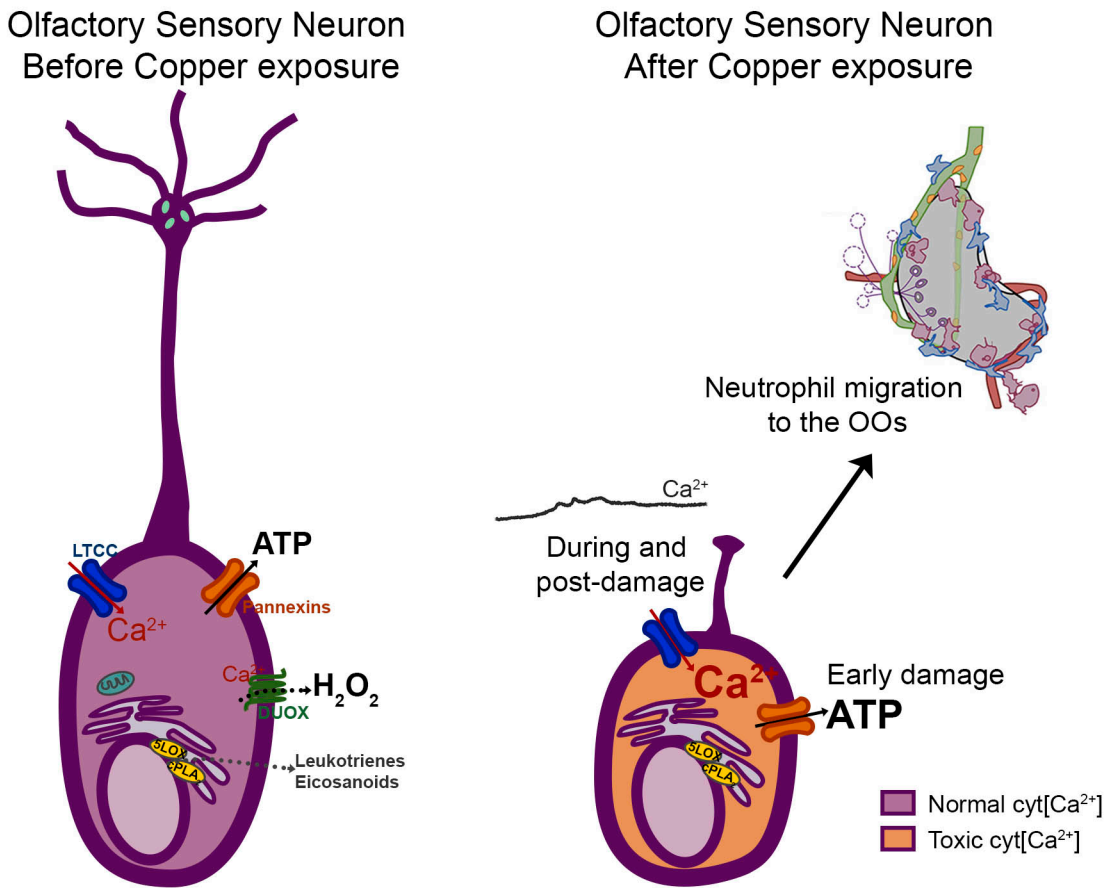
Olfactory Sensory Neuron
Before Copper exposure
LTCC
ATP
Pannexins
Ca2+
Ca2+
H2O2
DUOX
5LOX
cPLA
Leukotrienes
Eicosanoids
Olfactory Sensory Neuron
After Copper exposure
Neutrophil migration
to the OOs
Ca2+
During and
post-damage
Ca2+
Early damage
ATP
5LOX
cPLA
Normal cyt[Ca2+]
Toxic cyt[Ca2+]

Figure 3

Figure 3. Summary: LTCC-dependent Ca^{2+} increases in OSNs are necessary for neutrophil recruitment to the olfactory organs.

OSNs coordinate responses to odors. Ca^{2+}, H_2O_2, ATP, leukotrienes, and eicosanoids are the first signals that orchestrate immune cell recruitment after injury (Shestopalov and Slepak, 2014; Niethammer, 2016; De Oliveira et al., 2016). LTCCs and Pannexin1 are found to be expressed in OSNs. DUOX presence in the OSNs is hypothetical. 5-LOX (Rådmark et al.,2014) catalyze the synthesis of leukotrienes, inflammatory bioactive molecules that amplify local cell death signals (Lämmermann et al., 2013) to recruit neutrophils rapidly. The Ca^{2+}-dependent cytosolic phospholipase $cPLA_2$ regulates the synthesis of eicosanoids, early stimulators of wound signaling (Niethammer, 2016). Chemokines are later synthesized. After Cu, OSN showed long-lasting cytosolic Ca^{2+} increases (orange), swelling, and cilia degeneration by the end of the treatment. LTCC-dependent calcium waves are needed for neutrophil recruitment during and post-Cu administration (blockade by Furnidipine). In contrast, ATP release (blockage by using Probenecid, a Pannexin1 channel blocker) is needed only during the first 2 hours of damage, but not after copper removal. Neutrophil recruitment to the OOs is first controlled of Ca^{2+} and ATP changes in the olfactory sensory organ mediated by LTCC and Pannexin1 channels. After copper removal, Ca^{2+} but not ATP is needed for sustained neutrophil migration.

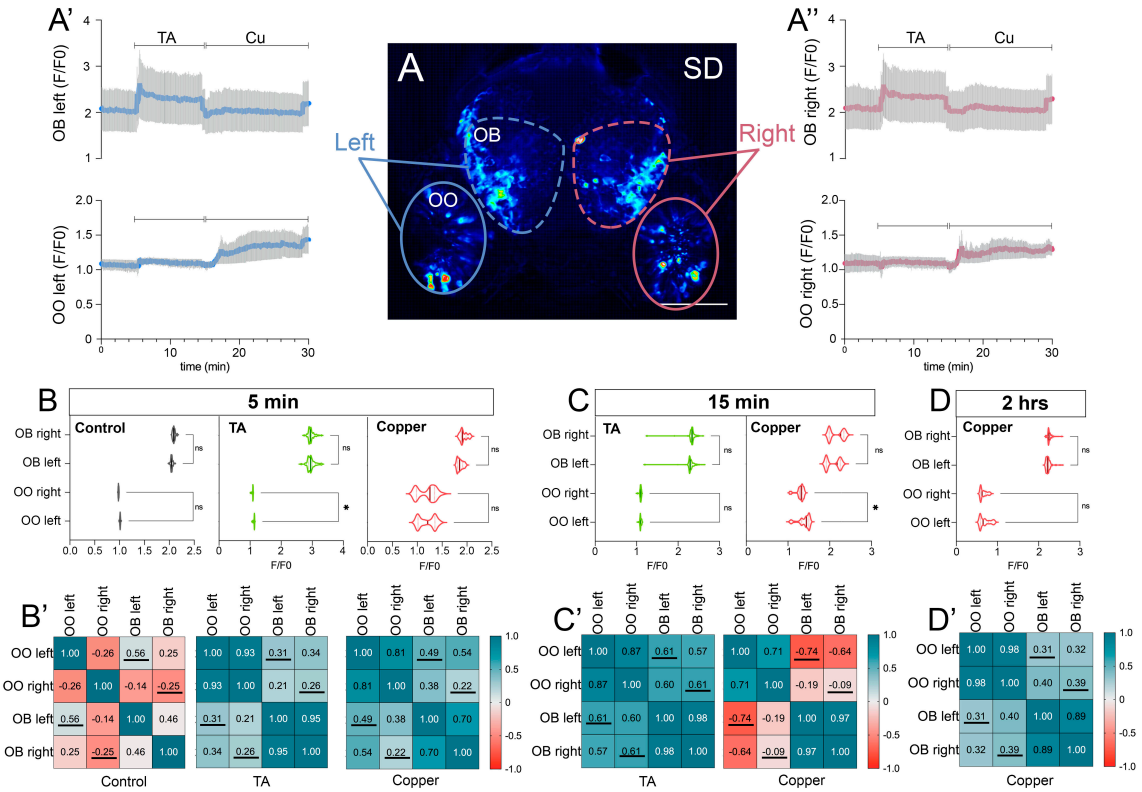

FIGURE ANNEX 1

Appendix Figure 1. Asymmetric responses of the olfactory sensory system during damage.

(A) Representative image showing standard deviation of the response to Copper (Cu) in a 5 dpf HuC:GGaMP3 larvae. (A') Calcium responses of the left (A', blue) and right (A'', red) OO and OB during taurocholic acid (TA) and copper exposure. Standard error is graphed in gray. F/F_0 mean responses to TA and copper after 5 (B), 15 (C), and 2 hrs (D) of left and right OO and OB. Correlation matrix between left and right OO and OB of the F/F_0 mean responses to TA and copper at 5 (B'), 15 (C') and 2 hrs (D'). The correlation coefficient ranges between -1.0 and 1.0. (A-D, B'-D') n= 3 larvae 5 dpf HuC:GCaMP3. 2-way ANOVA, Tukey test, $p < 0.005$. Frames were taken every 410 milliseconds. For F/F_0 calculation 10 cells in each OO and OB were selected using the standard deviation image of each recording.

CHAPTER 5: DISCUSSION

Discussion

The ability to smell depends on olfactory sensory neurons (OSNs) that lie in the peripherally-located olfactory epithelium (OE). This group of continually renewing neurons extends their axons across the cribriform plate where they make their first synapses in the olfactory bulbs (OBs) (Sakano et al., 2010; Whitlock, 2005) thus creating a potential route for chemical/biological agents to enter the brain. In the present study we characterized the presence of immune cells, and lymphatic and blood vasculature cells associated with the zebrafish olfactory sensory system during development (Palominos and Whitlock, 2021; Chapter 2) and adulthood (Palominos et al., 2021, submitted, Chapter 3). Furthermore, we demonstrated that damage induced increases in $Ca2^{+}$-triggers the migration of immune cells to the olfactory organs in the developing zebrafish (Chapter 4). We propose that olfactory organs, because of their unique anatomical structure, have the extensive immune architecture described in this study, in order to rapidly resolve inflammation and protect against infectious agents, thus protecting the central nervous system.

The development of the lymphatic vasculature around the olfactory system begins to be visible after one-week post fertilization (Palominos & Whitlock, 2021; Chapter 2), in accordance with the migration and formation of the lateral facial, otolithic, and branchial arch lymphatic branches (Okuda et al., 2012; Astin et al., 2014; Semo et al., 2016) between 5-7 days post fertilization. In mammals, immune cell are generated from the primary lymphoid tissues (bone and thymus) and mature in secondary lymphoid tissues (like peripheral lymph nodes and the spleen). In addition, tertiary lymphoid structures, resembling lymph nodes, can be found at the sites of chronic inflammation (Drayton et al., 2006,; Ruddle et al., 2014). In mammals, the arborization of the lymphatic vasculature in lymph nodes, is extensive and composed of internal High Endothelial Venules (HEVs). Although fish do not have lymph nodes, we describe HEV-like cells in the olfactory organs of the adult zebrafish, which may have a function similar to what has been

described in mammals (Girard et al., 2012; Hampton et al., 2015; Bogolowski et al., 2018; Hampton and Chtanova, 2019): allowing the infiltration of immune cells into the olfactory tissues. Furthermore, in mammals immune cells are found regionalized within lymphatic nodes, having different functionalities associated with their spatial location (Gray and Cyster, 2012; Kastenmüller et al 2012; Qi et al., 2014; Hampton and Chtanova, 2016). We propose that this unique situation where the OOs have resident neutrophils under normal conditions, coupled with the morphologies we described may reflect different region specific functions within the OOs (Chapter 3).

Our studies showed a surprising correlation between damage to the olfactory organ of the adult zebrafish and the appearance of neutrophils in the CNS, where neutrophils appeared along the ventral olfactory bulbs and ventral telencephalic ventricle. These data raise the possibility that the olfactory organs could be a host defense niche for the brain where immune cells move into the CNS in response to damage. Future research will shed light on how the olfactory-associated network of lymphatic and blood vasculature regulates the brain response to damage and the movement of immune cells in the peripheral and central olfactory sensory system.

Numerous studies have shown that vaccines as well as certain medications can be delivered nasally to generate systemic effects on immunity (Neutra and Kozlowski, 2005; Tacchi et al., 2014; Sepahi et al., 2017) and hormonal regulation (Fortuna et al., 2014; Al Bakri et al., 2018). These treatments are effective because of the known extensive vascularization of the olfactory epithelia in mammals (Kumar et al., 2016) that allows physiological responses in the organism through continuous connections between the nasal and the systemic blood vasculature. Furthermore, there is increasing evidence that cross-talk between neurons and blood vessels, the neurovascular unit (NVU), is a powerful signaling system controlling different cellular processes such as differentiation, migration and connectivity of neurons and glia (Segarra et al., 2019; De Luca et al., 2020). The neurovascular unit we described here (Chapter 3) linking the blood and

lymphatic vascular system with the OSNs and then, together, extending across the cribriform plate to the CNS, may orchestrate responses in both the peripheral and central nervous system to stimuli (odors, damage,) detected in the olfactory epithelia.

In order to further dissect the responses of neutrophils to OSN damage, we demonstrated the necessity of calcium in triggering the migration of neutrophils to the site of damage. Probenecid, normally used in the treatment of gout (a type of inflammatory arthritis caused by the elevated level of uric acid in the blood), has been shown to inhibit the production of Interleukin-1 β through Pannexin 1 (Pelegrin and Surprenant 2006; Yang et al., 2019). Blocking Pannexin 1 hemichannels with Probenecid revealed an early effect on neutrophil recruitment to the site of damage, however, we don't know if levels of Interleukin-1β were also reduced. Chronic exposure to L-type calcium channels blockers during development has been shown to disrupt the development of the olfactory sensory system in zebrafish (Yoshida et al., 2009). Here we used acute exposure to the L-type calcium channel blocker, Furnidipine, and demonstrated that immune cell migration was inhibited for the duration of the experiment. These results support potential use for LTCC blockers in modulating processes related to immune cell migration, such as scar-free regeneration in the CNS (Li et al., 2020; Dorrier et al., 2021). Furthermore, we found that the use of Furnidipine inhibited damage-induced calcium signals in OSN (data not shown). In the future, it will be interesting to investigate potential effects on intracellular calcium signals of migrating neutrophils.

The research presented here demonstrates that the zebrafish olfactory sensory system can be used as a novel model to study the neural immune interface protecting the brain from the outside world taking into account the neurogenic capacities of the adult olfactory organs. In conclusion, our studies present new pathways for understanding the immune response with emphasis on the

special role of the olfactory organs in the control of peripheral and potentially central inflammatory responses in the nervous system

References

Ager, A. (2017). High endothelial venules and other blood vessels: Critical regulators of lymphoid organ development and function. *Frontiers in Immunology*, *8*(FEB), 1–16. https://doi.org/10.3389/fimmu.2017.00045

Al Bakri, W., Donovan, M. D., Cueto, M., Wu, Y., Orekie, C., & Yang, Z. (2018). Overview of intranasally delivered peptides: key considerations for pharmaceutical development. *Expert Opinion on Drug Delivery*, *15*(10), 991–1005. https://doi.org/10.1080/17425247.2018.1517742

Astin, J. W., Haggerty, M. J. L., Okuda, K. S., Le Guen, L., Misa, J. P., Tromp, A., Hogan, B. M., Crosier, K. E., & Crosier, P. S. (2014). Vegfd can compensate for loss of Vegfc in zebrafish facial lymphatic sprouting. *Development (Cambridge)*, *141*(13), 2680–2690. https://doi.org/10.1242/dev.106591

Bogoslowski, A., Butcher, E. C., & Kubes, P. (2018). Neutrophils recruited through high endothelial venules of the lymph nodes via PNAd intercept disseminating Staphylococcus aureus. *Proceedings of the National Academy of Sciences of the United States of America*, *115*(10), 2449–2454. https://doi.org/10.1073/pnas.1715756115

De Luca, C., Colangelo, A. M., Virtuoso, A., Alberghina, L., & Papa, M. (2020). Neurons, glia, extracellular matrix and neurovascular unit: A systems biology approach to the complexity of synaptic plasticity in health and disease. *International Journal of Molecular Sciences*, *21*(4), 1–25. https://doi.org/10.3390/ijms21041539

Dorrier, C. E., Aran, D., Haenelt, E. A., Sheehy, R. N., Hoi, K. K., Pintarić, L., Chen, Y., Lizama, C. O., Cautivo, K. M., Weiner, G. A., Popko, B., Fancy, S. P. J., Arnold, T. D., & Daneman, R. (2021). CNS fibroblasts form a fibrotic scar in response to immune cell infiltration. *Nature Neuroscience*, *24*(2), 234–244. https://doi.org/10.1038/s41593-020-00770-9

Drayton, D. L., Liao, S., Mounzer, R. H., & Ruddle, N. H. (2006). Lymphoid organ development: From ontogeny to neogenesis. *Nature Immunology*, *7*(4), 344–353. https://doi.org/10.1038/ni1330

Fortuna, A., Alves, G., Serralheiro, A., Sousa, J., & Falcão, A. (2014). Intranasal delivery of systemic-acting drugs: small-molecules and biomacromolecules. *European Journal of Pharmaceutics and Biopharmaceutics : Official Journal of Arbeitsgemeinschaft Für Pharmazeutische Verfahrenstechnik e.V*, *88*(1), 8–27. https://doi.org/10.1016/j.ejpb.2014.03.004

Girard, J. P., Moussion, C., & Förster, R. (2012). HEVs, lymphatics and homeostatic immune cell trafficking in lymph nodes. *Nature Reviews Immunology*, *12*(11), 762–773. https://doi.org/10.1038/nri3298

Gray, E. E., & Cyster, J. G. (2012). Lymph node macrophages. *Journal of Innate Immunity*, *4*(5–6), 424–436. https://doi.org/10.1159/000337007

Hampton, H. R., & Chtanova, T. (2016). The lymph node neutrophil. *Seminars in Immunology*, *28*(2), 129–136. https://doi.org/10.1016/j.smim.2016.03.008

Hampton, H. R., & Chtanova, T. (2019). Lymphatic migration of immune cells. *Frontiers in Immunology*, *10*(MAY), 19–23. https://doi.org/10.3389/fimmu.2019.01168

Jafarnejad, M., Ismail, A. Z., Duarte, D., Vyas, C., Ghahramani, A., Zawieja, D. C., Lo Celso, C., Poologasundarampillai, G., & Moore, J. E. (2019). Quantification of the Whole Lymph Node Vasculature Based on Tomography of the Vessel Corrosion Casts. *Scientific Reports*, *9*(1), 1–11. https://doi.org/10.1038/s41598-019-49055-7

Kastenmüller, W., Torabi-Parizi, P., Subramanian, N., Lämmermann, T., & Germain, R. N. (2012). A spatially-organized multicellular innate immune response in lymph nodes limits systemic pathogen spread. *Cell*, *150*(6), 1235–1248. https://doi.org/10.1016/j.cell.2012.07.021

Kumar, N. N., Gautam, M., Lochhead, J. J., Wolak, D. J., Ithapu, V., Singh, V., & Thorne, R. G. (2016). Relative vascular permeability and vascularity across different regions of the rat nasal

mucosa: Implications for nasal physiology and drug delivery. *Scientific Reports*, *6*(July), 1–14. https://doi.org/10.1038/srep31732

Li, Y., He, X., Kawaguchi, R., Zhang, Y., Wang, Q., Monavarfeshani, A., Yang, Z., Chen, B., Shi, Z., Meng, H., Zhou, S., Zhu, J., Jacobi, A., Swarup, V., Popovich, P. G., Geschwind, D. H., & He, Z. (2020). Microglia-organized scar-free spinal cord repair in neonatal mice. *Nature*, *587*(7835), 613–618. https://doi.org/10.1038/s41586-020-2795-6

Neutra, M. R., & Kozlowski, P. A. (2006). Mucosal vaccines: The promise and the challenge. *Nature Reviews Immunology*, *6*(2), 148–158. https://doi.org/10.1038/nri1777

Okuda, K. S., Astin, J. W., Misa, J. P., Flores, M. V, Crosier, K. E., & Crosier, P. S. (2012). lyve1 Expression Reveals Novel Lymphatic Vessels and New Mechanisms for Lymphatic Vessel Development in Zebrafish. *Development*, *139*, 2381–2391. https://doi.org/10.1242/dev.077701

Palominos, M. F., & Whitlock, K. E. (2021). The Olfactory Organ Is Populated by Neutrophils and Macrophages During Early Development. *Frontiers in Cell and Developmental Biology*, *8*(January), 1–15. https://doi.org/10.3389/fcell.2020.604030

Pelegrin, P., & Surprenant, A. (2006). Pannexin-1 mediates large pore formation and interleukin-1β release by the ATP-gated P2X7 receptor. *EMBO Journal*, *25*(21), 5071–5082. https://doi.org/10.1038/sj.emboj.7601378

Qi, H., Kastenmüller, W., & Germain, R. N. (2014). Spatiotemporal basis of innate and adaptive immunity in secondary lymphoid tissue. *Annual Review of Cell and Developmental Biology*, *30*(1), 141–167. https://doi.org/10.1146/annurev-cellbio-100913-013254

Ruddle, N. H. (2014). Lymphatic vessels and tertiary lymphoid organs. *Journal of Clinical Investigation*, *124*(3), 953–959. https://doi.org/10.1172/JCI71611

Sakano, H. (2010). Neural map formation in the mouse olfactory system. *Neuron*, *67*(4), 530–542. https://doi.org/10.1016/j.neuron.2010.07.003

Whitlock, K. E. (2004). A New Model for Olfactory Placode Development. *Brain, Behavior and Evolution*, *64*(3), 126–140. https://doi.org/10.1159/000079742

Yang, Y., Delalio, L. J., Best, A. K., Macal, E., Milstein, J., Donnelly, I., Miller, A. M., McBride, M., Shu, X., Koval, M., Isakson, B. E., & Johnstone, S. R. (2020). Endothelial Pannexin 1 Channels Control Inflammation by Regulating Intracellular Calcium. *The Journal of Immunology*, *204*(11), 2995–3007. https://doi.org/10.4049/jimmunol.1901089

Yoshida, T., Uchida, S., & Mishina, M. (2009). Regulation of synaptic vesicle accumulation and axon terminal remodeling during synapse formation by distinct Ca2+signaling. *Journal of Neurochemistry*, *111*(1), 160–170. https://doi.org/10.1111/j.1471-4159.2009.06309.x